Aus dem Experimental and Clinical Research Center (ECRC)
der Medizinischen Fakultät Charité – Universitätsmedizin Berlin und
Max-Delbrück-Centrum für Molekulare Medizin (MDC) in der Helmholtz-
Gemeinschaft

DISSERTATION

Bestimmung der Steifheit weicher Biomaterialien und potenziell
assoziierter Ziellipide
Determination of soft biomaterials stiffness and potentially
associated target lipids

zur Erlangung des akademischen Grades
Doctor medicinae (Dr. med.)

vorgelegt der Medizinischen Fakultät
Charité – Universitätsmedizin Berlin

von

Herrn Guanlin Wu

aus Tongling, China

Datum der Promotion: 04.03.2022

Table of Contents

List of abbreviations

Eff: effective Young's modulus

E: Young's modulus

ICC: Intraclass Correlation Coefficient

CI: Confidence Interval

COV: within-subject coefficient of variation

RBC: red blood cell

CKD: chronic kidney disease

ESRD: end-stage renal disease

LC–MS/MS: liquid chromatography tandem mass

PUFA: polyunsaturated fatty acid

CYP: cytochrome P450

LOX: lipoxygenase

sEH: soluble epoxide hydrolase

HODE: hydroxyoctadecadienoic acid

HpODE: hydroperoxylinoleic acid

EpOME: epoxyoctadecenoic acid

DiHOME: dihydroxyctadecenoic acid

EET: epoxyeicosatrienoic acid

EEQ: epoxyeicosatetraenoic acid

EDP: epoxydocosapentaenoic acid

DHET: dihydroxyeicosatrienoic acid

DiHETE: dihydroxyeicosatetraenoic acid

DiHDHA: dihydroxydocosahexaenoic acid

DiHDPA: dihydroxydocosapentaenoic acid

HETE: hydroxyeicosatetraenoic acid

HPETE: hydroperoxyeicosatetraenoic acid

HEPE: hydroxyeicosapentaenoic acid

HDHA: hydroxydocosahexaenoic acid

LTB: leukotriene B

LXA: lipoxin A

LXB: lipoxin B

TXB2:   thromboxane B2

PGI2:   prostaglandin I2

PGE2:   prostaglandin E2

PGD2:   prostaglandin D2

PGJ2:   prostaglandin J2

PGF2a: prostaglandin F2a

TXB3:   thromboxane B3

PGE3:   prostaglandin E2

MAR 1:   pro-resolving lipid mediator maresin 1

7-epi-MAR1: inactive 7(S) epimer of maresin 1

RvD1:   resolvin D1

RvD2:   resolvin D2

RvD3:   resolvin D3

RvD5:   resolvin D5

RvE1:   resolvin E1

LA: linoleic acid, C18:2

EPA: eicosapentaenoic acid, C20:5 n-3

AA: arachidonic acid, C20:4

DHA: docosahexaenoic acid,C22:6 n-3

EDHF: endothelium-derived hyperpolarizing factor

Abstract

The connection between organ mechanical properties and disease has been widely recognized. Accurately measuring the mechanical properties of tissues contributes to the diagnosis and research of diseases. Indentation nanotechnology is often used to measure the stiffness of tough biomaterials. But it is still unknown about its reliability in analyzing soft biomaterials. In addition, it is not clear whether some lipids are able to become potential targets for regulating organ physiology and pathophysiology. In order to investigate the reliability of nanoindentation technology in soft biomaterials, we used a displacement-controlled nanoindenter to double measure the stiffness of several liver, kidney, uterus and spleen samples reaped from C57BL/6N mice, and compared the variations between test and retest via intraclass correlation coefficients (ICCs), within-subject coefficients of variation (COVs) and Bland-Altman plots. According to the analysis results, we found that among the three stiffness calculation models of Hertzian, JKR, and Oliver & Pharr, the results calculated only in the Hertzian model can consistently provide reliability (ICC>0.8, COV<15%). In addition, for the purpose to explore the lipids that may cause fibrosis of human organs, the expression level of certain lipids in both red blood cell (RBC) and plasma between some healthy people and chronic kidney disease (CKD) patients was compared. Furthermore, we also explored whether dialysis has an effect on the lipid levels in RBC and plasma of CKD patients. After testing all lipids by LC–MS/MS spectrometry, we found that the expression of some lipids in the blood of healthy people and CKD patients was different, and dialysis treatment was also able to cause alterations in several blood lipid levels of CKD patients. In conclusion, it revealed that the nanoindentation technique we used to measure the hardness of the liver, kidney, uterus and spleen is feasible and the Hertzian model provides the most reliable way to measure the stiffness of organs in vitro. Besides, these lipid metabolites could be potential targets for organ fibrosis formation due to their ability in impacting different hemodynamic and metabolic in various physiological or morbid conditions. Our studies are able to provide theoretical foundation and technical support for future research on organ fibrotic diseases.

Zusammenfassung

Der Zusammenhang zwischen den mechanischen Eigenschaften von Organen und Krankheiten ist weithin bekannt. Die genaue Messung der mechanischen Eigenschaften von Geweben trägt zur Diagnose und Erforschung von Krankheiten bei. Indentation Nanotechnologie wird häufig verwendet, um die Steifigkeit von zähen Biomaterialien zu messen. Über seine Zuverlässigkeit bei der Analyse weicher Biomaterialien ist jedoch noch nichts bekannt. Darüber hinaus ist nicht klar, ob einige Lipide potenzielle Ziele für die Regulierung der Organphysiologie und Pathophysiologie werden können. Um die Zuverlässigkeit der Nanoindentation-Technologie in weichen Biomaterialien zu untersuchen, haben wir einen verdrängungskontrollierten Nanoindenter verwendet, um die Steifigkeit mehrerer Leber-, Nieren-, Uterus- und Milzproben, die von C57BL/6N-Mäusen gewonnen wurden, doppelt zu messen und die Variationen zwischen Test und Retest verglichen über Intraklassen-Korrelationskoeffizienten (ICCs), Innersubjekt-Variationskoeffizienten (COVs) und Bland-Altman-Plots. Den Analyseergebnissen zufolge haben wir festgestellt, dass von den drei Steifigkeitsberechnungsmodellen von Hertzian, JKR und Oliver & Pharr die nur im Hertzschen Modell berechneten Ergebnisse konsistent eine Zuverlässigkeit bieten (ICC>0,8, COV<15%). Um die Lipide zu erforschen, die eine Fibrose menschlicher Organe verursachen können, wurde außerdem der Expressionsspiegel bestimmter Lipide sowohl in den roten Blutkörperchen (RBC) als auch im Plasma zwischen einigen gesunden Menschen und Patienten mit chronischer Nierenerkrankung (CKD) verglichen. Darüber hinaus untersuchten wir auch, ob die Dialyse einen Einfluss auf die Lipidspiegel in Erythrozyten und Plasma von CKD-Patienten hat. Nachdem wir alle Lipide durch LC-MS/MS-Spektrometrie getestet hatten, stellten wir fest, dass die Expression einiger Lipide im Blut von gesunden Menschen und von CNE-Patienten unterschiedlich war und die Dialysebehandlung auch in der Lage war, verschiedene Blutfettwerte von CNE-Patienten zu verändern. Zusammenfassend zeigte sich, dass die von uns verwendete Nanoindentation-Technik zur Messung der Härte von Leber, Niere, Gebärmutter und Milz machbar ist und das Hertzsche Modell die zuverlässigste Methode zur Messung der Steifigkeit von Organen in vitro bietet. Außerdem könnten diese Lipidmetaboliten potenzielle Ziele für die Bildung von Organfibrose sein, da sie verschiedene hämodynamische und metabolische Faktoren unter verschiedenen physiologischen oder morbiden Bedingungen beeinflussen können. Unsere Studien

sind in der Lage, die zukünftige Forschung zu organfibrotischen Erkrankungen theoretisch fundiert und technisch zu unterstützen.

1. Introduction

Changes in the stiffness of tissues or cells influences the physiological function or structure of certain organs in the body. Similarly, diseases are also able to alter organs stiffness and thus affect the progression of the illness. For example, heart and arteries of patients with cardiovascular diseases present varying degrees of hardening [1-2]. The connection between aortic stiffness and cardiac dysfunction in patients with inflammatory bowel disease has been confirmed [3]. The therapeutic strategy and effect to hepatitis virus have a significant impact on the patients liver stiffness [4-5]. The arterial stiffness of patients with different degrees of chronic kidney disease showed parallel changes [6]. The hardness of the central arteries are significantly affected by type 2 diabetes [7].

Multiple technologies have been applied in clinical diagnosis to detect changes in patients organs stiffness, examples include ultrasound, instantaneous elastography, magnetic resonance elastography, acoustic radiation force pulse elastography and point shear wave elastography [8-15]. In addition to vivo measurements, varieties of techniques have been utilized for characterizing the stiffness of some biomaterials *ex vivo*. Mark R. Buckley et al. utilized a technique that combines force measurement, shear testing and confocal imaging to study articular cartilage shear properties [16]. Damien Cuvelier et al. studied some biomechanical characteristics of tethers via a combined device of micropipette manipulation and optical tweezers [17]. AFM was applied by Kozaburo Hayashi and Mayumi Iwata in measuring the stiffness of cancer cells [18]. Yuhui Li et al. presented a magnetic mechanical testing system in viscoelastic tensile testing for micrometer-scale biological materials [19]. D.B. MacManus et al. developed a custom-made micro-indentation device to study brain tissue local mechanical properties [20]. Badar Rashid et al. used a high-rate tension device to obtain brain tissue dynamic properties in extension at different strain rates [21].

Piuma nanoindenter is an advanced technology to be used in testing the elastic properties of biomaterials. This facility has been applied to measure the mechanical properties of hard organs like bones and cartilage [22-25]. However, since only very few studies [26-30] reported the utilization of nanoindentation technology in the elasticity measurement of soft biomaterials, the strategy for analyzing the stiffness of organs *ex vivo* by this technology is still unclear. In our study, we took mouse kidney, liver, spleen and uterus to analyze the feasibility of nanoindentation technology in soft biomaterials.

Prostaglandins (PGS) and other eicosanes, such as leukotrienes (LTs), thromboalkanes (TXs), hydro(peroxy) fatty acids (or oxylipins) and epoxides, are lipid peroxidation products of 20-carbon (eicosa-) polyunsaturated fatty acids (PUFA). They are produced by three independent enzyme families, cytochrome P450 (CYP) expoygenases, cyclooxygenase (COX) and lipoxygenase (LOX), which catalyse lipid peroxidation in regio-specific products and a highly regulated manner generating stereo (**Figure 1**). Their expression is highly localized to tissues and varies in response to inflammatory activation that affects the fibrosis of the target organs. According to the cell type, the main products of COX, LOX and CYP are metabolized into secondary eicosanoids and their metabolites, some of which have strong biological activity (**Figure 1**). The main metabolic pathways of PUFA epoxides are the incorporation of their phospholipids and hydrolysis to the corresponding PUFA diols by soluble epoxide hydrolase (sEH) [31].

Oxipides play an important role in our bodies, but sometimes they can have harmful effects [32-34]. Therefore, it has clinical significance in practical practice because of the biological activity of these products. For example, dihydroxy eicosatrienoic acid (DHETs) and epoxyeicosatrienoic acids (EETs) are considered candidates for vascular dilatation endothelial-derived hyperpolarization factors (EDHFs) [35], whose release is activated by shear stress and Ca^{2+}- *via* the CYP pathway [36-37]. While epoxyoctadecenoic acids (EpOMEs) and their diols decrease the functional recovery of cardiac post-ischemic [38], 5-HETE stimulates neutrophil chemotaxis and degranulation [39-41] and inhibits endothelial prostaglandin I2 (PGI2) production with consecutive effects on platelet aggregation and vasotonus [42]. PGs is believed to be an essential ingredient in healing wounds, tissues and fibrosis [43-44]. Researches on the relationship between other lipids and organ fibrosis are limited. In our study, we tested all epoxides derived from cytochromes P450 monooxygenase and lipoxygenase (LOX)/CYP ω/(ω-1)-hydroxylase pathways in chronic kidney disease and hemodialysis treatment patients to see whether they could be taken as potential drug targets to regulate organ physiology and pathophysiology, in particular organ fibrosis.
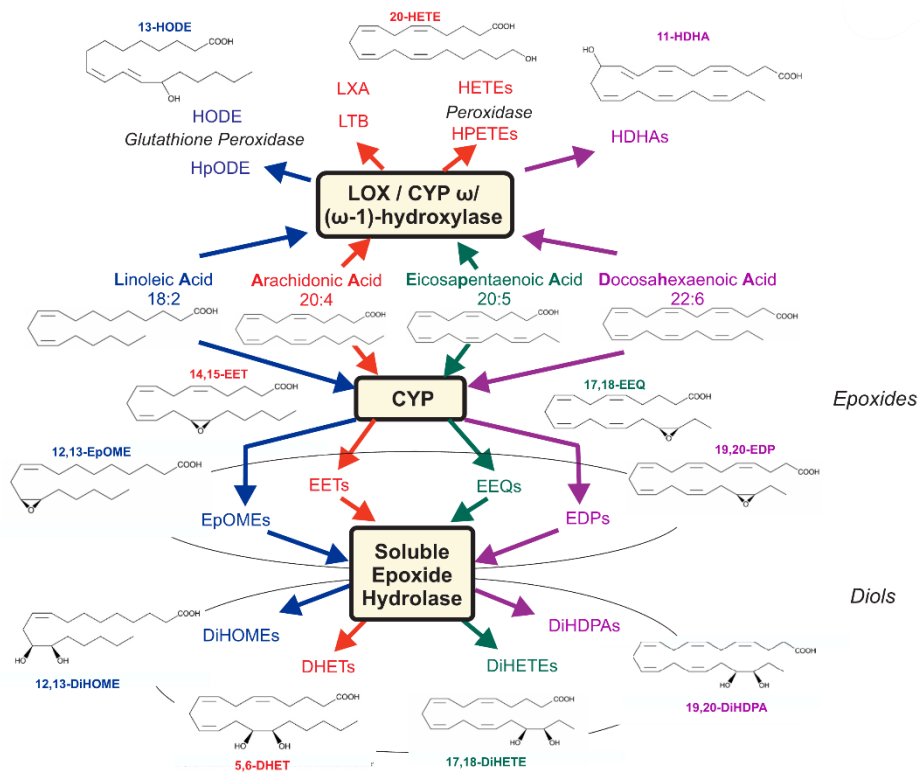
Figure 1: **12- and 15-lipoxygenase (LOX) / CYP (omega-1)-hydroxylase and cytochrome P450 epoxygenase (CYP) pathways**. Arachidonic (AA), linoleic (LA), docosahexaenoic acids (DHA) and eicosapentaenoic (EPA) are converted by CYP epoxygenase to epoxyeicosatrienoic acid (EETs), epoxyoctadecenoic acids (EpOMEs, e.g. 12,13-EpOME), epoxydocosapentaenoic acids (EDPs) and epoxyeicosatetraenoic acids (EEQs). EETs, EEQs, EDPs and EpOMEs can be converted to dihydroxyeicosatrienoic acids (DHETs, e.g. 5,6-DHET), dihydroxyctadecenoic acids (DiHOMEs), dihydroxydocosapentaenoic acids (DiHDPAs) and dihydroxyeicosatetraenoic acids (DiHETEs, e.g. 5,6-DiHETE, 17,18-DiHETE) by soluble epoxide hydrolase (sEH). EPA, LA, DHA, and AA are converted to hydroxyoctadecadienoic acids (HODEs), hydroperoxylinoleic acids (HpODEs), lipoxin A (LXA), leukotriene B (LTB), hydroxydocosahexaenoic acids (HDHAs), hydroxyeicosatetraenoic acids (HETEs) and hydroperoxyeicosatetraenoic acids (HPETEs) by LOX, CYP omega/(omega-1)- peroxidase and hydroxylase pathways. The changes of EPA, LA, DHA, and AA are tracked by the metabolites measured in these pathways. (This figure was cited from [45]).

2. Methodology

2.1 Animals and Matrigen hydrogels:

The strain of mice included in this study is C57BL/6N. For kidney and spleen, 2 mice of each sex and age (5 week-, 10 week-, 20 week- and 30 week-old) were used. For liver, five 5 week-old (3 males, 2 females), five 5 week-old (2 males, 3 females), six 20 week-old (2 males, 4 females) and four 30 week-old (2 males, 2 females) mice were used. In terms of the uterus, eight mice were used in the experiment, all of which were about 100 days old. The experiment was authorized by the animal welfare officers at the Max Delbrück Center for Molecular Medicine (MDC) (No. X 9011/19) and the local animal care committee (LAGeSo, Berlin, Germany).

Ten hydrogels (Softwell, Matrigen, Matrigen Life Technologies, Brea, CA) in different stiffness (1x1 kPa, 1x2 kPa, 2x4 kPa, 1x8 kPa, 3x12 kPa and 2x25 kPa) were taken as quality control.

2.2 Tissues preparation:

Front and back profiles of both left and right kidneys were dissected and measured. Left lobe of liver, intact spleen and opened left uterine horn were harvested for indentation. It is critical to clean all the impurities around tissues without damaging their essence. Shellac (Sigma) was used for immobilization of all biomaterials. PBS (NaCl 0.137 M, KCl 0.0027 M, Na_2HPO_4 0.01 M, KH_2PO_4 0.0018 M; pH 7.4) was the medium for all samples in the experiment.

2.3 Nanoindentation and stiffness determination:

For the measurement of stiffness, we used the nanoindenter instrument (Piuma; Optics11, Amsterdam, The Netherlands) contained a ferrule-top cantilever probe [46-47] (**Figure 2A**) with 50 μm radius and 0.5 N/m cantilever stiffness. The probe should focus on a flat and wide area on tissue surface (**Figure 2B**) after calibration. Each gel was indented 25 times (5x5 matrix) in an 800x800 μm grid scan with 200 μm distance between measurements. Kidney, liver and spleen samples were indented with 9 indentations (3x3 matrix) in a 200x200 μm grid scan. In uterus, three indentation matrixes with 4 single indentations in 100x100 μm grid were tested in proximal, middle and distal parts of uterus, respectively. The applied indentation scheme consists of a 4-second loading phase at an

indentation depth of 8000 nm, holding for 1 second, and then a 4-second unloading phase. All scans were performed twice for reliability analysis.

The mean value of the scan results from four renal sections of each mouse was presented as the elasticity of kidney. The average value of all results in each scan was taken as the stiffness for gel, liver and spleen. Uterine hardness was expressed by the mean results from three scans. All indentation values were processed and exported by Piuma Dataviewer version 2.2 (Piuma; Optics11, Amsterdam, The Netherlands).

2.4 Volunteers and patients:

The dialysis study had 15 healthy volunteers (6 men and 9 women) and 15 patients with CKD (7 men and 8 women) receiving routine hemodialysis signed an informed consent form outlining the treatment to be taken and the possible risks involved. None of the healthy control subjects received medication. The healthy subjects were 50 ± 18 years old and the hemodialysis (HD) patients were 47 ± 12 years old. BMI was 24.8 ± 3.4 kg/m^2 and 24.7 ± 4.6 kg/m^2, respectively. The use of humans in this study was approved by the Charité University Medicine institutional review board.

2.5 Human blood samples treatment:

For healthy subjects and patients with CKD in the dialysis treatment study, venous blood from each healthy subject was collected by subcutaneous arm venipuncture in sitting status. Blood samples from the fistula arm were collected from dialysis patients before the beginning of dialysis (pre-HD) and at the end of dialysis (5-15min before the end of dialysis, post-HD). Patients received dialysis 3 times a week, lasting 3 hours 45 minutes to 5 hours, based on a high-throughput AK200 dialyzer (Gambro GmbH, Hechingen, Germany). All samples were analyzed for plasma oxylipins and RBC lipids.

All lipidomics was performed using liquid chromatography tandem mass (LC–MS/MS) spectrometry.

2.6 Statistical analysis:

The reliability analysis of the test-retest depends on the results of Bland-Altman plot [48-49], Within-subject coefficient of variations (COVs) and Intraclass correlation coefficients (ICCs). In general, the difference value of test-retest results in Bland-Altman plot is between 95% limits of agreement, and/or ICC is greater than 0.8, and/or COV is less than 15%, which indicates that there is good reliability between test and retest.

The values of CKDs were compared with those of the control group by the Mann-Whitney test or the t-test. The paired t-test or paired Wilcoxon test was used to compare pre-HD and post-HD values. To determine the statistical differences between the four epoxide metabolites present in the cycle after hydrolysis, the Friedman's test was used, followed by the Dunn's multiple comparison test. 0.05 was selected as level significance (P). All data were expressed as Mean $\pm$ SD.

All analyses were performed using MedCalc 19.3 software (Belgium), SPSS 19.0 (Chicago, USA) or GraphPad Prism 7.0 (San Diego, USA).

For a complete description of the methods see:

G. Wu, M. Gotthardt, and M. Gollasch, Assessment of nanoindentation in stiffness measurement of soft biomaterials: kidney, liver, spleen and uterus. Sci Rep, 2020. 10(1): p. 18784.

B. Gollasch, **G. Wu**, I. Dogan, M. Rothe, M. Gollasch, and F. C. Luft, Effects of hemodialysis on plasma oxylipins. Physiol Rep, 2020. 8(12): p. e14447.

B. Gollasch, **G. Wu**, T. Liu, I. Dogan, M. Rothe, M. Gollasch, and F. C. Luft, Hemodialysis and erythrocyte epoxy fatty acids. Physiol Rep, 2020. 8(20): p. e14601.

3. Results

3.1 Stiffness determination in different models:

All results were calculated in three different models, which are Oliver & Pharr, JKR and Hertzian models.

The effective Young's modulus (Eff) calculation in Hertzian model [50-51] (**Figure 2C, D, F**) follows equation:

$$Eff = \frac{P*3/4}{\sqrt{R} \cdot h_t^{3/2}}$$

In JKR model [52] (**Figure 2C, D, G**), equations used for the calculation of Eff are:

$$h_t - h_0 = \frac{a_0^2}{R}\left(\frac{1 + \sqrt{1 - \frac{P}{P_{adh}}}}{2}\right)^{\frac{4}{3}} - \frac{2}{3}\frac{a_0^2}{R}\left(\frac{1 + \sqrt{1 - \frac{P}{P_{adh}}}}{2}\right)^{\frac{1}{3}}$$

$$P_{adh} = -\frac{3}{2}\pi\Delta r R$$

$$Eff = \frac{9\pi R^2 \Delta r}{2a_0^3}$$

When no sticky is displayed in the unload section, there would be no result from this model as no fit is applicable (**Figure 2E**).

Eff in Oliver & Pharr model [53-54] (**Figure 2C, D, H**) was processed by using the following formula:

$$Eff = \frac{dP}{dh}\frac{1}{2\sqrt{R(h_t + h_r)}}$$

The JKR model, the Hertzian model, and the Oliver & Pharr model were fitted at 100%, 100%, and 65-85%, respectively.

In addition to Eff, Young's modulus (E) also enable present stiffness. Poisson's ratio [55] v relates Eff and E by the following equation:

$$Eff = \frac{E}{1 - v^2}$$

Due to the unknown of tissues' material property and the Poisson's ratios, we determined both Eff and E for each biomaterial. We took the default value (0.5) in Piuma software for Poisson's ratio.
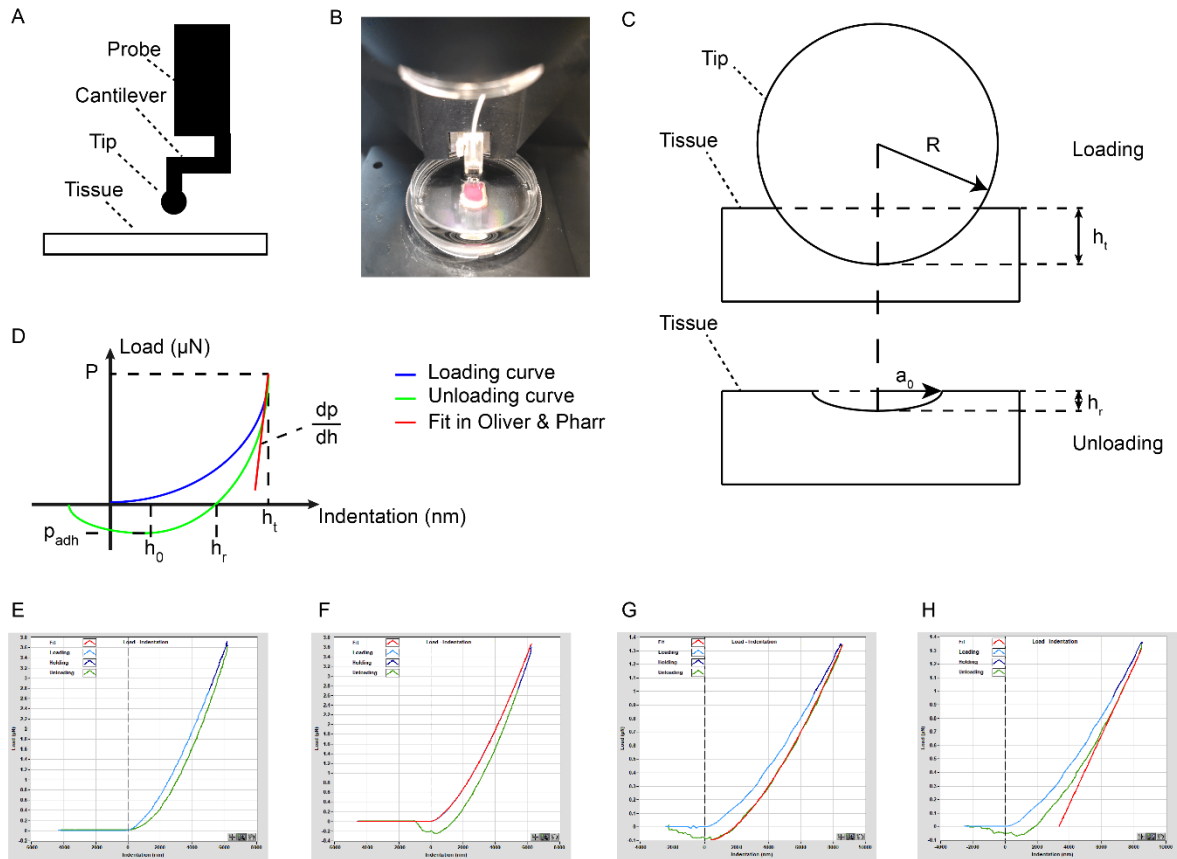
Figure 2: Effective Young's modulus calculational principle. (A) Components of probe and localization between the probe and tissue. (B) Focuse of the nanoindenter probe. (C) Schematic diagram from loading to unloading indentation. (D) Schematic diagram of load-indentation. (E) Non-adhesion indentation. (F) Indentation in Hertzian model (100% fit). (G) Indentation in JKR model (100% fit). (H) Indentation in Oliver & Pharr model (65-85% fit). (This figure was cited from [56]).

3.2 Stiffness reliability of Matrigen hydrogels and organs:

As shown in the Bland-Altman diagram of the hydrogel **(Figure 3)**, it revealed that almost all of the retest differences were within the 95% concordant range (-1.96 SD to 1.96 SD).In addition, ICC values of all models were greater than 0.8 and COV values were less than 15% **(Table 1)**, indicating that the three models all provided reliable results for gel samples.
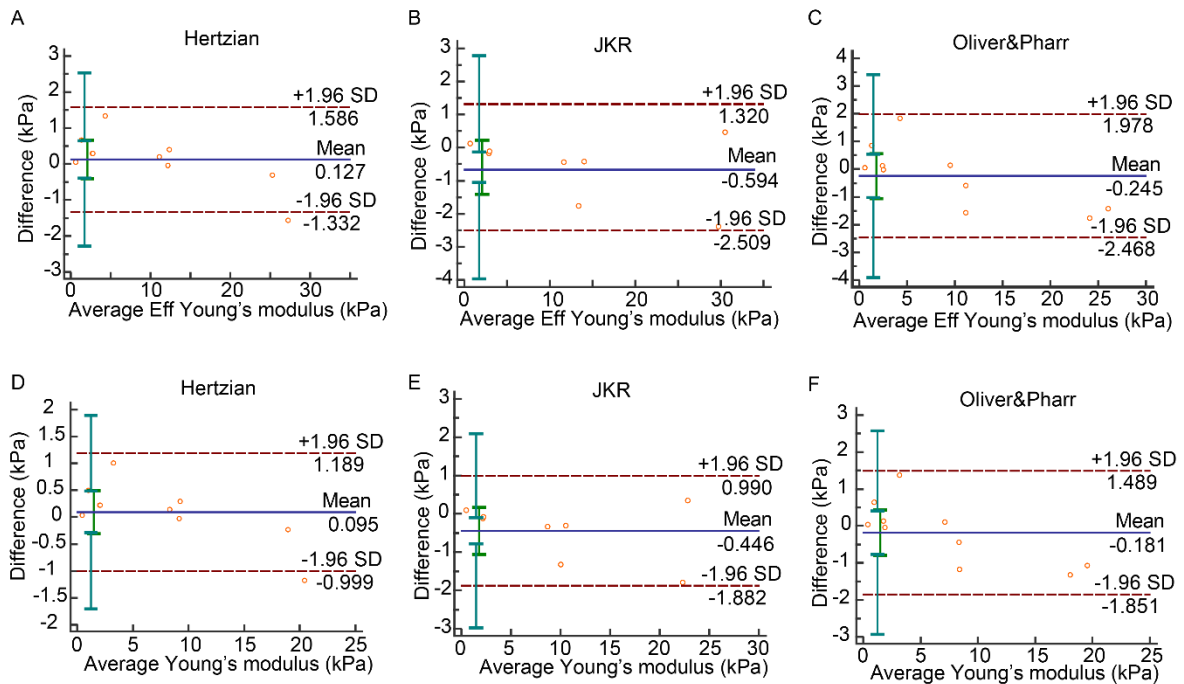
Figure 3. Bland-Altman plot of Matrigen hydogels. (A) Bland-Altman plot of *Eff* in Hertzian model. (B) Bland-Altman plot of *Eff* in JKR model. (C) Bland-Altman plot of *Eff* in Oliver & Pharr model. (D) Bland-Altman plot of *E* in Hertzian model. (E) Bland-Altman plot of *E* in JKR model. (F) Bland-Altman plot of *E* in Oliver & Pharr model. (This figure was cited from [56]).

Table 1. Reliability of test-retest in Matrigen gels

	ICC, 95% CI	COV (%)
Eff in Hertzian	**0.9986 (0.9948,0.9997)**	**5.0666**
Eff in JKR	**0.9978 (0.9900,0.9996)**	**5.8171**
Eff in Oliver & Pharr	**0.9964 (0.9865, 0.9991)**	**8.3703**
E in Hertzian	**0.9986 (0.9948,0.9997)**	**5.0665**
E in JKR	**0.9978 (0.9900,0.9996)**	**5.8171**
E in Oliver & Pharr	**0.9964 (0.9865,0.9991)**	**8.3787**

Note: Values in bold indicate that they are in the good reliability range.

(This table was cited from [56]).

In the kidney, only Hertzian model has ICC value greater than 0.8 and COV less than 15%, while other models do not show the character (**Table 2**).

Table 2. Reliability of test-retest in kidney

	ICC, 95% CI	**COV (%)**
Eff in Hertzian	**0.9686 (0.9124,0.9889)**	**5.0723**
Eff in JKR	0.5951 (-0.1287,0.8572)	18.2387
Eff in Oliver & Pharr	0.5929 (-0.1347,0.8565)	16.6833
E in Hertzian	**0.9693 (0.9143,0.9892)**	**5.0194**
E in JKR	0.6699 (0.07971,0.8836)	16.0643
E in Oliver & Pharr	0.6422 (0.002628,0.8738)	16.2013

Note: Values in bold indicate that they are in the good reliability range.

(This table was cited from [56]).

In the liver, only the Hertzian model has ICCs of E and Eff that consistently exceeds 0.8, while the Oliver & Pharr and JKR models do not. The COVs of Hertzian and Oliver & Pharr models were less than 15%, while the COVs of JKR model were not (**Table 3**).

Table 3. Reliability of test-retest in liver

	ICC, 95% CI	**COV (%)**
Eff in Hertzian	**0.9303 (0.8269,0.9722)**	**5.0091**
Eff in JKR	0.6240 (0.06673,0.8501)	19.1874
Eff in Oliver & Pharr	0.7507 (0.3811,0.9006)	**12.0356**
E in Hertzian	**0.9251 (0.8142,0.9702)**	**5.1724**
E in JKR	0.6078 (0.02648,0.8437)	20.5038
E in Oliver & Pharr	**0.8048 (0.5155,0.9222)**	**10.0323**

Note: Values in bold indicate that they are in the good reliability range.

(This table was cited from [56]).

In the spleen, ICCs of *Eff* and *E* were consistently greater than 0.8 in Hertzian and JKR models, but not in Olivier & Pharr model. The COVs of *E* and *Eff* in Hertzian model were less than 15%, but not in other models(**Table 4**).

Table 4. Reliability of test-retest in spleen

	ICC, 95% CI	**COV (%)**
Eff in Hertzian	**0.9924 (0.9787,0.9973)**	**3.1172**
Eff in JKR	**0.8675 (0.6307,0.9533)**	15.0115
Eff in Oliver & Pharr	0.3334 (-0.8583,0.7649)	20.3557
E in Hertzian	**0.9931 (0.9807,0.9976)**	**2.9890**
E in JKR	0.5113 (-0.3622,0.8277)	27.1063
E in Oliver & Pharr	-0.3404 (-2.7364,0.5274)	42.3569

Note: Values in bold indicate that they are in the good reliability range.

(This table was cited from [56]).

In the uterus, the Oliver & Pharr and Hertzian models had ICC values greater than 0.8, while the JKR model had ICC values less than 0.8. In contrast, only the Hertzian model had COVs less than 15%, while the other models did not(**Table 5**).

Table 5. Reliability of test-retest in uterus

	ICC, 95% CI	**COV (%)**
Eff in Hertzian	**0.9861 (0.9371,0.9972)**	**11.6893**
Eff in JKR	0.7926 (0.0607,0.9577)	64.4623
Eff in Oliver & Pharr	**0.8295 (0.2278,0.9652)**	34.7149
E in Hertzian	**0.9780 (0.9002,0.9955)**	**14.1841**
E in JKR	0.7512 (-0.1267,0.9492)	71.0078
E in Oliver & Pharr	**0.8778 (0.4465,0.9751)**	31.8501

Note: Values in bold indicate that they are in the good reliability range.

(This table was cited from [56]).

Similar to the Matrigen hydrogels, Bland-Altman diagrams of the kidney, liver, spleen, and uterus showed only a few difference for *Eff* and *E* out of the 95% concordant limit in all models.

3.3 Lipids in CKD:

In plasma, we detected increased 9,10-EpOME, 12,13-EpOME, 8,9-EET, 5,6-EET, 14,15-EET, 11,12-EET, 11,12-EEQ, 5,6-EEQ, 17,18-EEQ, 14,15-EEQ, 14,15-DiHETE, 10,11-EDP, 7,8-EDP, 19,20-EDP, 16,17-EDP, 5,6-DHET, 19-HEPE, 5-HEPE and 12-HEPE total levels and 13,14-EDP, 9-HEPE, 8-HEPE, 18-HEPE, 12-HEPE, 16-HDHA, 10-HDHA, 20-HDHA and 17-HDHA free levels in our end-stage renal disease (ESRD) patients, compared to the healthy subjects. Moreover, 9,10-DiHOME, 13-HODE, 11,12-DHET, 8,9-DHET, 8-HETE, 14,15-DHET, 11-HETE, 9-HETE, 15-HETE, 12-HETE, 19-HETE, 16-HETE, 8-HEPE, 20-HETE, 15-HEPE, 9-HEPE, 4-HDHA, 18-HEPE, 8-HDHA, 7-HDHA, 11-HDHA, 10-HDHA, 14-HDHA, 13-HDHA, 20-HDHA, 16-HDHA and 17-HDHA total levels and 9,10-DiHOME, 5,6-EET, 11,12-EET, 11,12-DiHETE, 17,18-DiHETE, 14,15-DiHETE, 11-HETE, 9-HETE, 15-HETE, 12-HETE, 15-HEPE, 14-HDHA and 13-HDHA free levels were decreased in our ESRD patients, compared to healthy volunteers. In addition, all total level individual metabolite diol/epoxide ratios in CKD patients were lower than controls. And total level EpOMEs and EDPs are better metabolized into their diols than EETs and EEQs in CKD patients (DiHOMEs/EpOMEs = DiHDPA/EDPs > DHETs/EETs = DiHETEs/EEQs).

In RBCs, CKD patients showed increased total levels of various epoxides, namely 14,15-DHET, 8,9-DHET, 11,12-EEQ, 5,6-EEQ, 17,18-EEQ, 14,15-EEQ, 13,14-DiHDPA, 7,8-DiHDPA, 5-HETE, 16,17-DiHDPA, 9-HETE, 8-HETE, 12-HETE, 11-HETE, 19-HETE and 15-HETE, and free levels of several lipids, namely 13-HODE, 8-HETE, 5-HETE, 11-HETE, 9-HETE, 15-HETE, 12-HETE, 5-HEPE, 16-HETE, 9-HEPE, 8-HEPE, 15-HEPE, 12-HEPE, 4-HDHA, 18-HEPE, 8-HDHA, 7-HDHA, 11-HDHA, 10-HDHA, 14-HDHA, 13-HDHA, 17-HDHA, 16-HDHA, 22-HDHA and 21-HDHA. We also found that various oxylipins total levels (19,20-EDP, 10,11-DiHDPA) and free levels (such as 5,6-EEQ, 8,9-EET and 14,15-EET) were decreased in the CKD patients. Regarding hydrolysis efficiency of these lipids, ESRD patients showed increased ratios for DHETs/EETs and DiHDPAs/EDPs in total level. In fact, compared to total level EETs and EEQs, EpOMEs

and EDPs are preferentially metabolized into their diols in controls (DiHOMEs/EpOMEs = DiHDPA/EDPs > DHETs/EETs = DiHETEs/EEQs).

3.4 Lipids in hemodialysis:

In plasma, hemodialysis treatment increases the majority of epoxy-metabolites in total level, including 13-HODE, 12,13-EpOME, 9,10-EpOME, 12,13-DiHOME, 9,10-DiHOME, 14,15-EET, 5,6-EET, 11,12-DHET, 8,9-DHET, 11,12-EEQ, 8,9-EEQ, 17,18-EEQ, 14,15-EEQ, 17,18-DiHETE, 14,15-DiHETE, 10,11-EDP, 7,8-EDP, 16,17-EDP, 13,14-EDP, 7,8-DiHDPA, 19,20-EDP, 13,14-DiHDPA, 10,11-DiHDPA, 19,20-DiHDPA, 16,17-DiHDPA, 20-HETE, 15-HEPE, 5-HEPE, 18-HEPE, 11-HDHA and 7-HDHA, and several free level lipids including 9,10-DiHOME, 11,12-EET, 16,17-EDP and 19,20-DiHDPA. Moreover, hemodialysis only decreased 19-HEPE in total level and 12-HpETE in free level. Nevertheless, ratios of diols/epoxides were not influenced by hemodialysis.

In RBCs, hemodialysis treatment increased several CYP epoxides and LOX/CYP ω/(ω-1)-hydroxylase metabolites in free state, such as 13-HODE, 11,12-DHET, 8-HETE, 5-HETE, 11-HETE, 9-HETE, 5-HEPE, 15-HETE, 10-HDHA, 8-HDHA, 17-HDHA, 13-HDHA and 16-HDHA. However, the diols/epoxides ratios were not altered due to dialysis.

For a complete description of the results see:

G. Wu, M. Gotthardt, and M. Gollasch, Assessment of nanoindentation in stiffness measurement of soft biomaterials: kidney, liver, spleen and uterus. Sci Rep, 2020. 10(1): p. 18784.

B. Gollasch, **G. Wu**, I. Dogan, M. Rothe, M. Gollasch, and F. C. Luft, Effects of hemodialysis on plasma oxylipins. Physiol Rep, 2020. 8(12): p. e14447.

B. Gollasch, **G. Wu**, T. Liu, I. Dogan, M. Rothe, M. Gollasch, and F. C. Luft, Hemodialysis and erythrocyte epoxy fatty acids. Physiol Rep, 2020. 8(20): p. e14601.

4. Discussion

4.1 Hard and soft biomaterials:

Piuma nanoindentation technology has been reported to measure the hardness of tough organs in animals (such as ear [25], bone [24], septum [25], ala nasi [25], articular cartilage [23] and knee joint [22]) and human tissues (like fibrotic intestinal tissue [29], donor cornea [26], particularly calcified aneurysmal abdominal aortas [28], pancreatic acellular scaffolds [30] and soft plates [27]). The feasibility and reliability of this technology in measuring the hardness of soft biomaterials *ex vivo* has not been confirmed. Compared with hard biomaterials, the viscoelasticity and structural complexity of soft biomaterials are more likely to cause deviations in the results of nanoindentation. Our research is the first to use this technique to test the stiffness of vitro soft biological organs in mice, which are often used to simulate human and animal diseases.

Our Bland-Altman plots, ICCs and COVs proved that the stiffness test results of hydrogels have perfect reliability, indicating that the gel can be used as a reference for the quality control of the hardness measurement results. Therefore, through the reliability analysis of other soft tissues, we concluded that nanoindentation technology can work well on these soft biological materials. All in all, we have indeed overcome the possible technical limitations of nanoindentation technology to measure the stiffness of soft organs by selecting the appropriate measurement model and using appropriate methods to prepare samples.

4.2 Reliability in different models and specimens:

Since the results in Bland-Altman plots are qualified, the reliability of the results from kidney, liver, spleen and uterine stiffness in different models can only be verified by comparing COVs and ICCs. Among these four organs, the data of Hertzian model are consistent with the quantitative standards of ICCs and COVs, indicating the results are reliable. Results from JKR or Oliver & Pharr models do not always meet high quality criteria. The reason for the observed differences may depend on the differences in viscosity of the sample in the unloaded state. For example, in the JKR model, even on the same sample, there are some points sticking, while some single indentations are not adhered, as shown in **Figure 2E**, which could increase the difference between the test and the retest. Therefore, our results uncover that the Hertzian model can best calculate the stiffness of the four organs. Remarkably, other researchers chose this model in their

measurements [26-28], while other related studies did not report which model they used [29-30].

Additionally, comparing the uterus results with the other three organs', it reveals that even in the Hertzian model, the COV values of the uterus are 11.6893% in *Eff* and 14.1844% in *E*. These values are very close to the threshold and much higher than the COVs of the other three organs in the Hertzian model, indicating that the variability between repeated measurements of the uterus is higher than that of the spleen, liver and kidney. The most likely reason for these results is that the uterus is thinner and smaller than the other three organs. During the experiment, we noticed that the edges of the uterus were easily rolled up due to its small and size, which is expected to affect the measurement results. Therefore, it is possible that this method is more reliable in measuring the hardness of thick and large soft organs *ex vivo.*

4.3 Limitations of nanoindentation:

In addition to the system operation and measurement strategy, the successful application of nanoindentation also highly depends on factors such as shape, preparation and fixation of tissue. Since the device can only recognize flat and stable surface, it is unable to test irregular tissues. For example, for tissue with marginal barriers, this technology is impossible to test its sunk surface. The lumpy surface affects not only the accuracy of the measurement results, but also damages the cantilever of the probe due to jamming. Furthermore, the calculation of hardness is also affected by the condition of the sample. For instance, if the surface to be measured is inclined, the contact area would not be fully pressed by the tip of the probe, which means that the lost depth and force may cause stiffness measurement errors. Globose organs are also unable to be tested because they cannot be stabilized during the measurement. In short, it is critical that the tested tissue needs to be prepared into an appropriate shape and size.

When the tissue is manually transformed into a testable material, it is unknown whether its elasticity maintains the same characteristics as the original organ, and whether a part of the organ's elasticity can represent its overall elasticity. Therefore, in some cases, in *vivo* testing may be better or even the only option to discover the mechanical properties of organs. However, in *vivo* testing may be interfered and affected by other factors during the measurement process, so it may be an advantage that nanoindenter could directly contact with the target material in measurement.

4.4 Lipids in regulating organ physiology and pathophysiology:

The release of EETs and their diols (DHETs) may affect blood pressure and vascular tone, reduce inflammation and produce pro-fibrinolysis [57-59]. Several recent studies reported EETs activate smooth muscle BK_{Ca} channels [60] and produce vasodilation [61]. It has been speculated that elevated levels of EETs in the body's blood and tissues may also have harmful cardiovascular side effects, such as an increased risk of ischemic stroke [62] and in humans, the recurrence rate of atrial fibrillation after catheter ablation was higher [63], and survival was reduced in mice after cardiac arrest and cardiopulmonary resuscitation [64]. Experimental evidence suggests that inhibition of sEH alters EETs levels, which can prevent the development of atherosclerosis, hypertension, fatty liver, heart failure and organ fibrosis [65].

Both EEQs and EDPs are potent vasodilators [66-69]. EDPs have antiangiogenic [70], anti-fibrotic [71] and protective effect on functional recovery after ischemia, at least by maintaining mitochondrial function and reducing inflammation [72-73].Their diols (DiHDPAs) may also be bioactive and may play a beneficial role in arrhythmias [74]. DiHDPAs dilate coronary microvessels with similar potency to EEQ isomers in canine and porcine models [75] and their inhibition on human platelet aggregation has a low efficacy on EDPs and EEQs [76]. HETEs are involved in many chronic diseases such as cardiovascular disease, inflammation, obesity, cancer and kidney disease [32]. There was a demonstration that a novel omega-3 fatty acid metabolite 19,20-EDP contributes to prevent unilateral ureteral obstruction induced renal fibrosis in mice [71].

Recent findings suggest that EpOMEs exhibit cardio-depressant [77-79] and vasoactive properties [80]. New data also suggest that their diols (DiHOMEs) cause detrimental effects on post-ischemic cardiac function [81-82]. Besides, it has been proved that several DiHOMEs could be potential biomarkers for liver cirrhosis prediction [83].

4.5 Future perspectives:

At present, there is no standardized procedure for nanoindentation of biomaterials. Thus, we are not sure whether it will become an indispensable tool in the biomechanical research of soft organs and tissues. However, with the deepening of research and development of this technology, we hope that it will have a great opportunity to be applied in multiple research fields, such as physiology and pathophysiology of soft organs.

Based on our research and other studies, we can clarify that numerous lipids have significant effects on the physiology and pathophysiology of certain organs. More of their

mechanism of action will be uncovered so that we can use these lipids as regulatory targets for certain diseases to make corresponding animal disease models. And with the support of nanoindenter, the changes in the mechanical properties of specific organs in these disease models would also be well explored.

5. Bibliography

1. M. R. Zile, C. F. Baicu, J. S. Ikonomidis, R. E. Stroud, P. J. Nietert, A. D. Bradshaw, R. Slater, B. M. Palmer, P. Van Buren, M. Meyer, M. M. Redfield, D. A. Bull, H. L. Granzier, and M. M. LeWinter, *Myocardial stiffness in patients with heart failure and a preserved ejection fraction: contributions of collagen and titin.* Circulation, 2015. **131**(14): p. 1247-59.
2. O. Trojnarska, L. Szczepaniak-Chichel, M. Gabriel, A. Bartczak-Rutkowska, J. Rupa-Matysek, A. Tykarski, and S. Grajek, *Arterial stiffness and arterial function in adult cyanotic patients with congenital heart disease.* J Cardiol, 2017. **70**(1): p. 62-67.
3. A. N. Aslan, C. Sari, S. Ozer Sari, O. Tayfur Yurekli, S. Bastug, S. Sivri, O. Ersoy, and E. Bozkurt, *Association between aortic stiffness and left ventricular function in inflammatory bowel disease.* Cardiol J, 2016. **23**(2): p. 202-10.
4. S. Singh, A. Facciorusso, R. Loomba, and Y. T. Falck-Ytter, *Magnitude and Kinetics of Decrease in Liver Stiffness After Antiviral Therapy in Patients With Chronic Hepatitis C: A Systematic Review and Meta-analysis.* Clin Gastroenterol Hepatol, 2018. **16**(1): p. 27-38 e4.
5. F. A. Gonzalez, E. Van den Eynde, S. Perez-Hoyos, J. Navarro, A. Curran, J. Burgos, V. Falco, I. Ocana, E. Ribera, and M. Crespo, *Liver stiffness and aspartate aminotransferase levels predict the risk for liver fibrosis progression in hepatitis C virus/HIV-coinfected patients.* HIV Med, 2015. **16**(4): p. 211-8.
6. M. Briet, E. Bozec, S. Laurent, C. Fassot, G. M. London, C. Jacquot, M. Froissart, P. Houillier, and P. Boutouyrie, *Arterial stiffness and enlargement in mild-to-moderate chronic kidney disease.* Kidney Int, 2006. **69**(2): p. 350-7.
7. E. Kimoto, T. Shoji, K. Shinohara, M. Inaba, Y. Okuno, T. Miki, H. Koyama, M. Emoto, and Y. Nishizawa, *Preferential stiffening of central over peripheral arteries in type 2 diabetes.* Diabetes, 2003. **52**(2): p. 448-52.
8. D. Attia, H. Bantel, H. Lenzen, M. P. Manns, M. J. Gebel, and A. Potthoff, *Liver stiffness measurement using acoustic radiation force impulse elastography in overweight and obese patients.* Aliment Pharmacol Ther, 2016. **44**(4): p. 366-79.
9. M. Endo, Y. Soroida, M. Sato, T. Kobayashi, H. Hikita, M. Sato, H. Gotoh, T. Iwai, S. Sone, T. Sasano, Y. Sumi, K. Koike, Y. Yatomi, and H. Ikeda, *Ultrasound evaluation of liver stiffness: accuracy of ultrasound imaging for the prediction of liver cirrhosis as evaluated using a liver stiffness measurement.* J Med Dent Sci, 2017. **64**(2-3): p. 27-34.
10. L. Grass, N. Szekely, A. Alrajab, T. T. T. Bui-Ta, G. F. Hoffmann, E. Wuhl, and J. P. Schenk, *Point shear wave elastography (pSWE) using Acoustic Radiation Force Impulse (ARFI) imaging: a feasibility study and norm values for renal parenchymal stiffness in healthy children and adolescents.* Med Ultrason, 2017. **19**(4): p. 366-373.
11. G. Low, N. E. Owen, I. Joubert, A. J. Patterson, M. J. Graves, K. J. Glaser, G. J. Alexander, and D. J. Lomas, *Reliability of magnetic resonance elastography using multislice two-dimensional spin-echo echo-planar imaging (SE-EPI) and three-dimensional inversion reconstruction for assessing renal stiffness.* J Magn Reson Imaging, 2015. **42**(3): p. 844-50.
12. A. Pawlus, M. S. Inglot, K. Szymanska, K. Kaczorowski, B. D. Markiewicz, A. Kaczorowska, J. Gasiorowski, A. Szymczak, M. Inglot, J. Bladowska, and U. Zaleska-Dorobisz, *Shear wave elastography of the spleen: evaluation of spleen stiffness in healthy volunteers.* Abdom Radiol (NY), 2016. **41**(11): p. 2169-2174.
13. D. Tokuhara, Y. Cho, and H. Shintaku, *Transient Elastography-Based Liver Stiffness Age-Dependently Increases in Children.* PLoS One, 2016. **11**(11): p. e0166683.

14. D. Wu, E. Chen, T. Liang, M. Wang, B. Chen, B. Lang, and H. Tang, *Predicting the risk of postoperative liver failure and overall survival using liver and spleen stiffness measurements in patients with hepatocellular carcinoma.* Medicine (Baltimore), 2017. **96**(34): p. e7864.

15. C. Yang, M. Yin, K. J. Glaser, X. Zhu, K. Xu, R. L. Ehman, and J. Chen, *Static and dynamic liver stiffness: An ex vivo porcine liver study using MR elastography.* Magn Reson Imaging, 2017. **44**: p. 92-95.

16. M. R. Buckley, J. P. Gleghorn, L. J. Bonassar, and I. Cohen, *Mapping the depth dependence of shear properties in articular cartilage.* J Biomech, 2008. **41**(11): p. 2430-7.

17. D. Cuvelier, I. Derenyi, P. Bassereau, and P. Nassoy, *Coalescence of membrane tethers: experiments, theory, and applications.* Biophys J, 2005. **88**(4): p. 2714-26.

18. K. Hayashi and M. Iwata, *Stiffness of cancer cells measured with an AFM indentation method.* J Mech Behav Biomed Mater, 2015. **49**: p. 105-11.

19. Yuhui Li, Yuan Hong, Guang-Kui Xu, Shaobao Liu, Qiang Shi, Deding Tang, Hui Yang, Guy M. Genin, Tian Jian Lu, and Feng Xu, *Non-contact tensile viscoelastic characterization of microscale biological materials.* Acta Mechanica Sinica, 2018. **34**(3): p. 589-599.

20. D. B. MacManus, M. D. Gilchrist, and J. G. Murphy, *An empirical measure of nonlinear strain for soft tissue indentation.* R Soc Open Sci, 2017. **4**(11): p. 170894.

21. B. Rashid, M. Destrade, and M. D. Gilchrist, *Mechanical characterization of brain tissue in tension at dynamic strain rates.* J Mech Behav Biomed Mater, 2014. **33**: p. 43-54.

22. Parisa R. Moshtagh, Nicoline M. Korthagen, Saskia G. Plomp, Behdad Pouran, Rene M. Castelein, Amir A. Zadpoor, and Harrie Weinans, *Early Signs of Bone and Cartilage Changes Induced by Treadmill Exercise in Rats.* JBMR Plus, 2018. **2**(3): p. 134-142.

23. Parisa R. Moshtagh, Nicoline M. Korthagen, Mattie H. P. van Rijen, Rene M. Castelein, Amir A. Zadpoor, and Harrie Weinans, *Effects of non-enzymatic glycation on the micro- and nano-mechanics of articular cartilage.* Journal of the Mechanical Behavior of Biomedical Materials, 2018. **77**: p. 551-556.

24. Xiaohong Wang, Shunfeng Wang, Feng He, Emad Tolba, Heinz C. Schröder, Bärbel Diehl-Seifert, and Werner E. G. Müller, *Polyphosphate as a Bioactive and Biodegradable Implant Material: Induction of Bone Regeneration in Rats* Advanced Engineering Materials, 2016. **18**(8): p. 1406-1417.

25. E. J. Bos, M. Pluemeekers, M. Helder, N. Kuzmin, K. van der Laan, M. L. Groot, G. van Osch, and P. van Zuijlen, *Structural and Mechanical Comparison of Human Ear, Alar, and Septal Cartilage.* Plast Reconstr Surg Glob Open, 2018. **6**(1): p. e1610.

26. B. S. Shavkuta, M. Y. Gerasimov, N. V. Minaev, D. S. Kuznetsova, V. V. Dudenkova, I. A. Mushkova, B. E. Malyugin, S. L. Kotova, P. S. Timashev, S. V. Kostenev, B. N. Chichkov, and V. N. Bagratashvili, *Highly effective 525 nm femtosecond laser crosslinking of collagen and strengthening of a human donor cornea.* Laser Physics Letters, 2018. **15**(1): p. 015602.

27. A. H. Badreddine, S. Couitt, and C. Kerbage, *Histopathological and biomechanical changes in soft palate in response to non-ablative 9.3-mum CO_2 laser irradiation: an in vivo study.* Lasers Med Sci, 2020.

28. J. P. Meekel, G. Mattei, V. S. Costache, R. Balm, J. D. Blankensteijn, and K. K. Yeung, *A multilayer micromechanical elastic modulus measuring method in ex vivo human aneurysmal abdominal aortas.* Acta Biomater, 2019. **96**: p. 345-353.

29. A. Bokemeyer, P. R. Tepasse, L. Quill, P. Lenz, E. Rijcken, M. Vieth, N. Ding, S. Ketelhut, F. Rieder, B. Kemper, and D. Bettenworth, *Quantitative Phase Imaging Using Digital*

Holographic Microscopy Reliably Assesses Morphology and Reflects Elastic Properties of Fibrotic Intestinal Tissue. Sci Rep, 2019. **9**(1): p. 19388.

30. L. Xu, Y. Huang, D. Wang, S. Zhu, Z. Wang, Y. Yang, and Y. Guo, *Reseeding endothelial cells with fibroblasts to improve the re-endothelialization of pancreatic acellular scaffolds.* J Mater Sci Mater Med, 2019. **30**(7): p. 85.

31. A. A. Spector and H. Y. Kim, *Cytochrome P450 epoxygenase pathway of polyunsaturated fatty acid metabolism.* Biochim Biophys Acta, 2015. **1851**(4): p. 356-65.

32. M. Gabbs, S. Leng, J. G. Devassy, M. Monirujjaman, and H. M. Aukema, *Advances in Our Understanding of Oxylipins Derived from Dietary PUFAs.* Adv Nutr, 2015. **6**(5): p. 513-40.

33. M. A. Nayeem, *Role of oxylipins in cardiovascular diseases.* Acta Pharmacol Sin, 2018. **39**(7): p. 1142-1154.

34. B. E. Tourdot, I. Ahmed, and M. Holinstat, *The emerging role of oxylipins in thrombosis and diabetes.* Front Pharmacol, 2014. **4**: p. 176.

35. W. B. Campbell, D. Gebremedhin, P. F. Pratt, and D. R. Harder, *Identification of epoxyeicosatrienoic acids as endothelium-derived hyperpolarizing factors.* Circ Res, 1996. **78**(3): p. 415-23.

36. M. N. Graber, A. Alfonso, and D. L. Gill, *Recovery of Ca2+ pools and growth in Ca2+ pool-depleted cells is mediated by specific epoxyeicosatrienoic acids derived from arachidonic acid.* J Biol Chem, 1997. **272**(47): p. 29546-53.

37. W. B. Campbell and I. Fleming, *Epoxyeicosatrienoic acids and endothelium-dependent responses.* Pflugers Arch, 2010. **459**(6): p. 881-95.

38. M. Bannehr, L. Lohr, J. Gelep, W. Haverkamp, W. H. Schunck, M. Gollasch, and A. Wutzler, *Linoleic Acid Metabolite DiHOME Decreases Post-ischemic Cardiac Recovery in Murine Hearts.* Cardiovasc Toxicol, 2019. **19**(4): p. 365-371.

39. E. J. Goetzl, *A role for endogenous mono-hydroxy-eicosatetraenoic acids (HETEs) in the regulation of human neutrophil migration.* Immunology, 1980. **40**(4): p. 709-19.

40. F. H. Valone, M. Franklin, F. F. Sun, and E. J. Goetzl, *Alveolar macrophage lipoxygenase products of arachidonic acid: isolation and recognition as the predominant constituents of the neutrophil chemotactic activity elaborated by alveolar macrophages.* Cell Immunol, 1980. **54**(2): p. 390-401.

41. W. F. Stenson and C. W. Parker, *Monohydroxyeicosatetraenoic acids (HETEs) induce degranulation of human neutrophils.* J Immunol, 1980. **124**(5): p. 2100-4.

42. E. E. Gordon, J. A. Gordon, and A. A. Spector, *HETEs and coronary artery endothelial cells: metabolic and functional interactions.* Am J Physiol, 1991. **261**(4 Pt 1): p. C623-33.

43. D. W. Powell and J. I. Saada, *Mesenchymal stem cells and prostaglandins may be critical for intestinal wound repair.* Gastroenterology, 2012. **143**(1): p. 19-22.

44. Y. J. Li, N. Kanaji, X. Q. Wang, T. Sato, M. Nakanishi, M. Kim, J. Michalski, A. J. Nelson, M. Farid, H. Basma, A. Patil, M. L. Toews, X. Liu, and S. I. Rennard, *Prostaglandin E2 switches from a stimulator to an inhibitor of cell migration after epithelial-to-mesenchymal transition.* Prostaglandins Other Lipid Mediat, 2015. **116-117**: p. 1-9.

45. B. Gollasch, G. Wu, I. Dogan, M. Rothe, M. Gollasch, and F. C. Luft, *Effects of hemodialysis on plasma oxylipins.* Physiol Rep, 2020. **8**(12): p. e14447.

46. D. Chavan, T. C. van de Watering, G. Gruca, J. H. Rector, K. Heeck, M. Slaman, and D. Iannuzzi, *Ferrule-top nanoindenter: an optomechanical fiber sensor for nanoindentation.* Rev Sci Instrum, 2012. **83**(11): p. 115110.

47. M. R. VanLandingham, *Review of Instrumented Indentation.* J Res Natl Inst Stand Technol, 2003. **108**(4): p. 249-65.

48. J. Martin Bland and Douglas G. Altman, *Statistical methods for assessing agreement between two methods of clinical measurement.* Lancet, 1986. **1**(8476): p. 307-310.

49. J. M. Bland and D. G. Altman, *Measuring agreement in method comparison studies.* Stat Methods Med Res, 1999. **8**(2): p. 135-60.

50. David C. Lin and Ferenc Horkay, *Nanomechanics of polymer gels and biological tissues: A critical review of analytical approaches in the Hertzian regime and beyond.* Soft Matter, 2008. **4**(4): p. 669.

51. D. C. Lin, D. I. Shreiber, E. K. Dimitriadis, and F. Horkay, *Spherical indentation of soft matter beyond the Hertzian regime: numerical and experimental validation of hyperelastic models.* Biomech Model Mechanobiol, 2009. **8**(5): p. 345-58.

52. D. M. Ebenstein and K. J. Wahl, *A comparison of JKR-based methods to analyze quasi-static and dynamic indentation force curves.* J Colloid Interface Sci, 2006. **298**(2): p. 652-62.

53. W.C. Oliver and G.M. Pharr, *An improved technique for determining hardness and elastic modulus using load and displacement sensing indentation.* Journal of Materials Research, 1992. **7**(06): p. 1564-1583.

54. W.C. Oliver and G.M. Pharr, *Measurement of hardness and elastic modulus by instrumented indentation Advances in understanding and refinements to methodology.* Journal of Materials Research, 2004. **19**(1): p. 3-20.

55. A. P. C. Choi and Y.P. Zheng, *Estimation of Young's modulus and Poisson's ratio of soft tissue from indentation using two different-sized indentors: Finite element analysis of the finite deformation effect.* Medical and Biological Engineering and Computing, 2005. **43**(2): p. 258-264.

56. G. Wu, M. Gotthardt, and M. Gollasch, *Assessment of nanoindentation in stiffness measurement of soft biomaterials: kidney, liver, spleen and uterus.* Sci Rep, 2020. **10**(1): p. 18784.

57. H. Jiang, J. Quilley, A. B. Doumad, A. G. Zhu, J. R. Falck, B. D. Hammock, C. T. Stier, Jr., and M. A. Carroll, *Increases in plasma trans-EETs and blood pressure reduction in spontaneously hypertensive rats.* Am J Physiol Heart Circ Physiol, 2011. **300**(6): p. H1990-6.

58. H. Jiang, G. D. Anderson, and J. C. McGiff, *Red blood cells (RBCs), epoxyeicosatrienoic acids (EETs) and adenosine triphosphate (ATP).* Pharmacol Rep, 2010. **62**(3): p. 468-74.

59. H. Jiang, G. D. Anderson, and J. C. McGiff, *The red blood cell participates in regulation of the circulation by producing and releasing epoxyeicosatrienoic acids.* Prostaglandins Other Lipid Mediat, 2012. **98**(3-4): p. 91-3.

60. T. Lu, P. V. Katakam, M. VanRollins, N. L. Weintraub, A. A. Spector, and H. C. Lee, *Dihydroxyeicosatrienoic acids are potent activators of Ca(2+)-activated K(+) channels in isolated rat coronary arterial myocytes.* J Physiol, 2001. **534**(Pt 3): p. 651-67.

61. H. C. Hercule, W. H. Schunck, V. Gross, J. Seringer, F. P. Leung, S. M. Weldon, ACh da Costa Goncalves, Y. Huang, F. C. Luft, and M. Gollasch, *Interaction between P450 eicosanoids and nitric oxide in the control of arterial tone in mice.* Arterioscler Thromb Vasc Biol, 2009. **29**(1): p. 54-60.

62. A. Gschwendtner, S. Ripke, T. Freilinger, P. Lichtner, B. Muller-Myhsok, H. E. Wichmann, T. Meitinger, and M. Dichgans, *Genetic variation in soluble epoxide hydrolase (EPHX2) is associated with an increased risk of ischemic stroke in white Europeans.* Stroke, 2008. **39**(5): p. 1593-6.

63. A. Wutzler, C. Kestler, A. Perrot, L. Loehr, M. Huemer, A. S. Parwani, P. Attanasio, C. Ozcelik, W. H. Schunck, M. Gollasch, W. Haverkamp, and L. H. Boldt, *Variations in the human soluble epoxide hydrolase gene and recurrence of atrial fibrillation after catheter ablation.* Int J Cardiol, 2013. **168**(4): p. 3647-51.

64. M. P. Hutchens, T. Nakano, J. Dunlap, R. J. Traystman, P. D. Hurn, and N. J. Alkayed, *Soluble epoxide hydrolase gene deletion reduces survival after cardiac arrest and cardiopulmonary resuscitation.* Resuscitation, 2008. **76**(1): p. 89-94.

65. J. He, C. Wang, Y. Zhu, and D. Ai, *Soluble epoxide hydrolase: A potential target for metabolic diseases.* J Diabetes, 2016. **8**(3): p. 305-13.

66. H. C. Hercule, B. Salanova, K. Essin, H. Honeck, J. R. Falck, M. Sausbier, P. Ruth, W. H. Schunck, F. C. Luft, and M. Gollasch, *The vasodilator 17,18-epoxyeicosatetraenoic acid targets the pore-forming BK alpha channel subunit in rodents.* Exp Physiol, 2007. **92**(6): p. 1067-76.

67. B. Lauterbach, E. Barbosa-Sicard, M. H. Wang, H. Honeck, E. Kargel, J. Theuer, M. L. Schwartzman, H. Haller, F. C. Luft, M. Gollasch, and W. H. Schunck, *Cytochrome P450-dependent eicosapentaenoic acid metabolites are novel BK channel activators.* Hypertension, 2002. **39**(2 Pt 2): p. 609-13.

68. A. Ulu, K. S. Stephen Lee, C. Miyabe, J. Yang, B. G. Hammock, H. Dong, and B. D. Hammock, *An omega-3 epoxide of docosahexaenoic acid lowers blood pressure in angiotensin-II-dependent hypertension.* J Cardiovasc Pharmacol, 2014. **64**(1): p. 87-99.

69. C. Morin, S. Fortin, and E. Rousseau, *19,20-EpDPE, a bioactive CYP450 metabolite of DHA monoacyglyceride, decreases Ca(2)(+) sensitivity in human pulmonary arteries.* Am J Physiol Heart Circ Physiol, 2011. **301**(4): p. H1311-8.

70. D. R. McDougle, J. E. Watson, A. A. Abdeen, R. Adili, M. P. Caputo, J. E. Krapf, R. W. Johnson, K. A. Kilian, M. Holinstat, and A. Das, *Anti-inflammatory omega-3 endocannabinoid epoxides.* Proc Natl Acad Sci U S A, 2017. **114**(30): p. E6034-E6043.

71. A. Sharma, M. A. Hye Khan, S. P. Levick, K. S. Lee, B. D. Hammock, and J. D. Imig, *Novel Omega-3 Fatty Acid Epoxygenase Metabolite Reduces Kidney Fibrosis.* Int J Mol Sci, 2016. **17**(5).

72. C. Arnold, M. Markovic, K. Blossey, G. Wallukat, R. Fischer, R. Dechend, A. Konkel, C. von Schacky, F. C. Luft, D. N. Muller, M. Rothe, and W. H. Schunck, *Arachidonic acid-metabolizing cytochrome P450 enzymes are targets of {omega}-3 fatty acids.* J Biol Chem, 2010. **285**(43): p. 32720-33.

73. A. M. Darwesh, K. L. Jamieson, C. Wang, V. Samokhvalov, and J. M. Seubert, *Cardioprotective effects of CYP-derived epoxy metabolites of docosahexaenoic acid involve limiting NLRP3 inflammasome activation (1).* Can J Physiol Pharmacol, 2019. **97**(6): p. 544-556.

74. Y. Zhang, E. Guallar, E. Blasco-Colmenares, A. C. Harms, R. J. Vreeken, T. Hankemeier, G. F. Tomaselli, and A. Cheng, *Serum-Based Oxylipins Are Associated with Outcomes in Primary Prevention Implantable Cardioverter Defibrillator Patients.* PLoS One, 2016. **11**(6): p. e0157035.

75. Y. Zhang, C. L. Oltman, T. Lu, H. C. Lee, K. C. Dellsperger, and M. VanRollins, *EET homologs potently dilate coronary microvessels and activate BK(Ca) channels.* Am J Physiol Heart Circ Physiol, 2001. **280**(6): p. H2430-40.

76. M. VanRollins, *Epoxygenase metabolites of docosahexaenoic and eicosapentaenoic acids inhibit platelet aggregation at concentrations below those affecting thromboxane synthesis.* J Pharmacol Exp Ther, 1995. **274**(2): p. 798-804.

77. M. R. Siegfried, N. Aoki, A. M. Lefer, E. M. Elisseou, and R. E. Zipkin, *Direct cardiovascular actions of two metabolites of linoleic acid.* Life Sci, 1990. **46**(6): p. 427-33.

78. A. Fukushima, M. Hayakawa, S. Sugiyama, M. Ajioka, T. Ito, T. Satake, and T. Ozawa, *Cardiovascular effects of leukotoxin (9, 10-epoxy-12-octadecenoate) and free fatty acids in dogs.* Cardiovasc Res, 1988. **22**(3): p. 213-8.

79. S. Sugiyama, M. Hayakawa, S. Nagai, M. Ajioka, and T. Ozawa, *Leukotoxin, 9, 10-epoxy-12-octadecenoate, causes cardiac failure in dogs.* Life Sci, 1987. **40**(3): p. 225-31.

80. S. Okamura, S. Ameshima, Y. Demura, T. Ishizaki, S. Matsukawa, and I. Miyamori, *Leukotoxin-activated human pulmonary artery endothelial cell produces nitric oxide and superoxide anion.* Pulm Pharmacol Ther, 2002. **15**(1): p. 25-33.

81. K. R. Chaudhary, B. N. Zordoky, M. L. Edin, N. Alsaleh, A. O. El-Kadi, D. C. Zeldin, and J. M. Seubert, *Differential effects of soluble epoxide hydrolase inhibition and CYP2J2 overexpression on postischemic cardiac function in aged mice.* Prostaglandins Other Lipid Mediat, 2013. **104-105**: p. 8-17.

82. M. Bannehr, L. Lohr, J. Gelep, W. Haverkamp, W. H. Schunck, M. Gollasch, and A. Wutzler, *Linoleic Acid Metabolite DiHOME Decreases Post-ischemic Cardiac Recovery in Murine Hearts.* Cardiovasc Toxicol, 2019.

83. Yonghai Lu, Jinling Fang, Li Zou, Liang Cui, Xu Liang, Seng Gee Lim, Yock-Young Dan, and Choon Nam Ong, *Omega-6-derived oxylipin changes in serum of patients with hepatitis B virus-related liver diseases.* Metabolomics, 2018. **14**(3).

6. Detailed account of my contribution to the publications:

Guanlin Wu contributed the following to the below listed publications:

Publication 1: **G. Wu,** M. Gotthardt, and M. Gollasch, Assessment of nanoindentation in stiffness measurement of soft biomaterials: kidney, liver, spleen and uterus. Sci Rep, 2020. 10(1): p. 18784.

Contribution: Research plan design, organ collection and preparation, nanoindentation measurements, data analysis, figures drawing, tables forming, first draft of manuscript writing. Figure 1 was created based on my drawing and experiment. Figures 2, 3, 4, 5, 6 and tables 1, 2, 3, 4, 5 were created based on my statistical calculations. In other words, the contents of work described in "**2.1 Animals and Matrigen hydrogels**", "**2.2 Tissues preparation**", "**2.3 Nanoindentation and stiffness determination**", "**3.1 Stiffness determination in different models**" and "**3.2 Stiffness reliability of Matrigen hydrogels and organs**" of the synopsis were all done independently by me. Specifically, **figures 2, 3** and **tables 1, 2, 3, 4, 5** cited from the publication were created based on my statistical calculations.

Publication 2: B. Gollasch, **G. Wu**, I. Dogan, M. Rothe, M. Gollasch, and F. C. Luft, Effects of hemodialysis on plasma oxylipins. Physiol Rep, 2020. 8(12): p. e14447.

Contribution: Data analysis, discussion of data and contribution to writing. Tables 3 and 5 were created based on my statistical calculations. Some results, particularly the conversion ratios of lipids and their diols, in "**3.3 Lipids in CKD**" and "**3.4 Lipids in hemodialysis**" of the synopsis were analyzed by me.

Publication 3: B. Gollasch, **G. Wu**, T. Liu, I. Dogan, M. Rothe, M. Gollasch, and F. C. Luft, Hemodialysis and erythrocyte epoxy fatty acids. Physiol Rep, 2020. 8(20): p. e14601.

Contribution: Data analysis, discussion of data and contribution to writing. Tables 2 and 4 were created based on my statistical calculations. Some results, particularly the conversion ratios of lipids and their diols, in "**3.3 Lipids in CKD**" and "**3.4 Lipids in hemodialysis**" of the synopsis were analyzed by me.

7. Statutory Declaration

"I, Guanlin Wu, by personally signing this document in lieu of an oath, hereby affirm that I prepared the submitted dissertation on the topic Determination of soft biomaterials stiffness and potentially associated target lipids (Bestimmung der Steifheit weicher Biomaterialien und potenziell assoziierter Ziellipide), independently and without the support of third parties, and that I used no other sources and aids than those stated.
All parts which are based on the publications or presentations of other authors, either in letter or in spirit, are specified as such in accordance with the citing guidelines. The sections on methodology (in particular regarding practical work, laboratory regulations, statistical processing) and results (in particular regarding figures, charts and tables) are exclusively my responsibility.

[In the case of having conducted your doctoral research project completely or in part within a working group:] Furthermore, I declare that I have correctly marked all of the data, the analyses, and the conclusions generated from data obtained in collaboration with other persons, and that I have correctly marked my own contribution and the contributions of other persons (cf. declaration of contribution). I have correctly marked all texts or parts of texts that were generated in collaboration with other persons.

My contributions to any publications to this dissertation correspond to those stated in the below joint declaration made together with the supervisor. All publications created within the scope of the dissertation comply with the guidelines of the ICMJE (International Committee of Medical Journal Editors; www.icmje.org) on authorship. In addition, I declare that I shall comply with the regulations of Charité – Universitätsmedizin Berlin on ensuring good scientific practice.

I declare that I have not yet submitted this dissertation in identical or similar form to another Faculty.

The significance of this statutory declaration and the consequences of a false statutory declaration under criminal law (Sections 156, 161 of the German Criminal Code) are known to me."

Date   Signature

8. Declaration of your own contribution to the publications

Guanlin Wu contributed the following to the below listed publications:

Publication 1: **G. Wu,** M. Gotthardt, and M. Gollasch, Assessment of nanoindentation in stiffness measurement of soft biomaterials: kidney, liver, spleen and uterus. Sci Rep, 2020. 10(1): p. 18784. **Impact Factor (2019): 3.998**

Contribution (please set out in detail): Research plan design, organ collection and preparation, nanoindentation measurements, data analysis, figures drawing, tables forming, first draft of manuscript writing. Figure 1 was created based on my drawing and experiment. Figures 2, 3, 4, 5, 6 and tables 1, 2, 3, 4, 5 were created based on my statistical calculations.

Publication 2: B. Gollasch, **G. Wu**, I. Dogan, M. Rothe, M. Gollasch, and F. C. Luft, Effects of hemodialysis on plasma oxylipins. Physiol Rep, 2020. 8(12): p. e14447.

Contribution (please set out in detail): Data analysis, discussion of data and contribution to writing. Tables 3 and 5 were created based on my statistical calculations.

Publication 3: B. Gollasch, **G. Wu**, T. Liu, I. Dogan, M. Rothe, M. Gollasch, and F. C. Luft, Hemodialysis and erythrocyte epoxy fatty acids. Physiol Rep, 2020. 8(20): p. e14601.

Contribution (please set out in detail): Data analysis, discussion of data and contribution to writing. Tables 2 and 4 were created based on my statistical calculations.

_____

Signature, date and stamp of first supervising university professor / lecturer

_____

Signature of doctoral candidate

9. Selected Publications

9.1 Publication #1

Assessment of nanoindentation in stiffness measurement of soft biomaterials: kidney, liver, spleen and uterus.

G. Wu, M. Gotthardt, and M. Gollasch, Assessment of nanoindentation in stiffness measurement of soft biomaterials: kidney, liver, spleen and uterus. Sci Rep, 2020. 10(1): p. 18784. **Impact Factor (2019): 3.998**

Journal Data Filtered By: **Selected JCR Year: 2019** Selected Editions: SCIE,SSCI
Selected Categories: **"MULTIDISCIPLINARY SCIENCES"** Selected Category
Scheme: WoS
Gesamtanzahl: 71 Journale

Rank	Full Journal Title	Total Cites	Journal Impact Factor	Eigenfactor Score
1	NATURE	767,209	42.778	1.216730
2	SCIENCE	699,842	41.845	1.022660
3	National Science Review	2,775	16.693	0.009760
4	Science Advances	36,380	13.116	0.172060
5	Nature Human Behaviour	2,457	12.282	0.014190
6	Nature Communications	312,599	12.121	1.259510
7	Science Bulletin	5,172	9.511	0.014150
8	PROCEEDINGS OF THE NATIONAL ACADEMY OF SCIENCES OF THE UNITED STATES OF AMERICA	676,425	9.412	0.931890
9	Journal of Advanced Research	3,564	6.992	0.005470
10	GigaScience	4,068	5.993	0.016410
11	Scientific Data	5,761	5.541	0.028720
12	Research Synthesis Methods	2,572	5.299	0.006440
13	ANNALS OF THE NEW YORK ACADEMY OF SCIENCES	45,596	4.728	0.026370
14	FRACTALS-COMPLEX GEOMETRY PATTERNS AND SCALING IN NATURE AND SOCIETY	2,156	4.536	0.002210
15	iScience	1,410	4.447	0.004140
16	GLOBAL CHALLENGES	481	4.306	0.001440
17	Scientific Reports	386,848	3.998	1.231180
18	JOURNAL OF KING SAUD UNIVERSITY SCIENCE	1,640	3.819	0.002020
19	Journal of the Royal Society Interface	13,762	3.748	0.027670

Publication Ⅰ

scientific reports

OPEN

Assessment of nanoindentation in stiffness measurement of soft biomaterials: kidney, liver, spleen and uterus

Guanlin Wu[1,2]✉, Michael Gotthardt[1,3,6] & Maik Gollasch[2,4,5,6]✉

Nanoindentation technology with high spatial resolution and force sensitivity is widely used to measure the mechanical properties of hard biomaterials and tissues. However, its reliability to analyze soft biomaterials and organs has not been tested. Here, we evaluated the utility of nanoindentation to measure the passive mechanical properties of soft biological specimen. Kidney, liver, spleen and uterus samples were harvested from C57BL/6 N mice. We assessed test–retest repeatability in biological specimen and hydrogel controls using Bland–Altman diagrams, intraclass correlation coefficients (ICCs) and the within-subject coefficients of variation (COVs). The results were calculated using Hertzian, JKR and Oliver & Pharr models. Similar to hydrogels, Bland–Altman plots of all biological specimen showed good reliability in stiffness test and retest examinations. In gels, ICCs were larger than 0.8 and COVs were smaller than 15% in all three models. In kidney, liver, spleen and uterus, ICCs were consistently larger than 0.8 only in the Hertzian model but not in the JKR and Oliver & Pharr models. Similarly, COVs were consistently smaller than 15% in kidney, liver, spleen and uterus only in the Hertzian model but not in the other models. We conclude that nanoindentation technology is feasible in detecting the stiffness of kidney, liver, spleen and uterus. The Hertzian model is the preferred method to provide reliable results on ex vivo organ stiffness of the biological specimen under study.

Abbreviations
E_{ff}	Effective Young's modulus
E	Young's modulus
ICC	Intraclass Correlation Coefficient
CI	Confidence Interval
COV	Within-subject coefficient of variation

Several diseases lead to changes in stiffness in certain organs, which could give rise to illnesses. Potentially, there is also a possibility that a variation of stiffness in tissue or cells influences the function or structure in other organs in the body. For example, patients with heart failure and a preserved ejection fraction can exhibit increases in passive myocardial stiffness[1]. Cyanotic patients with congenital heart diseases are often characterized by increased arterial stiffness in comparison with healthy population[2]. There is a direct relationship between aortic stiffness and left ventricular systolic and diastolic dysfunction in patients with inflammatory bowel disease[3]. Eradication of hepatitis C virus infection causes a significant decline in liver stiffness -particularly in patients with high base-line level of inflammation or patients who received direct-acting antiviral agents[4,5]. Increased arterial stiffness can occur in parallel with the decline of glomerular filtration rate in patients with mild-to-moderate chronic kidney disease[6]. Type 2 diabetes had greater impact on pulse wave velocity of the central arteries than peripheral

[1]Max Delbrück Center for Molecular Medicine (MDC) in the Helmholtz Association, Robert-Rössle-Straße 10, 13125 Berlin, Germany. [2]Experimental and Clinical Research Center (ECRC), Charité–Universitätsmedizin Berlin, Berlin, Germany. [3]German Center for Cardiovascular Research (DZHK), Partner Site Berlin, Berlin, Germany. [4]Department of Internal and Geriatric Medicine, University of Greifswald, University District Hospital Wolgast, Greifswald, Germany. [5]Medical Clinic of Nephrology and Internal Intensive Care, Charité Universitätsmedizin Berlin, Berlin, Germany. [6]These authors jointly supervised this work: Michael Gotthardt and Maik Gollasch. ✉email: wuguanlin105109@gmail.com; maik.gollasch@charite.de

Publication I
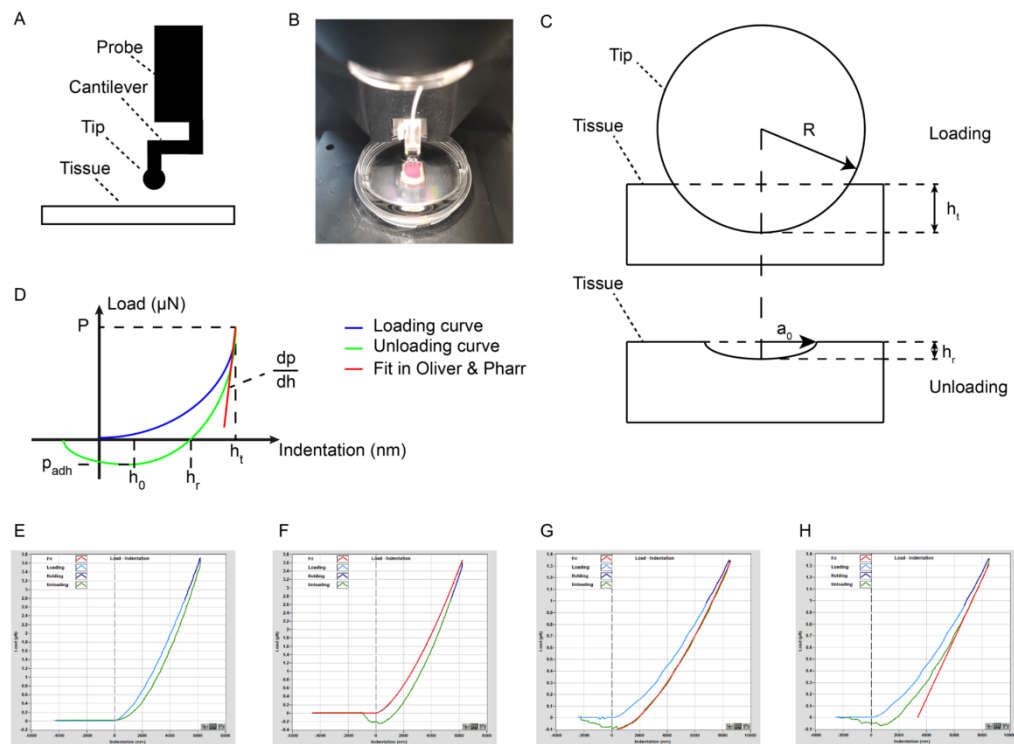
Figure 1. Principle of effective Young's modulus calculation. (**A**) Details of probe and relationship between the probe and tissue. (**B**) The probe of nanoindenter was focused on an appropriate area of tissue. (**C**) Schematic diagram of indentation from loading to unloading. (**D**) Load-indentation schematic diagram. (**E**) Schematic diagram of non-adhesion indentation. (**F**) Schematic diagram of indentation in Hertzian model with 100% fit. (**G**) Schematic diagram of indentation in JKR model with 100% fit. (**H**) Schematic diagram of indentation in Oliver & Pharr model with 65–85% fit.

arteries[7]. In clinical settings, a number of various techniques have been introduced to detect changes in stiffness of human organs, such as transient elastography, ultrasonography, acoustic radiation force impulse elastography, point shear wave elastography and magnetic resonance elastography[8–15], which are helpful and meaningful in diagnosis of organ fibrosis. Presently, a variety of testing techniques have been developed and utilized widespread from bulk scale to the micro/nano-scale for characterizing some biomaterials *ex vivo*[16–21]. Piuma nanoindenter is one of these technologies to be used to study elastic property of biomaterials. This technique has been widely used to test passive mechanical properties of hard biosamples, such as bone and cartilage[22–26]. However, so far there are only very few studies[27–31] which used the Nanoindentation technology to study organ stiffness of soft biomaterials, such as the kidney, liver, spleen and uterus samples. There is uncertainty on suitable ways in analyzing ex vivo organ stiffness by this technique.

Results
Hertzian, JKR and Oliver & Pharr models. We applied Hertzian, JKR and Oliver & Pharr models based on the following considerations. The calculation of the effective Young's modulus (*Eff*) by considering the Hertzian contact model[36,37], follows the fit of the loading curve (Fig. 1F) to the following equation:

$$Eff = \frac{P * 3/4}{\sqrt{R} \cdot h_t^{3/2}}$$

where P is the load in the peak of fit, R means the tip radius and h_t represents the indentation depth (Fig. 1C,D).

The JKR model[38] is often used for analysis of elastic adhesive materials and could allow a better estimation of *Eff* in the presence of adhesion forces which changes the contact area (Fig. 1G). However, if the unloading part shows no sticky character, it is expected that there would be no reliable result from this model (Fig. 1E). The equation used for the fitting is:

2

Publication Ⅰ

37

$$h_t - h_0 = \frac{a_0^2}{R}\left(\frac{1 + \sqrt{1 - \frac{P}{P_{adh}}}}{2}\right)^{\frac{4}{3}} - \frac{2}{3}\frac{a_0^2}{R}\left(\frac{1 + \sqrt{1 - \frac{P}{P_{adh}}}}{2}\right)^{\frac{1}{3}}$$

$$P_{adh} = -\frac{3}{2}\pi\,\Delta r R$$

$$Eff = \frac{9\pi R^2 \Delta r}{2a_0^3}$$

where h_t is indentation depth, h_0 means the contact point, a_0 represents the contact radius at zero load, R is the tip radius of the indenter, P is the load and P_{adh} is the pull-off force (minimum load), Δr means work of adhesion. h_0 and a_0 are fitting parameters (Fig. 1D).

For elastoplastic materials, the unloading part of the curve is often fitted by the so-called Oliver & Pharr model[39,40], which may exclude plasticity bias. This method derives the *Eff* from the slope of the unloading part of the stress–strain curve, indenter tip radius and final indentation depth using the following formula:

$$Eff = \frac{dP}{dh}\frac{1}{2\sqrt{R(h_t + h_r)}}$$

where $\frac{dP}{dh}$ is the slope at maximum indentation, R is the radius of the spherical indenter tip, h_t and h_r represent maximum indentation depth and final contact depth (Fig. 1C,D,H). In this study, the fits were set as 100%, 100% and 65–85% in Hertzian model, JKR model and Oliver & Pharr model, respectively. Poisson's ratio[41] ν relates effective Young's modulus (*Eff*) and Young's modulus (*E*) by the following equation:

$$Eff = \frac{E}{1 - \nu^2}$$

Except *Eff*, in all models the Piuma software also enabled to directly calculate *E*, for which a Poisson's ratio of 0.5 was pre-defined (for perfect incompressible materials). We determined both *Eff* and *E* for each biomaterial because the material property of tissues and the Poisson's ratios are unknown.

Stiffness of matrigen hydrogels and organs. Bland–Altman plots of Matrigen hydrogels showed mean stiffness differences in all measurements (Fig. 2). There was only one difference (spot) out of the 95% limits of agreement (− 1.96 SD to 1.96 SD) in the Hertzian model for both *Eff* and *E* (Fig. 2A,D). Differences in the other models were within the SD range (Fig. 2B,C,E,F). ICC values were larger than 0.8 and COVs were smaller than 15% in all models (Table 1), which demonstrates that all three models provide reliable results on gel specimen.

In the kidney, the Bland–Altman plots show that there was only one difference out of the 95% limits of agreement for *E* in JKR model, for *Eff* in the Oliver & Pharr model and for *E* in the Oliver & Pharr model (Fig. 3E,G,H). The differences in the other models were all within the SD range (Fig. 3C,D,F). Of note, the ICC value was larger than 0.8 and the COV was smaller than 15% only in the Hertzian model but not in the other models (Table 2).

In the liver, the Bland–Altman plots uncovered mean stiffness differences between test and retest data. Except for *Eff* in the Hertzian model and *E* in the JKR model, there were no differences out of the 95% limits of agreement (Fig. 4C-H). The ICC values of *E* and *Eff* exceeded 0.8 consistently only in the Hertzian model but not Oliver & Pharr and JKR models. The COV values were smaller than 15% in the Hertzian and Oliver & Pharr models but not in the JKR model (Table 3).

In the spleen, the Bland–Altman plots showed that the average stiffness differences of test–retest data were within the SD range in the JKR model. There was only one difference result out of the scope in the Hertzian and Oliver & Pharr models (Fig. 5C-H). The ICC values of *E* and *Eff* were consistently larger than 0.8 in the Hertzian and JKR models but not in the Oliver & Pharr model. The COVs of the *E* and *Eff* values were smaller than 15% in Hertzian but not in the other models (Table 4).

In uterus, Bland–Altman plots revealed only one difference out of the 95% limits of agreement between indentations in both the Hertzian and JKR models (Fig. 6D,E,G,H) but not in Oliver & Pharr model (Fig. 6F,I). ICC values were larger than 0.8 in Hertzian and Oliver & Pharr models but not JKR model. In contrast, COVs were smaller than 15% only in Hertzian model but not other models (Table 5).

Discussion

Piuma nanoindentation technology has been widely used in research on biomaterial stiffness of hard animal organs, for example in bone[25], in ear, ala nasi, and septum on both the cellular and the extracellular matrix (ECM) levels[24,26], in the knee joint[22], in articular cartilage[23]. Other examples are human donor cornea[27], fibrotic intestinal tissue[30], pancreatic acellular scaffolds[31], soft plates[28] and particularly calcified aneurysmal abdominal aortas[29]. The feasibility and reliability of this technology in measuring the stiffness of soft biological materials, particularly organs ex vivo, is unknown. Compared with hard biomaterials, certain properties of soft biomaterials, such as viscoelasticity and adhesion, are more prone to deviations in nanoindentation. Our study is the first to use this technology to test the stiffness of soft biological organs ex vivo, particularly from mice, which are widely used for modeling human and animal diseases. We applied the Piuma nanoindentation technology, which is easy to use and utilizes a specific probe to measure Young's Moduli to match with the specific sample properties
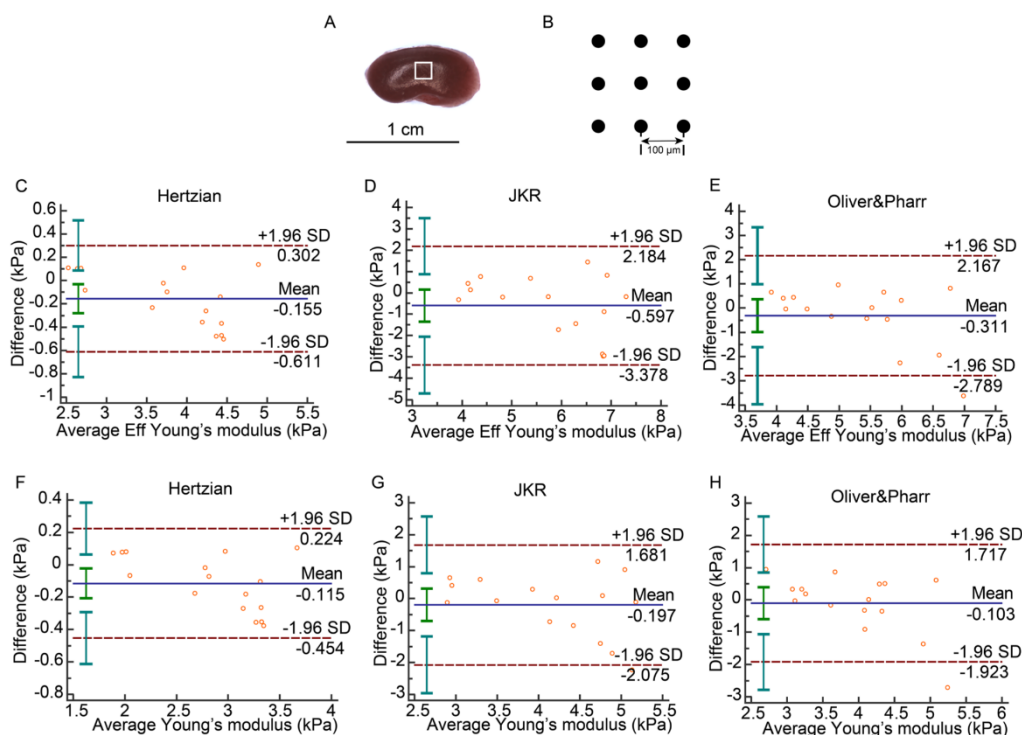
Publication I

38
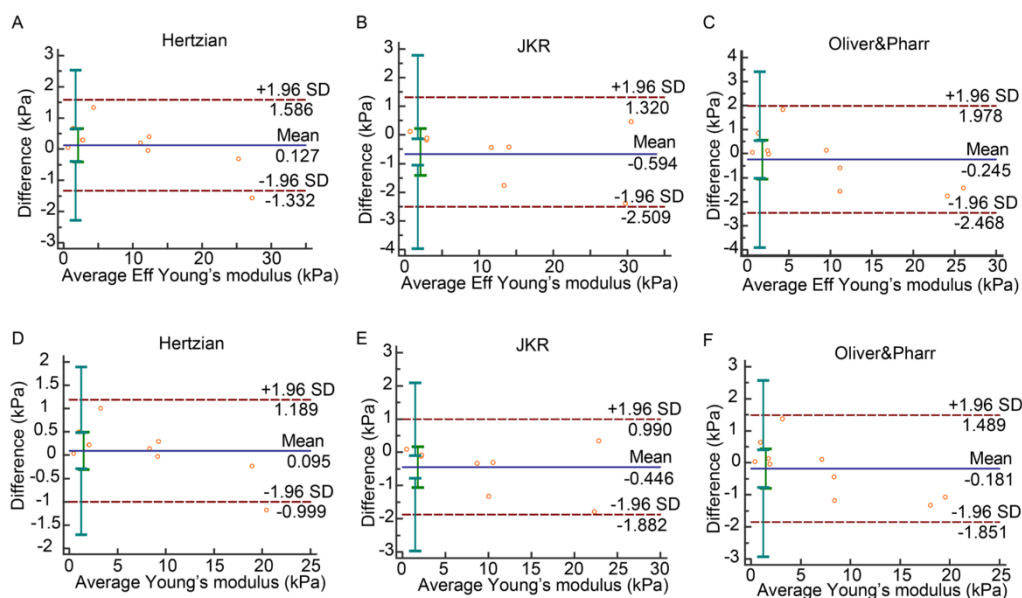
Figure 2. Bland–Altman plot of Matrigen hydogels. (**A**) Bland–Altman plot of *Eff* in Hertzian model. (**B**) Bland–Altman plot of *Eff* in JKR model. (**C**) Bland–Altman plot of *Eff* in Oliver & Pharr model. (**D**) Bland–Altman plot of *E* in Hertzian model. (**E**) Bland–Altman plot of *E* in JKR model. (**F**) Bland–Altman plot of *E* in Oliver & Pharr model.

	Bland–Altman, 95% limits of agreement (kPa)	ICC, 95% CI	COV (%)
Eff in Hertzian	0.127 (−1.332,1.586)	**0.9986 (0.9948,0.9997)**	5.0666
Eff in JKR	−0.594 (−2.509,1.320)	**0.9978 (0.9900,0.9996)**	5.8171
Eff in Oliver & Pharr	−0.245 (−2.468,1.978)	**0.9964 (0.9865, 0.9991)**	8.3703
E in Hertzian	0.095 (−0.999,1.189)	**0.9986 (0.9948,0.9997)**	5.0665
E in JKR	−0.446 (−1.882,0.990)	**0.9978 (0.9900,0.9996)**	5.8171
E in Oliver & Pharr	−0.181 (−1.851,1.489)	**0.9964 (0.9865,0.9991)**	8.3787

Table 1. Reliability of test–retest in Matrigen gels. Values that are in the range of good reliability are in bold.

of the tissue[42–44]. Different tissue contains different mechanical properties, therefore, different protocols should be applied in tissues with some special characterizations[45]. Since there is no way to judge the feature of tested samples before an experiment, we analyzed both the loading and unloading parts for their elastic behavior detection. In addition to the operation of the system and the development of measurement strategies, the preparation and fixation of tissue is expected to be important. An irregular tissue is impossible to be tested as the device only recognizes flat and stable surfaces, and the calculation of stiffness would be affected by the condition of sample. For example, if the tested surface is a slope (Supplement 1, Fig 1A), the contacted area would not be fully indented by the tip of probe, which means the losing depth and force could led to a mistake in stiffness measurement. A globose organ (Supplement 1 Fig 1B) is also untestable because it cannot be stabilized during the process of measurement. Furthermore, it is impossible for this technology to test a sunk surface (Supplement 1 Fig 1C) due to the obstacle at the edge of the tissue. A lumpy surface (Supplement 1 Fig 1D) would not only affect the accuracy of the measurement results but also cause the probe cantilever to be damaged due to jamming. Together, the tested tissue needs to be prepared testable in an appropriate shape and size. We did overcome these possible limitations for the feasibility and reliability of the nanoindentation technology to measure soft organ stiffness by using isolated kidneys, liver, spleen and uterus dissected in an appropriate manner. We confirmed the feasibility and reliability of the results by a comparative study of this technology to Matrigen hydrogels. Matrigen hydrogels at a given stiffness, stable shape, appropriate thickness and flat surface were taken as a quality control, although their given stiffness is not considered golden-standard. Nevertheless, our Bland–Altman plots, ICCs and COVs demonstrated a good reliability of the gels used. Therefore, we conclude that nanoindentation technology works well and is reliable in our laboratory settings and on this material.

Publication Ⅰ

Figure 3. Renal indentation strategy and Bland–Altman plot. (**A**) Half of kidney was chopped from the middle line of side. White frame was the scan area on the tissue. (**B**) Sample was indented 9 times (3×3 matrix) in a 200×200 μm grid scan with 100 μm distance between measurements. (**C**) Bland–Altman of *Eff* in Hertzian model. (**D**) Bland–Altman plot of *Eff* in JKR model. (**E**) Bland–Altman plot of *Eff* in Oliver & Pharr model. (**F**) Bland–Altman plot of *E* in Hertzian model. (**G**) Bland–Altman plot of *E* in JKR model. (**H**) Bland–Altman plot of *E* in Oliver & Pharr model.

	Bland–Altman, 95% limits of agreement (kPa)	ICC, 95% CI	COV (%)
Eff in Hertzian	−0.155 (−0.611,0.302)	**0.9686 (0.9124,0.9889)**	5.0723
Eff in JKR	−0.597 (−3.378,2.184)	0.5951 (−0.1287,0.8572)	18.2387
Eff in Oliver & Pharr	−0.311 (−2.789,2.167)	0.5929 (−0.1347,0.8565)	16.6833
E in Hertzian	−0.115 (−0.454,0.224)	**0.9693 (0.9143,0.9892)**	5.0194
E in JKR	−0.197 (−2.075,1.680)	0.6699 (0.0797,0.8836)	16.0643
E in Oliver & Pharr	−0.103 (−1.923,1.717)	0.6422 (0.0026,0.8738)	16.2013

Table 2. Reliability of test–retest in kidney. Values that are in the range of good reliability are in bold.

We next tested the technology in measuring the stiffness of four organs ex vivo, namely the kidney, liver, spleen and uterus. Although the Bland–Altman plots did not give us numerous out-of-qualification results, the reliability of the results from the four organs hardness in different models can only be validated by comparing the ICCs and COVs. In the four organs, all Hertzian model's results followed the quantified criteria of ICCs and COVs showed reliable results. The results in JKR or Oliver & Pharr models did not always meet the high quality criteria. The reason for the observed differences may rely on differences between specimens in stickiness under unloading state.

For example, in the JKR model, even on the same sample, some spots are sticky, while some single indentations show no adhesion, as shown in Fig. 1E, which would increase the variation between test and retest. Thus, our results show that the hardness of the four organs under study is best calculated using the Hertzian model under forced indentation. Of note, this model has been used by others researchers who utilized the nanoindentation

5

Publication Ⅰ

40
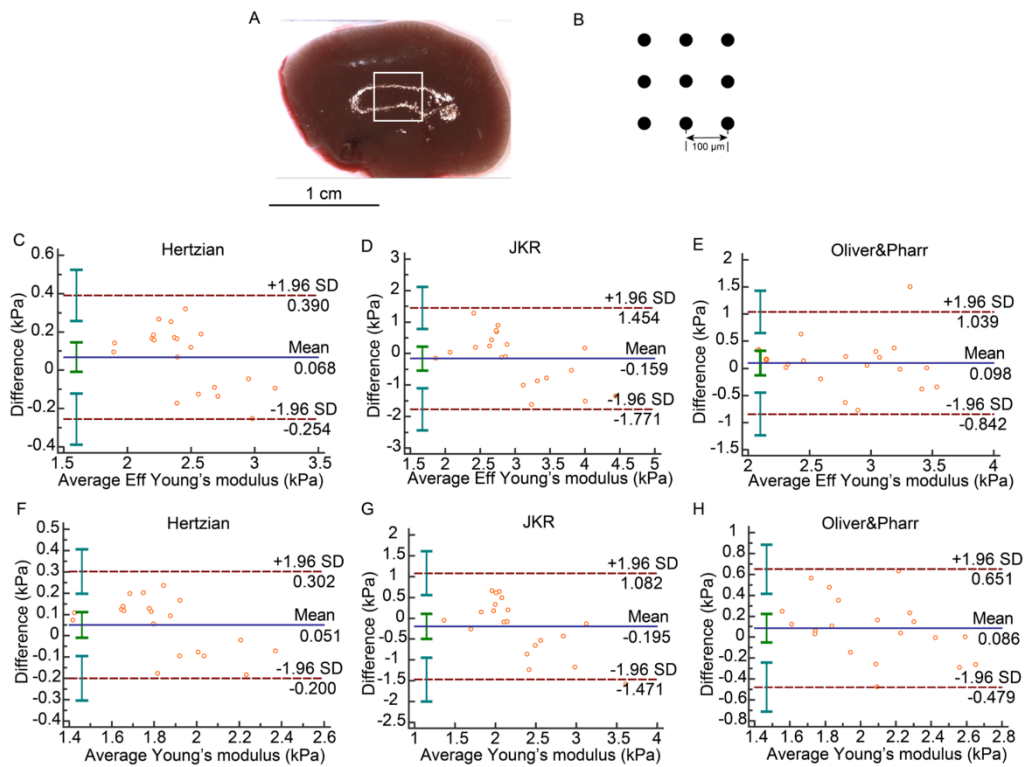
Figure 4. Hepatic indentation strategy and Bland–Altman plot. (**A**) A piece of liver was harvested from the left lobe. White frame was the scan area on the tissue. (**B**) Sample was indented 9 times (3 × 3 matrix) in a 200 × 200 μm grid scan with 100 μm distance between measurements. (**C**) Bland–Altman plot of *Eff* in Hertzian model. (**D**) Bland–Altman pot of Eff in JKR model. (**E**) Bland–Altman plot of *Eff* in Oliver & Pharr model. (**F**) Bland–Altman plot of *E* in Hertzian model. (**G**) Bland–Altman plot of *E* in JKR model. (**H**) Bland–Altman plot of *E* in Oliver & Pharr model.

	Bland–Altman, 95% limits of agreement (kPa)	ICC, 95% CI	COV (%)
Eff in Hertzian	0.679 (−0.254,0.390)	**0.9303 (0.8269,0.9722)**	**5.0091**
Eff in JKR	−0.159 (−1.771,1.454)	0.6240 (0.0667,0.8501)	19.1874
Eff in Oliver & Pharr	0.098 (−0.842,1.039)	0.7507 (0.3811,0.9006)	**12.0356**
E in Hertzian	0.051 (−0.200,0.302)	**0.9251 (0.8142,0.9702)**	**5.1724**
E in JKR	−0.195 (−1.472,1.082)	0.6078 (0.0265,0.8437)	20.5038
E in Oliver & Pharr	0.086 (−0.479,0.651)	**0.8048 (0.5155,0.9222)**	**10.0323**

Table 3. Reliability of test–retest in liver. Values that are in the range of good reliability are in bold.

technology in their studies[27–29], while other studies did not report the model used[30,31]. In addition, comparing the results of the uterus with the three other organs, we found that even in the Hertzian mode, the COV value of the uterus is 11.6893% in the case of calculating the hardness according to *Eff* and 14.1841% in the case of calculating the stiffness according to *E*, which were very close to the threshold and much higher than the COV values of the other three organs in the Hertzian model. This indicates that the variability between repeated measurements of the uterus is greater than that of the liver, kidney and spleen. A possible reason is that the uterus is smaller and thinner than the other three organs, and in the course of the experiment, we found that the edge of the smaller and thinner organ uterus was more likely to be rolled up causing a similar situation shown in Supplement 1 Fig 1B, which is expected to affect the results of the measurements. Therefore, the reliability of the method is better in relatively large and thick soft organs ex vivo.

Publication Ⅰ

41
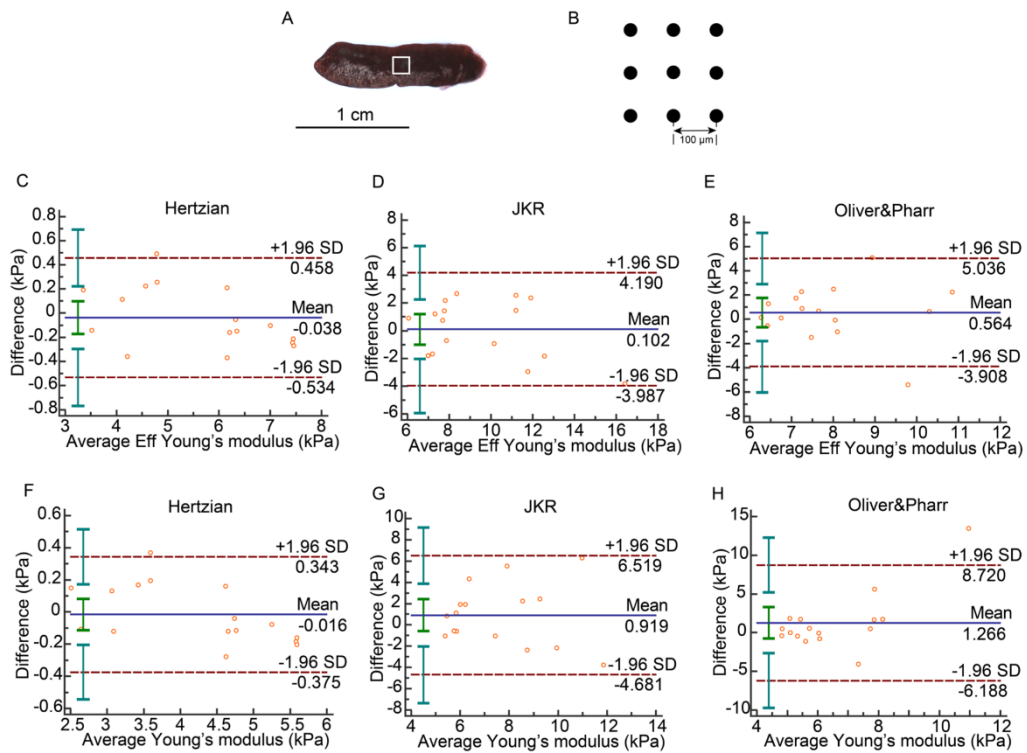
Figure 5. Splenic indentation strategy and Bland–Altman plot. (**A**) An intact spleen of mouse. White frame was the scan area on the tissue. (**B**) Sample was indented 9 times (3×3 matrix) in a 200×200 μm grid scan with 100 μm distance between measurements. (**C**) Bland–Altman plot of *Eff* in Hertzian model. (**D**) Bland–Altman of *Eff* in JKR model. (**E**) Bland–Altman plot of *Eff* in Oliver & Pharr model. (**F**) Bland–Altman plot of *E* in Hertzian model. (**G**) Bland–Altman plot of *E* in JKR model. (**H**) Bland–Altman plot of *E* in Oliver & Pharr model.

	Bland–Altman, 95% limits of agreement (kPa)	ICC, 95% CI	COV (%)
Eff in Hertzian	−0.038 (−0.534,0.458)	**0.9924 (0.9787,0.9973)**	**3.1172**
Eff in JKR	0.102 (−3.987,4.190)	**0.8675 (0.6307,0.9533)**	15.0115
Eff in Oliver & Pharr	0.564 (−3.908,5.036)	0.3334 (−0.8583,0.7649)	20.3557
E in Hertzian	−0.016 (−0.375,0.343)	**0.9931 (0.9807,0.9976)**	**2.9890**
E in JKR	0.919 (−4.681,6.519)	0.5113 (−0.3622,0.8277)	27.1063
E in Oliver & Pharr	1.266 (−6.188,8.720)	−0.3404 (−2.7364,0.5274)	42.3569

Table 4. Reliability of test–retest in spleen. Values that are in the range of good reliability are in bold.

Moreover, the successful application of nanoindentation is highly depended on material features such as the shape of the tissue being measured; measurement of biological materials with complicated rough surface tends to be difficult. When a tissue is manually transformed into a material that can be tested, it is unknown that whether its elasticity keeps the same property as the elasticity of the original organ, and whether part of the elasticity of the organ can represent its overall elasticity. Accordingly, for certain organ studies, in vivo testing may be a better or sometimes even the only option to provide detailed insights into the organ's mechanical properties. However, in vivo tests are likely interfered and affected by other factors during the measurement process, so perhaps it is an advantage that the nanoindenter can be directly contacted with the target material for measurement. At present, there are more limitations and shortcomings in the application of this technology. For example, its validity and authenticity still need to be further verified, and the standardized routine for biomaterial nanoindentation has

Publication Ⅰ
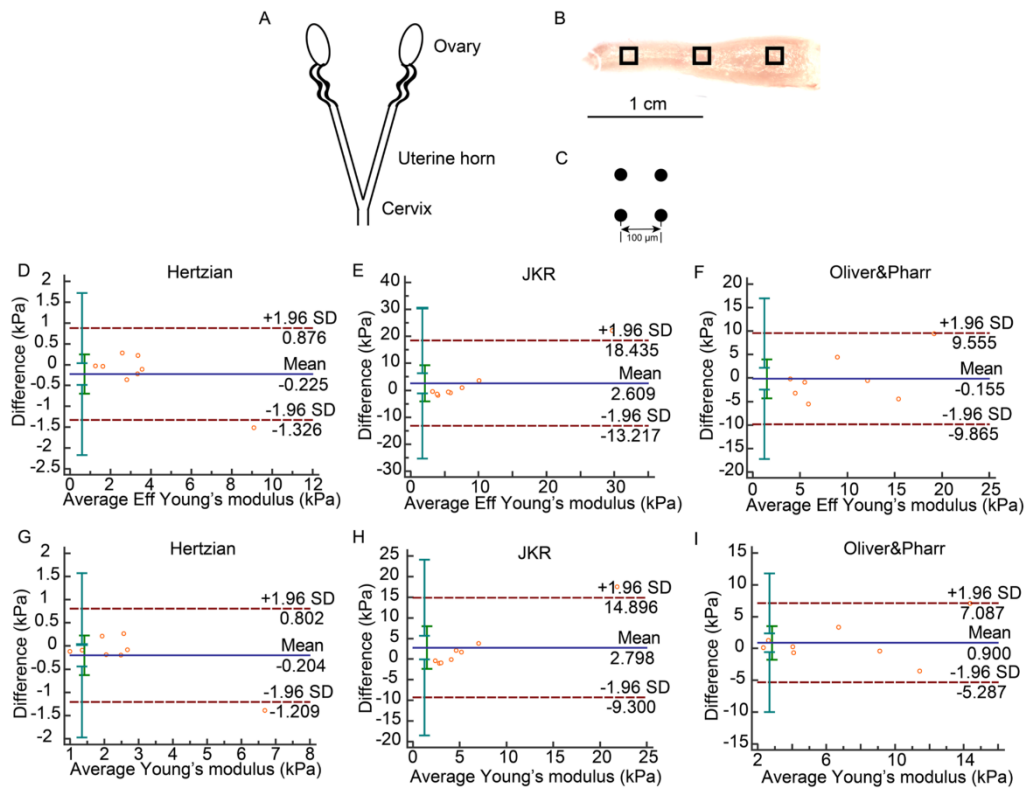
Figure 6. Uterine indentation strategy and Bland–Altman plot. (**A**) Schematic diagram of mouse whole uterus. (**B**) Opened left uterus horn. Black frames were three scan areas located on proximal, middle and distal parts, respectively. (**C**) In each scan, there were four indentation spots with 100 μm distance between measurements in a 100×100 μm square. (**D**) Bland–Altman plot of *Eff* in Hertzian model. (**E**) Bland–Altman plot of *Eff* in JKR model. (**F**) Bland–Altman plot of *Eff* in Oliver & Pharr model. (**G**) Bland–Altman plot of *E* in Hertzian model. (**H**) Bland–Altman plot of *E* in JKR model. (**I**) Bland–Altman plot of *E* in Oliver & Pharr model.

	Bland–Altman, 95% limits of agreement (kPa)	ICC, 95% CI	COV (%)
Eff in Hertzian	−0.225 (−1.326,0.876)	**0.9861 (0.9371,0.9972)**	**11.6893**
Eff in JKR	2.609 (−13.217,18.435)	0.7926 (0.0607,0.9577)	64.4623
Eff in Oliver & Pharr	−0.155 (−9.865,9.555)	**0.8295 (0.2278,0.9652)**	34.7149
E in Hertzian	−0.204 (−1.209,0.802)	**0.9780 (0.9002,0.9955)**	**14.1841**
E in JKR	2.798 (−9.300,14.896)	0.7512 (−0.1267,0.9492)	71.0078
E in Oliver & Pharr	0.900 (−5.287,7.087)	**0.8778 (0.4465,0.9751)**	31.8501

Table 5. Reliability of test–retest in uterus. Values that are in the range of good reliability are in bold.

not yet been established. Therefore, we cannot be certainly sure whether it will become an indispensable tool in the research of mechanical biology and biomechanics of soft organs and tissues. However, as the research and development of this technology is going more and more in-depth, we expect it will have great opportunities to be applied to research in multiple fields such as physiology and pathology of soft organs.

Publication Ⅰ

Conclusion

Piuma nanoindentation technology is an easy and feasible method to test the stiffness of ex vivo organs, such as kidney, liver, spleen and uterus. In small and thin tissues with disorder surface, we expect that the variation of results will increase. The Hertzian model is the most reliable method to measure the passive mechanical property of soft organs and biomaterials ex vivo. JKR and Oliver & Pharr models did not thoroughly provide reliable results.

Materials and methods

Animals. Kidneys, liver and spleen were dissected from 5 week-, 10 week-, 20 week- and 30 week-old C57BL/6 N mice. For kidneys and spleen, 2 mice of each sex and age were used. For liver, 2 to 4 mice of each sex and age were used. For uterus, eight mice were used, all these mice were around 100 days old. The experiments were approved by the regulations of local animal care committee (LAGeSo, Berlin, Germany) and the animal welfare officers of the Max Delbrück Center for Molecular Medicine (MDC) (No. X 9011/19).

Matrigen hydrogels. Hydrogels with different stiffness (1 kPa, 2 kPa, 4 kPa, 8 kPa, 12 kPa and 25 kPa) were purchased from Softwell, Matrigen, Matrigen Life Technologies, Brea, CA and used for quality control (1 kPa, 2 kPa, 4 kPa, 8 kPa, 12 kPa and 25 kPa; N = 1 to 3).

Preparation of tissues. Left and right kidneys were respectively divided into two from the middle line of side (Fig. 3A), the four parts were all taken into indentation. Liver samples were taken from left lobe (Fig. 4A). Spleens were whole harvested for usage in the experiments (Fig. 5A). Left uterus horn was selected and opened (Fig. 6A,B). All organs were cleaned with removal of visible blood, fat, membrane or vessels on the surface of organs, but avoiding damage the parenchyma of them. To obtain a flat surface, we pasted all samples to the bottom of 4 cm diameter petri-dishes with Shellac (Sigma) so that the outer surface was leveled. Tissue samples were immersed in PBS (NaCl 0.137 M, KCl 0.0027 M, Na_2HPO_4 0.01 M, KH_2PO_4 0.0018 M; pH 7.4).

Nanoindentation. To determine elastic properties, we used a displacement-controlled nanoindenter instrument (Piuma; Optics11, Amsterdam, The Netherlands). The device utilizes a ferrule-top cantilever probe[32,33] to apply load and simultaneously measure indentation depth using a fiber optic based readout (Fig. 1A). We used a spherical probe with a radius of 50 μm and a cantilever stiffness of 0.5 N/m. Cantilever bending calibrations were performed before each series of experiments by indenting a rigid surface and equating cantilever bending to probe displacement. Afterwards, the probe was focused on an appropriate area on tissue surface (Figs. 1B, 3A, 4A, 5A, 6B). Each gel was indented 25 times (5 × 5 matrix) in an 800 × 800 μm grid scan with 200 μm distance between measurements. Kidney, liver and spleen samples were indented with 9 indentations (3 × 3 matrix) in a 200 × 200 μm grid scan (Figs. 3B, 4B, 5B). In uterus, three indentation matrixes with 4 single indentations in 100 × 100 μm grid were tested in proximal, middle and distal parts of uterus, respectively (Fig. 6B,C). The applied indentation protocol was composed of a loading phase for 4 s at 8000 nm indentation depth, which was held for one second, and then an unloading phase for 4 s. All scans were done twice for the analysis of reliability. The average of all the results in the four sections from left and right kidneys was presented as renal elasticity. The stiffness of gel, liver and spleen was expressed as the mean value of all results in each scan. Three scans results' average was taken as uterine hardness. All single indentation values were calculated by Piuma Dataviewer version 2.2 (Piuma; Optics11, Amsterdam, The Netherlands).

Bland–Altman plots and coefficients. Bland–Altman plots (a graphical method to plot the difference scores of two measurements against the mean for each subject)[34,35], intraclass correlation coefficients (ICCs) and within-subject coefficient of variations (COVs) were used to analyze the reliability of test–retest results. If the difference value of test–retest results is between 95% limits of agreement in the Bland–Altman plots, it means the reliability is good. If the value of ICC is greater than 0.8, there is good reliability between the measurement and re-measurements. If COVs are smaller than 15%, it is considerable that the test–retest result is reliable.

All analyses were performed using SPSS 19.0 (Chicago, USA), GraphPad Prism 7.0 (San Diego, USA) or MedCalc 19.3 software (Belgium).

Ethics approval and consent to participate. The usage of mice was abided by the regulations of local animal care committee (LAGeSo, Berlin, Germany) and the animal welfare officers of the Max Delbrück Center for Molecular Medicine (MDC) (No. X 9011/16). There are no ethical concerns.

Data availability

The data and protocol can be obtained by contacting Michael Gotthardt.

References

1. Zile, M. R. *et al.* Myocardial stiffness in patients with heart failure and a preserved ejection fraction: contributions of collagen and titin. *Circulation* **131**, 1247–1259. https://doi.org/10.1161/CIRCULATIONAHA.114.013215 (2015).
2. Trojnarska, O. *et al.* Arterial stiffness and arterial function in adult cyanotic patients with congenital heart disease. *J. Cardiol.* **70**, 62–67. https://doi.org/10.1016/j.jjcc.2016.09.003 (2017).

Publication Ⅰ

3. Aslan, A. N. *et al.* Association between aortic stiffness and left ventricular function in inflammatory bowel disease. *Cardiol. J.* **23**, 202–210. https://doi.org/10.5603/CJ.a2016.0008 (2016).
4. Singh, S., Facciorusso, A., Loomba, R. & Falck-Ytter, Y. T. Magnitude and Kinetics of Decrease in Liver Stiffness After Antiviral Therapy in Patients With Chronic Hepatitis C: A Systematic Review and Meta-analysis. *Clin. Gastroenterol. Hepatol. Off. Clin. Pract. J. Am. Gastroenterol. Assoc.* **16**, 27–38. https://doi.org/10.1016/j.cgh.2017.04.038 (2018).
5. Gonzalez, F. A. *et al.* Liver stiffness and aspartate aminotransferase levels predict the risk for liver fibrosis progression in hepatitis C virus/HIV-coinfected patients. *HIV Med.* **16**, 211–218. https://doi.org/10.1111/hiv.12197 (2015).
6. Briet, M. *et al.* Arterial stiffness and enlargement in mild-to-moderate chronic kidney disease. *Kidney Int.* **69**, 350–357. https://doi.org/10.1038/sj.ki.5000047 (2006).
7. Kimoto, E. *et al.* Preferential stiffening of central over peripheral arteries in type 2 diabetes. *Diabetes* **52**, 448–452. https://doi.org/10.2337/diabetes.52.2.448 (2003).
8. Attia, D. *et al.* Liver stiffness measurement using acoustic radiation force impulse elastography in overweight and obese patients. *Aliment. Pharmacol. Ther.* **44**, 366–379. https://doi.org/10.1111/apt.13710 (2016).
9. Endo, M. *et al.* Ultrasound evaluation of liver stiffness: accuracy of ultrasound imaging for the prediction of liver cirrhosis as evaluated using a liver stiffness measurement. *J. Med. Dent. Sci.* **64**, 27–34. https://doi.org/10.11480/jmds.640301 (2017).
10. Grass, L. *et al.* Point shear wave elastography (pSWE) using Acoustic Radiation Force Impulse (ARFI) imaging: a feasibility study and norm values for renal parenchymal stiffness in healthy children and adolescents. *Med. Ultrasonogr.* **19**, 366–373. https://doi.org/10.11152/mu-1078 (2017).
11. Low, G. *et al.* Reliability of magnetic resonance elastography using multislice two-dimensional spin-echo echo-planar imaging (SE-EPI) and three-dimensional inversion reconstruction for assessing renal stiffness. *J. Magnet. Reson. Imaging JMRI* **42**, 844–850. https://doi.org/10.1002/jmri.24826 (2015).
12. Pawlus, A. *et al.* Shear wave elastography of the spleen: evaluation of spleen stiffness in healthy volunteers. *Abdom. Radiol.* **41**, 2169–2174. https://doi.org/10.1007/s00261-016-0834-4 (2016).
13. Tokuhara, D., Cho, Y. & Shintaku, H. Transient elastography-based liver stiffness age-dependently increases in children. *PLoS ONE* **11**, e0166683. https://doi.org/10.1371/journal.pone.0166683 (2016).
14. Wu, D. *et al.* Predicting the risk of postoperative liver failure and overall survival using liver and spleen stiffness measurements in patients with hepatocellular carcinoma. *Medicine* **96**, e7864. https://doi.org/10.1097/MD.0000000000007864 (2017).
15. Yang, C. *et al.* Static and dynamic liver stiffness: An ex vivo porcine liver study using MR elastography. *Magn. Reson. Imaging* **44**, 92–95. https://doi.org/10.1016/j.mri.2017.08.009 (2017).
16. Buckley, M. R., Gleghorn, J. P., Bonassar, L. J. & Cohen, I. Mapping the depth dependence of shear properties in articular cartilage. *J. Biomech.* **41**, 2430–2437. https://doi.org/10.1016/j.jbiomech.2008.05.021 (2008).
17. Cuvelier, D., Derenyi, I., Bassereau, P. & Nassoy, P. Coalescence of membrane tethers: experiments, theory, and applications. *Biophys. J* . **88**, 2714–2726. https://doi.org/10.1529/biophysj.104.056473 (2005).
18. Hayashi, K. & Iwata, M. Stiffness of cancer cells measured with an AFM indentation method. *J. Mech. Behav. Biomed. Mater.* **49**, 105–111. https://doi.org/10.1016/j.jmbbm.2015.04.030 (2015).
19. Li, Y. *et al.* Non-contact tensile viscoelastic characterization of microscale biological materials. *Acta. Mech. Sin.* **34**, 589–599. https://doi.org/10.1007/s10409-017-0740-1 (2018).
20. MacManus, D. B., Gilchrist, M. D. & Murphy, J. G. An empirical measure of nonlinear strain for soft tissue indentation. *R. Soc. Open Sci.* **4**, 170894. https://doi.org/10.1098/rsos.170894 (2017).
21. Rashid, B., Destrade, M. & Gilchrist, M. D. Mechanical characterization of brain tissue in tension at dynamic strain rates. *J. Mech. Behav. Biomed. Mater.* **33**, 43–54. https://doi.org/10.1016/j.jmbbm.2012.07.015 (2014).
22. Moshtagh, P. R. *et al.* Early signs of bone and cartilage changes induced by treadmill exercise in rats. *JBMR Plus* **2**, 134–142. https://doi.org/10.1002/jbm4.10029 (2018).
23. Moshtagh, P. R. *et al.* Effects of non-enzymatic glycation on the micro- and nano-mechanics of articular cartilage. *J. Mech. Behav. Biomed. Mater.* **77**, 551–556. https://doi.org/10.1016/j.jmbbm.2017.09.035 (2018).
24. Bos, E. J. *et al.* Noninvasive measurement of ear cartilage elasticity on the cellular level: a new method to provide biomechanical information for tissue engineering. *Plast. Reconstr. Surg. Glob. Open* **5**, e1147. https://doi.org/10.1097/GOX.0000000000001147 (2017).
25. Wang, X. *et al.* Polyphosphate as a bioactive and biodegradable implant material: induction of bone regeneration in rats. *Adv. Eng. Mater.* **18**, 1406–1417. https://doi.org/10.1002/adem.201600057 (2016).
26. Bos, E. J. *et al.* Structural and mechanical comparison of human ear, alar, and septal cartilage. *Plast. Reconstr. Surg. Glob. Open* **6**, e1610. https://doi.org/10.1097/GOX.0000000000001610 (2018).
27. Shavkuta, B. S. *et al.* Highly effective 525 nm femtosecond laser crosslinking of collagen and strengthening of a human donor cornea. *Laser Phys. Lett.* **15**, 015602. https://doi.org/10.1088/1612-202X/aa963b (2018).
28. Badreddine, A. H., Couitt, S. & Kerbage, C. Histopathological and biomechanical changes in soft palate in response to non-ablative 93-mum CO2 laser irradiation: an in vivo study. *Lasers Med. Sci.* https://doi.org/10.1007/s10103-020-03087-y (2020).
29. Meekel, J. P. *et al.* A multilayer micromechanical elastic modulus measuring method in ex vivo human aneurysmal abdominal aortas. *Acta Biomater.* **96**, 345–353. https://doi.org/10.1016/j.actbio.2019.07.019 (2019).
30. Bokemeyer, A. *et al.* Quantitative phase imaging using digital holographic microscopy reliably assesses morphology and reflects elastic properties of fibrotic intestinal tissue. *Sci. Rep.* **9**, 19388. https://doi.org/10.1038/s41598-019-56045-2 (2019).
31. Xu, L. *et al.* Reseeding endothelial cells with fibroblasts to improve the re-endothelialization of pancreatic acellular scaffolds. *J. Mater. Sci. Mater. Med.* **30**, 85. https://doi.org/10.1007/s10856-019-6287-x (2019).
32. Chavan, D. *et al.* Ferrule-top nanoindenter: an optomechanical fiber sensor for nanoindentation. *Rev. Sci. Instrum.* **83**, 115110. https://doi.org/10.1063/1.4766959 (2012).
33. VanLandingham, M. R. Review of Instrumented Indentation. *J. Res. Nat. Inst. Stand. Technol.* **108**, 249–265. https://doi.org/10.6028/jres.108.024 (2003).
34. Bland, J. M. & Altman, D. G. Statistical methods for assessing agreement between two methods of clinical measurement. *Lancet* **1**, 307–310 (1986).
35. Bland, J. M. & Altman, D. G. Measuring agreement in method comparison studies. *Stat. Methods Med. Res.* **8**, 135–160. https://doi.org/10.1177/096228029900800204 (1999).
36. Lin, D. C. & Horkay, F. Nanomechanics of polymer gels and biological tissues: a critical review of analytical approaches in the Hertzian regime and beyond. *Soft Matter* **4**, 669. https://doi.org/10.1039/b714637j (2008).
37. Lin, D. C., Shreiber, D. I., Dimitriadis, E. K. & Horkay, F. Spherical indentation of soft matter beyond the Hertzian regime: numerical and experimental validation of hyperelastic models. *Biomech. Model. Mechanobiol.* **8**, 345–358. https://doi.org/10.1007/s10237-008-0139-9 (2009).
38. Ebenstein, D. M. & Wahl, K. J. A comparison of JKR-based methods to analyze quasi-static and dynamic indentation force curves. *J. Colloid Interface Sci.* **298**, 652–662. https://doi.org/10.1016/j.jcis.2005.12.062 (2006).
39. Oliver, W. C. & Pharr, G. M. An improved technique for determining hardness and elastic modulus using load and displacement sensing indentation. *J. Mater. Res.* **7**, 1564–1583 (1992).
40. Oliver, W. C. & Pharr, G. M. Measurement of hardness and elastic modulus by instrumented indentation Advances in understanding and refinements to methodology. *J. Mater. Res.* **19**, 3–20 (2004).

Publication Ⅰ

45

41. Choi, A. P. C. & Zheng, Y. P. Estimation of Young's modulus and Poisson's ratio of soft tissue from indentation using two different-sized indentors: Finite element analysis of the finite deformation effect. *Med. Biol. Eng. Comput.* **43**, 258–264 (2005).
42. Chen, W., Li, M., Zhang, T., Cheng, Y.-T. & Cheng, C.-M. Influence of indenter tip roundness on hardness behavior in nanoindentation. *Mater. Sci. Eng. A* **445–446**, 323–327. https://doi.org/10.1016/j.msea.2006.09.050 (2007).
43. Shih, C. W., Yang, M. & Li, J. C. M. Effect of tip radius on nanoindentation. *J. Mater. Res.* **6**, 2623–2628 (1991).
44. Tang, B. & Ngan, A. H. W. Accurate measurement of tip–sample contact size during nanoindentation of viscoelastic materials. *J. Mater. Res.* **18**, 1141–1148. https://doi.org/10.1557/jmr.2003.0156 (2011).
45. Cheng, Y.-T. & Cheng, C.-M. Relationships between initial unloading slope, contact depth, and mechanical properties for spherical indentation in linear viscoelastic solids. *Mater. Sci. Eng. A* **409**, 93–99. https://doi.org/10.1016/j.msea.2005.05.118 (2005).

Competing interests

The authors declare no competing interests.

Additional information

Supplementary information is available for this paper at https://doi.org/10.1038/s41598-020-75738-7.

Correspondence and requests for materials should be addressed to G.W. and M.Gol.

Reprints and permissions information is available at www.nature.com/reprints.

Publisher's note Springer Nature remains neutral with regard to jurisdictional claims in published maps and institutional affiliations.

Publication I

9.2 Publication #2

Effects of hemodialysis on plasma oxylipins.

B. Gollasch, **G. Wu**, I. Dogan, M. Rothe, M. Gollasch, and F. C. Luft, Effects of hemodialysis on plasma oxylipins. Physiol Rep, 2020. 8(12): p. e14447.

Not included in SCIE and SSCI.

Physiological Reports is a peer-reviewed open access online only scientific journal covering original research in all areas of physiology. It is published by Wiley-Blackwell on behalf of The Physiological Society and the American Physiological Society.

ORIGINAL RESEARCH

The Physiological Society | american physiological society | **Physiological** Reports

Effects of hemodialysis on plasma oxylipins

Benjamin Gollasch[1,2] [ID] | Guanlin Wu[1,3] | Inci Dogan[4] | Michael Rothe[4] | Maik Gollasch[1,5] | Friedrich C. Luft[1]

[1]Experimental and Clinical Research Center (ECRC), a joint institution between the Charité University Medicine and Max Delbrück Center (MDC) for Molecular Medicine, Berlin-Buch, Germany

[2]HELIOS Klinikum Berlin-Buch, Berlin, Germany

[3]Max Delbrück Center for Molecular Medicine (MDC) in the Helmholtz Association, Berlin, Germany

[4]LIPIDOMIX GmbH, Berlin, Germany

[5]Department of Geriatrics, University of Greifswald, University District Hospital Wolgast, Greifswald, Germany

Correspondence
Benjamin Gollasch, Experimental and Clinical Research Center (ECRC), Lindenberger Weg 80, 13125 Berlin, Germany.
Email: benjamin.gollasch@charite.de

Abstract

Chronic kidney disease (CKD) is an important risk factor for cardiovascular and all-cause mortality. Survival rates among end-stage renal disease (ESRD) hemodialysis patients are poor and most deaths are related to cardiovascular disease. Oxylipins constitute a family of oxygenated natural products, formed from fatty acid by pathways involving at least one step of dioxygen-dependent oxidation. They are derived from polyunsaturated fatty acids (PUFAs) by cyclooxygenase (COX) enzymes, by lipoxygenases (LOX) enzymes, or by cytochrome P450 epoxygenase. Oxylipins have physiological significance and some could be of regulatory importance. The effects of decreased renal function and dialysis treatment on oxylipin metabolism are unknown. We studied 15 healthy persons and 15 CKD patients undergoing regular hemodialysis treatments and measured oxylipins (HPLC-MS lipidomics) derived from cytochrome P450 (CYP) monooxygenase and lipoxygenase (LOX)/CYP ω/(ω-1)-hydroxylase pathways in circulating blood. We found that all four subclasses of CYP epoxy metabolites were increased after the dialysis treatment. Rather than resulting from altered soluble epoxide hydrolase (sEH) activity, the oxylipins were released and accumulated in the circulation. Furthermore, hemodialysis did not change the majority of LOX/CYP ω/(ω-1)-hydroxylase metabolites. Our data support the idea that oxylipin profiles discriminate ESRD patients from normal controls and are influenced by renal replacement therapies.

KEYWORDS
dialysis, eicosanoids, fatty acids, lipidomics, oxylipins

1 | INTRODUCTION

Chronic kidney disease (CKD) is an important risk factor for cardiovascular and all-cause mortality. The 5-year survival rate among end-stage renal disease (ESRD) hemodialysis patients is nearly 50% (McGill, 2019) and most of these deaths are related to cardiovascular disease (CVD), making ESRD a catastrophic risk factor (Luft, 2000). Conceivably, the hemodialysis treatment per se has a counterproductive effect on cardiovascular risk. Oxylipins are a superclass of lipid mediators with potent biological activities. They are derived from the oxidation of polyunsaturated fatty acids (PUFA). In addition to the well-known eicosanoids derived from arachidonic acid (C20:4 n–6, AA), recent developments in lipidomics methodologies have raised awareness of, and interest in, the many hitherto unknown oxylipins. These products include octadecanoids derived from

Publication Ⅱ

linoleic acid (C18:2 n–6, LA) and α-linolenic acid (C18:3 n–3, ALA), eicosanoids derived from dihomo-γ-linolenic acid (C20:3 n–6), eicosapentanoic acid (C20:5 n–3, EPA), and docosanoids derived from adrenic acid (C22:4 n–6, AdA) or docosahexaenoic acid (22:6 n–3, DHA) (Gabbs, 2015). Oxylipins are primarily produced via the cytochromes P450 (CYP) monooxygenase, cyclooxygenase (COX), and lipoxygenase (LOX)/ CYP ω/(ω-1)-hydroxylase pathways (Figure 1), resulting in the formation of mono-, di-, and trihydroxy fatty acids, epoxy fatty acids, prostaglandins, thromboxanes, lipoxins, resolvins, and maresin (Gabbs, 2015). Epoxyoctadecenoic acids (EpOMEs), epoxyeicosatrienoic acids (EETs), epoxyeicosatetraenoic acids (EEQs), and epoxydocosapentaenoic acids (EDPs) represent the principal subclasses of CYP epoxygenase products. The primary metabolic fate of EETs (Figure 1), EpOMEs, EEQs, and EDPs in many cells is conversion into DHETs, DiHOMEs, DiHETEs, and DiHDPAs by the soluble epoxide hydrolase enzyme (sEH) (Spector, 2004).
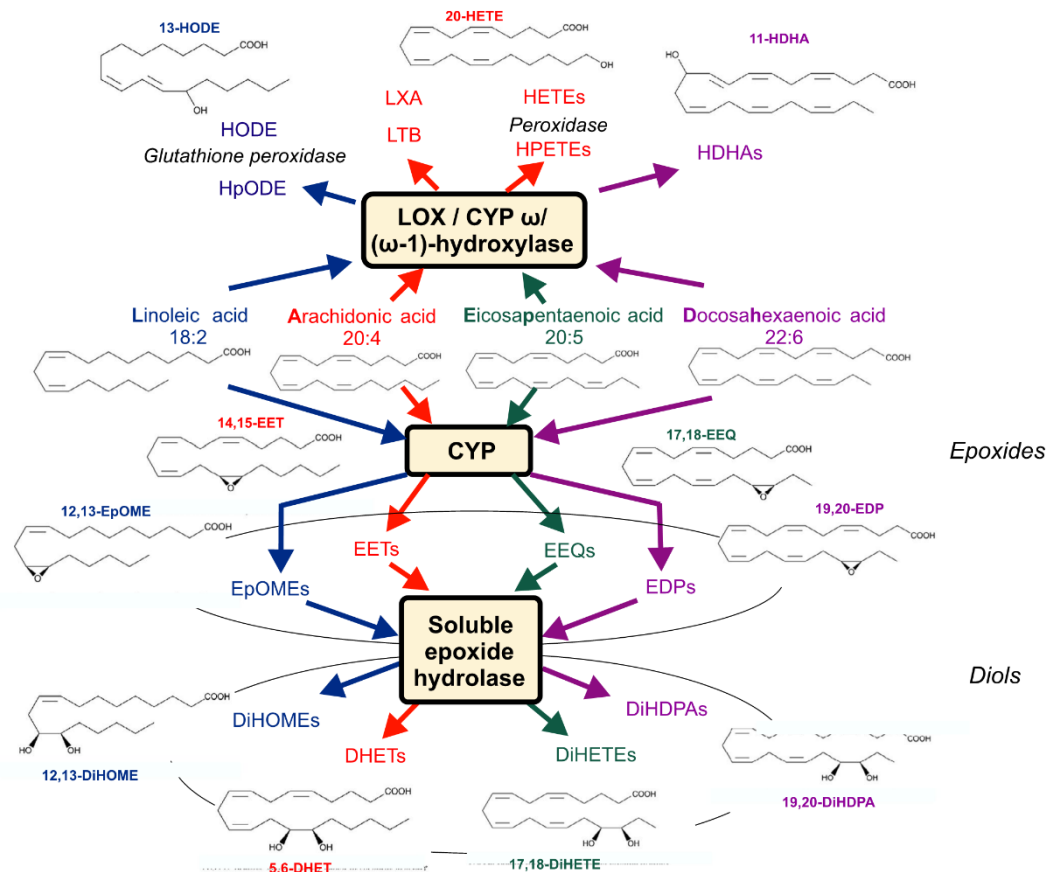
FIGURE 1 Cytochrome P450 epoxygenase (CYP) and 12- and 15-lipoxygenase (LOX)/ CYP (omega-1)-hydroxylase pathways evaluated in response hemodialysis. Linoleic (LA), arachidonic (AA), eicosapentaenoic (EPA), and docosahexaenoic acids (DHA) are converted to epoxyoctadecenoic acids (EpOMEs, e.g., 12,13-EpOME), epoxyeicosatrienoic acid (EETs), epoxyeicosatetraenoic acids (EEQs), and epoxydocosapentaenoic acids (EDPs) by CYP epoxygenase, respectively. EpOMEs, EETs, EEQs, and EDPs primary metabolic fate is conversion to dihydroxyctadecenoic acids (DiHOMEs, e.g., 12, 13-DiHOME), dihydroxyeicosatrienoic acids (DHETs, e.g., 5,6-DHET), dihydroxyeicosatetraenoic acids (DiHETEs, e.g., 5,6-DiHETE, 17,18-DiHETE) and dihydroxydocosapentaenoic acids (DiHDPAs, 19, 20-DiHDPA), respectively, by the soluble epoxide hydrolase (sEH) enzyme. LA, AA, EPA, and DHA are converted to hydroperoxylinoleic acids (HpODEs), hydroxyoctadecadienoic acids (HODEs), leukotriene B (LTB), lipoxin A (LXA), hydroxydocosahexaenoic acids (HDHAs), hydroperoxyeicosatetraenoic acids (HPETEs), and hydroxyeicosatetraenoic acids (HETEs) by LOX, CYP omega/(omega-1)-hydroxylase and peroxidase pathways. The metabolites measured within these pathways track the changes observed in LA, AA, EPA, and DHA, respectively

Publication Ⅱ

Oxylipins are not only important in normal physiology, but can also have detrimental effects (for review see (Gabbs, 2015; Nayeem, 2018; Tourdot, Ahmed, & Holinstat, 2014)). They could exhibit either beneficial or harmful cardiovascular effects (Afshinnia, 2018; Fan & Roman, 2017; Schunck, 2018). Oxylipin profiling of human plasma in uremic ESRD patients before fistula construction surgery has been reported (Hu, 2018). The authors identified decreases in 5,6-dihydroxyeicosatrienoic acid (5,6-DHET) and 5-hydroxyeicosatetraenoic acid (5-HETE), but increases in 9,10-EpOME and 12,13-EpOME as key markers that discriminated between ESRD patients and controls. The products are biologically active. For example, EETs and DHETs are considered candidates for vasodilatory endothelium-derived hyperpolarizing factors (EDHFs) (Campbell, 1996), whose release is triggered by Ca^{2+} and shear stress via the CYP pathway (Campbell & Fleming, 2010; Graber, Alfonso, & Gill, 1997). While EpOMEs and their diols decrease cardiac postischemic functional recovery (Bannehr, 2019a), 5-HETE stimulates neutrophil chemotaxis and degranulation, (Goetzl, 1980; Stenson & Parker, 1980; Valone, 1980) and inhibits endothelial PGI2 production with consecutive effects on platelet aggregation and vasomotor tone (Gordon, Gordon, & Spector, 1991). Hemodialysis treatment per se increases levels of plasma 6-keto PGF1 alpha and PGF2 isoprostanes, which may also play a role in platelet aggregation and vasodilation (Kim, 2004; Kovac, 1992). Whether or not the hemodialysis treatment itself affects oxylipin profiles is unknown. We tested the hypothesis that oxylipin profiles differ in normal subjects and ESRD patients and that the hemodialysis treatment per se would affect plasma concentrations.

2 | METHODS

The Charité University Medicine Institutional Review Board approved this registered study (ClinicalTrials.gov, Identifier: NCT03857984). In total, 15 healthy volunteers (6 male and 9 female) and 15 ESRD patients (7 men and 8 women) participated in the study (Table 1). Inclusion criteria for the group of CKD patients were: history of renal failure requiring hemodialysis/hemofiltration therapy, age over 18 years, the ability to consent, and written consent of the study participant. The patients in the group CKD were diagnosed for the following conditions: diabetes mellitus (4 patients), hypertension (3 patients), membranous glomerulonephritis (2 patients), ADPKD (autosomal dominant polycystic kidney disease) (1 patient), other or unknown (5 patients). Exclusion criteria for healthy volunteers were: age under 18 years, chronic illness requiring any medication, pregnancy, inability to follow simple instructions, relevant or severe abnormalities in medical

TABLE 1 Characteristics of hemodialysis (HD) patients and control subjects ($n = 15$ each)

	HD patients	Controls
Age (years)	50 18	47 12
Sex		
Male (*n*)	7	6
Female (*n*)	8	9
Body mass index (kg/m^2)	24.8 3.4	24.7 4.6
Race (*n*)		
	Caucasian = 14	Caucasian = 14
	Black = 1	Asian = 1
Cause of end-stage renal disease		
Diabetes (*n*)	4	
Hypertension (*n*)	3	
Membranous glomerulonephritis (*n*)	2	
ADPKD (*n*)	1	
Other or unknown	5	
Complications		
Cardiovascular (*n*)	2	
Cerebrovascular (*n*)	1	
Peripheral artery disease (*n*)	3	

Note: Data are presented as mean   *SD* or frequencies.

history, or physical examination (Gollasch, 2020). Patients underwent thrice weekly dialysis, which lasted from 3 hr 45 min to 5 hr, based on high flux AK 200 dialyzers (Gambro GmbH, Hechingen, Germany).

Venous blood was collected in each healthy subject by subcutaneous arm vein puncture in the sitting position. In the group of dialyzed patients (CKD group), all the blood samples were collected on the fistula arm right before beginning of the dialysis (pre-HD) and at the end of the dialysis (5–15 min before termination, post-HD). All blood samples were obtained by 4°C precooled EDTA vacuum extraction tube systems. Cells were separated from plasma by centrifugation for 10 min at 1,000–2,000 g using a refrigerated centrifuge. Following centrifugation, supernatant plasma was immediately transferred into clean polypropylene tubes using an Eppendorf pipette. The samples were maintained at 2–8°C while handling. Aliquots (0.5 ml) were then stored at −80°C until further processing and extraction. Overall, the processing took no longer than 10 min. All samples were analyzed for free and total plasma oxylipins. Oxylipins were determined by high-performance liquid chromatography mass spectrometry (HPLC-MS) spectrometry described in (Fischer, 2014) (Gollasch, 2019a). Descriptive statistics were

Publication Ⅱ

calculated and variables were examined for meeting assumptions of normal distribution without skewness and kurtosis. We used the Shapiro–Wilk test to determine if they were normally distributed. In order to determine statistical significance, a two-tailed t test or Mann–Whitney test were used to compare values of CKD versus control groups. Homogeneity of variances was asserted using Levene's test. Paired t test or paired Wilcoxon test were used to compare pre-HD versus post-HD values. In order to determine the statistical significance between the four classes of epoxy metabolites hydrolyzed to appear in the circulation, Friedman's test was used followed by applying Dunn's multiple comparison test (Gollasch, 2019a, 2019b). The .05 level of significance (p) was chosen. All data are presented as mean SD. All statistical analyses were performed using SPSS Statistics software (IBM Corporation, Armonk, NY, USA).

3 | RESULTS

3.1 | Clinical characteristics

Table 1 shows the demographics of the ESRD hemodialysis (HD) patients and control subjects. The results show that age and body mass indices between HD patients and the healthy subjects were not different ($p > .05$ each). Subjects were Caucasians, with the exception of one African and one Asian subject in each group. The ESRD patients had diabetes mellitus, hypertension, membranous glomerulonephritis, ADPKD, and other or unknown disease, as underlying causes. Major cardiovascular complications were cardiovascular and cerebrovascular events, and peripheral artery disease.

3.2 | Oxylipins in ESRD

We first determined the total levels of oxylipins in plasma of the HD patients (Table 2) and compared the results with the healthy control subjects. We were particularly interested in 9,10-EpOME, 12,13-EpOME, 5,6-DHET, and 5-HETE, which have been recently identified as the key markers to discriminate uremic ESRD patients from controls (Hu, 2018). Our results confirm these findings. However, we also detected increased 5,6-EET, 8,9-EET, 11,12-EET, 14,15-EET, 5,6-EEQ, 11,12-EEQ, 14,15-EEQ, 17,18-EEQ, 14,15-DiHETE, 7,8-EDP, 10,11-EDP, 16,17-EDP, 19,20-EDP, 5-HEPE, 12-HEPE, and 19-HEPE levels in our ESRD patients undergoing regular hemodialysis treatments, compared to the control subjects (Table 2A). Moreover, 13-HODE, 9,10-DiHOME, 8,9-DHET, 11,12-DHET, 14,15-DHET, 8-HETE, 9-HETE, 11-HETE, 12-HETE, 15-HETE, 16-HETE, 19-HETE, 20-HETE, 8-HEPE, 9-HEPE, 15-HEPE, 18-HEPE, 4-HDHA, 7-HDHA, 8-HDHA, 10-HDHA, 11-HDHA, 13-HDHA,

14-HDHA, 16-HDHA, 17-HDHA, and 20-HDHA levels were decreased in our ESRD patients, compared to controls. Our dialysis patients showed 12,13-DiHOME, 8,9-EEQ, 5,6-DiHETE, 8,9-DiHETE, 11,12-DiHETE, 17,18-DiHETE, 13,14-EDP, 7,8-DiHDPA, 10,11-DiHDPA, 13,14-DiHDPA, 16,17-DiHDPA, 19,20-DiHDPA, 17-HETE, 18-HETE, 12-HpETE, 20-HEPE, 21-HDHA, and 22-HDHA levels, which were similar to values observed in the control group. Metabolites in free state may have been contributed to changes of total 9,10-DiHOME, 11-HETE, 12-HETE, or 12-HEPE levels (Table 2B) since both total and free oxylipins showed similar data grouping effects (right columns in Table 2A and B). With exception of decreased PGE2 and PGD2 levels (Table 2B), our CKD patients showed similar or nondetectable levels of TXB2, 11-dehydro TXB2, 15-keto-PGE2, 13,14-dihydro-15-keto-PGE2, 13,14-dihydro-15-keto-PGD2, PGJ2, 15-deoxy-delta 12,14-PGJ2, PGF2a, 8-iso-PGF2a, TXB3, 11-dehydro TXB3, PGE3, 6(S)-LXA4, LXA4, 15(R)-LXA4, LXB4, LXA5, MAR 1, 7-epi-MAR1, RvD1, 17(R)-RvD1, RvD2, RvD3, RvD5, and RvE1, compared to healthy controls (detection level of 0.05 ng/g, each).

Together, the findings indicate that ESRD is associated with an altered plasma oxylipins status namely an individual signature, which shows decreases in the majority of LOX/CYP ω/(ω-1)-hydroxylase-dependent metabolites (HETEs, HEPEs, HDTAs, and 13-HODE) and increases in all four classes of CYP epoxy metabolites (i.e., EET, EpOME, EEQ, and EDP).

3.3 | Diol/epoxide ratios

As shown in Figure 1, the main pathway of EET, EpOME, EEQ, and EDP metabolism in many cells is conversion into DHETs, DiHOMEs, DiHETEs, and DiHDPAs by the soluble epoxide hydrolase enzyme (sEH), even though epoxy-polyunsaturated fatty acids (EpPUFA) can also be nonenzymatically hydrolyzed into dihydroxymetabolites (DiHPUFA) (Spector, 2004). Since ESRD might have caused EET, EpOME, EEQ, and EDP production rapidly degraded to their diols, we next analyzed the sums of the individual CYP epoxy metabolites and their diols (Table 3A). We found that ESRD was associated with increased levels of the majority of those CYP metabolites (Table 3A). To provide insights into possible mechanisms underlying this increase, we calculated diol/epoxide ratios of the epoxy metabolites (Table 3B and C). We found that the four classes of epoxy metabolites are unequally hydrolyzed to appear in the circulation (Friedman's test, $p < .05$). We found that EpOMEs and EDPs are better metabolized into their diols (ratio of DiHOMEs/EPOMEs and DiHDPAs/EDPs; 0.156 0.301 and 0.114 0.141, respectively; Dunn's multiple comparison test, $p > .05$) than EETs and EEQs (ratios of those diols/epoxy metabolites,

Publication Ⅱ

T A B L E 2   Comparison of oxylipins between control subjects versus. CKD patients before hemodialysis (HD) ($n = 15$)

Amount ng/mL	Control (Mean	SD)	HD (mean	SD)	p-value t-Test (#Mann-Whitney Test)	Data grouping effect
A. Total oxylipins in plasma.						
9,10-EpOME	17.22	11.11	57.77	53.82	.001#	HD > Control
12,13-EpOME	19.42	16.22	57.80	58.55	.004#	
5,6-EET	15.66	7.34	47.09	53.73	.013#	
8,9-EET	4.97	2.07	13.12	13.52	.009#	
11,12-EET	2.02	064	7.29	8.74	<.001#	
14,15-EET	8.02	3.62	35.11	39.14	.001#	
5,6-EEQ	7.87	5.32	28.3	32.4	.028	
11,12-EEQ	0.42	0.27	1.48	1.60	.019#	
14,15-EEQ	0.32	0.20	1.22	1.37	.011#	
17,18-EEQ	1.00	0.68	4.45	4.74	.002#	
14,15-DiHETE	0.02	0.01	0.04	0.09	.041#	
7,8-EDP	1.53	0.52	3.65	2.36	.002#	
10,11-EDP	0.33	0.19	0.75	0.54	.005#	
16,17-EDP	1.33	0.48	5.34	4.55	<.001#	
19,20-EDP	1.56	0.55	7.75	5.99	<.001#	
5-HEPE	1.07	0.62	1.12	2.19	.023#	
12-HEPE	1.09	0.65	1.33	3.32	.002#	
19-HEPE	0.77	0.31	1.80	5.06	.021#	
13-HODE	39.08	13.32	30.44	14.64	.041#	HD < Control
9,10-DiHOME	5.05	3.17	4.07	4.37	.041#	
5,6-DHET	1.60	0.76	0.85	0.45	.004#	
8,9-DHET	1.42	051	1.10	1.25	.016#	
11,12-DHET	0.41	0.15	0.31	0.16	.019#	
14,15-DHET	0.55	0.24	0.32	0.10	.003	
5-HETE	7.22	3.21	4.25	1.40	.001#	
8-HETE	5.60	2.41	3.16	4.49	.003	
9-HETE	6.60	2.23	3.78	1.38	<.001	
11-HETE	9.95	2.73	5.05	1.53	<.001	
12-HETE	11.82	4.23	6.52	3.42	<.001#	
15-HETE	17.22	5.36	8.82	3.30	<.001	
16-HETE	1.39	0.61	0.75	0.25	<.001#	
19-HETE	1.10	0.51	0.58	0.22	<.001#	
20-HETE	0.98	0.30	0.72	0.26	.019	
8-HEPE	0.50	0.28	0.46	1.04	.001#	
9-HEPE	0.53	0.29	0.48	1.05	.001#	
15-HEPE	0.78	0.44	0.66	1.40	<.001#	
4-HDHA	2.39	0.95	1.61	1.32	.009#	
7-HDHA	1.04	0.47	0.79	0.88	.045#	
8-HDHA	1.27	0.55	1.02	1.29	.026#	
10-HDHA	1.75	0.61	1.00	1.00	.001#	
11-HDHA	1.33	0.57	0.97	1.14	.013#	

(Continues)

Publication Ⅱ

TABLE 2 (Continued)

Amount ng/mL	Control (Mean	SD)	HD (mean	SD)	*p*-value *t*-Test (#Mann-Whitney Test)	Data grouping effect
13-HDHA	1.44	0.54	0.90	0.80	.002#	
14-HDHA	2.27	0.81	1.18	1.33	.001#	
16-HDHA	1.14	0.40	0.76	0.84	.002#	
17-HDHA	3.02	0.98	1.85	1.83	.001#	
20-HDHA	4.73	1.78	2.90	2.48	.002#	
12,13-DiHOME	3.76	1.67	3.18	2.56	.267#	No effect or not significant
8,9-EEQ	0.66	0.40	1.85	2.03	.098#	
5,6-DiHETE	0.25	0.15	0.38	0.69	.461#	
8,9-DiHETE	0.02	0.01	0.05	0.14	.102#	
11,12-DiHETE	0.01	0.01	0.02	0.07	.074#	
17,18-DiHETE	0.10	0.04	0.22	0.48	.838#	
13,14-EDP	0.20	0.11	0.45	0.40	.148#	
7,8-DiHDPA	0.24	0.13	0.28	0.37	.412#	
10,11-DiHDPA	0.05	0.02	0.05	0.09	.260#	
13,14-DiHDPA	0.04	0.01	0.04	0.05	.130#	
16,17-DiHDPA	0.10	0.04	0.11	0.11	.285#	
19,20-DiHDPA	0.57	0.25	0.90	0.23	.935#	
17-HETE	0.25	0.07	0.30	0.23	.967#	
18-HETE	0.72	0.36	0.56	0.24	.187#	
12-HpETE	6.23	3.23	12.32	10.44	.067#	
20-HEPE	0.13	0.07	0.35	0.81	.775#	
21-HDHA	0.70	0.23	1.53	3.35	.744#	
22-HDHA	0.21	0.07	0.63	1.55	.967#	
B. Free oxylipins in plasma.						
13,14-EDP	0.01	0.01	0.02	0.02	.019#	HD > Control
9-HEPE	0.04	0.03	0.08	0.25	.017#	
12-HEPE	1.65	1.25	3.26	9.64	.015#	
18-HEPE	0.38	0.20	0.58	1.67	.001#	
10-HDHA	0.20	0.10	0.23	0.50	.029#	
16-HDHA	0.06	0.05	0.12	0.37	.007#	
17-HDHA	0.59	0.28	0.85	2.33	.004#	
9,10-DiHOME	1.65	2.14	0.44	0.41	.046	HD < Control
5,6-EET	0.37	0.13	0.23	0.10	.003	
11,12-EET	0.06	0.04	0.03	0.02	.013#	
14,15-DiHETE	0.03	0.03	0.02	0.05	.008#	
17,18-DiHETE	0.27	0.34	0.12	0.20	.003#	
9-HETE	0.12	0.04	0.09	0.12	.013#	
11-HETE	0.74	0.22	0.24	0.12	<.001	
12-HETE	9.61	6.22	4.44	5.60	.006#	
15-HETE	1.19	0.85	0.41	0.22	<.001#	
15-HEPE	0.14	0.09	0.13	0.35	.001#	
13-HDHA	0.11	0.07	0.10	0.20	.022#	

(Continues)

Publication Ⅱ

T A B L E 2   (Continued)

Amount ng/mL	Control (Mean	SD)	HD (mean	SD)	p-value t-Test (#Mann-Whitney Test)	Data grouping effect
14-HDHA	1.80	0.96	1.30	2.23	.017#	
TXB2	0.38	0.19	0.14	0.16	.003#	
PGE2	0.09	0.04	0.04	0.03	.001#	
PGD2	0.05	0.02	0.03	0.02	.012#	
13-HODE	7.68	6.28	5.05	5.27	.098#	No effect or not significant
9,10-EpOME	0.70	0.59	1.73	2.01	.098#	
12,13-EpOME	0.78	0.70	1.59	1.89	.254#	
12,13-DiHOME	9.02	14.34	2.93	2.75	.080#	
8,9-EET	0.02	0.02	0.03	0.03	.180	
14,15-EET	0.31	0.19	0.39	0.28	.397	
5,6-DHET	0.01	0.01	0.01	0.01	.856#	
8,9-DHET	0.11	0.12	0.09	0.05	.719#	
11,12-DHET	0.11	0.09	0.08	0.04	.555#	
14,15-DHET	0.05	0.02	0.04	0.01	.067	
5,6-EEQ	0.37	0.12	0.32	0.19	.688	
8,9-EEQ	0.09	0.08	0.35	0.73	.241#	
11,12-EEQ	0.02	0.01	0.05	0.12	1.000#	
14,15-EEQ	0.09	0.08	0.22	0.59	.222#	
17,18-EEQ	0.27	0.22	0.75	2.15	.467#	
5,6-DiHETE	0.01	0.01	0.01	0.02	.098#	
8,9-DiHETE	0.01	0.01	0.01	0.03	.896#	
11,12-DiHETE	0.01	0.01	0.01	0.01	.047#	
7,8-EDP	0.15	0.8	0.15	0.21	.235#	
10,11-EDP	0.01	0.01	0.03	0.05	.316#	
16,17-EDP−233	0.04	0.06	0.02	0.02	.185#	
19,20-EDP	0.03	0.04	0.49	1.43	.072#	
7,8-DiHDPA	0.01	0.01	0.01	0.01	.650#	
10,11-DiHDPA	0.01	0.01	0.01	0.01	.200#	
13,14-DiHDPA	0.01	0.01	0.01	0.01	.142#	
16,17-DiHDPA	0.08	0.05	0.09	0.07	.717#	
19,20-DiHDPA	0.34	0.20	0.64	0.81	.363#	
5-HETE	0.07	0.03	0.09	0.11	.892#	
8-HETE	0.17	0.08	0.14	0.09	.294#	
16-HETE	0.29	0.08	0.25	0.10	.282	
17-HETE	0.05	0.02	0.11	0.19	.928#	
18-HETE	0.01	0.01	0.03	0.05	.339#	
19-HETE	0.04	0.01	0.04	0.02	.690	
20-HETE	0.25	0.10	0.35	0.19	.118#	
12-HpETE	0.04	0.04	0.05	0.04	.598	
5-HEPE	0.05	0.03	0.15	0.42	.440#	
19-HEPE	0.35	0.42	1.45	4.24	.339#	
20-HEPE	0.03	0.06	0.24	0.50	.823#	

(Continues)

Publication Ⅱ

T A B L E 2 (Continued)

Amount ng/mL	Control (Mean	SD)	HD (mean	SD)	p-value t-Test (#Mann-Whitney Test)	Data grouping effect
4-HDHA	0.03	0.03	0.23	0.73	.821[#]	
7-HDHA	0.01	0.01	0.05	0.14	.294[#]	
8-HDHA	0.02	0.02	0.07	0.19	.387[#]	
11-HDHA	0.12	0.07	0.28	0.74	.254[#]	
20-HDHA	0.16	0.09	0.16	0.37	.004[#]	
21-HDHA	0.39	0.51	2.02	5.94	.892[#]	
22-HDHA	0.32	0.43	1.10	3.00	.751[#]	
15-keto-PGE2	n.d.		n.d.			
13,14-dihydro−15-keto-PGE2	n.d.		n.d.			
13,14-dihydro−15-keto-PGD2	n.d.		n.d.			
PGJ2	n.d.		n.d.			
15-deoxy-delta 12,14-PGJ2	n.d.		n.d.			
PGF2a8-iso-PGF2a	n.d.		n.d.			
TXB3	n.d.		n.d.			
11-dehydro TXB3	n.d.		n.d.			
PGE3	n.d.		n.d.			
6(S)-LXA4	n.d.		n.d.			
LXA4	n.d.		n.d.			
15(R)-LXA4	n.d.		n.d.			
LXB4	n.d.		n.d.			
LXA5	n.d.		n.d.			
MAR 1	n.d.		n.d.			
7-epi-MAR1	n.d.		n.d.			
RvD1	n.d.		n.d.			
17(R)-RvD1	n.d.		n.d.			
RvD2	n.d.		n.d.			
RvD3	n.d.		n.d.			
RvD5	n.d.		n.d.			

0.047 ± 0.046 and 0.027 ± 0.031, respectively; Dunn's multiple comparison test, $p > .05$) (Table 3B). In fact, the following order of ratios was identified: DiHOMEs/ EpOMEs = DiHDPA/EDPs > DHETs/EETs = DiHETEs/ EEQs (Dunn's multiple comparison test, $p < .05$). This pattern was also found for the individual metabolites in vivo, as shown (Table 3C). Together, the findings indicate that CYP epoxy metabolites are released and accumulated in the circulation of ESRD HD patients, compared to controls, with epoxy metabolite substrate classes unequally hydrolyzed by sEH in vivo.

3.4 | Effects of hemodialysis

The effects of hemodialysis treatment on plasma oxylipins in ESRD HD patients are summarized (Table 4). The data demonstrate an increase in the majority of epoxy metabolites, including 9,10-EpOME, 12,13-EpOME, 9,10-DiHOME, 12,13-DiHOME, 5,6-EET, 14,15-EET, 8,9-DHET, 11,12-DHET, 8,9-EEQ, 11,12-EEQ, 14,15-EEQ, 17,18-EEQ, 14,15-DiHETE, 17,18-DiHETE, 7,8-EDP, 10,11-EDP, 13,14-EDP, 16,17-EDP, 19,20-EDP, 7,8-DiHDPA, 10,11-DiHDPA, 13,14-DiHDPA, 16,17-DiHDPA, and 19,20-DiHDPA (Table 4A). Moreover, hemodialysis also

Publication Ⅱ

TABLE 3 Comparison of oxylipins and their ratios between control subjects versus. CKD patients before hemodialysis (HD) ($n = 15$)

Epoxides or Diols (ng/mL)	Control (Mean	SD)	HD (Mean	SD)	p-value Mann-Whitney test	Data grouping effect
A. Concentrations of individual total epoxides plus their respective diols in plasma.						
9,10-EpOME + 9,10-DiHOME	22.27	12.62	61.84	53.16	.0025	HD > Control
12,13-EpOME + 12,13-DiHOME	23.18	17.10	60.97	58.41	.0062	
5,6-EET + 5,6-DHET	17.25	7.548	47.94	53.82	.0213	
8,9-EET + 8,9-DHET	6.213	2.207	14.22	13.81	.0421	
11,12 EET + 11,12-DHET	2.427	0.7535	7.601	8.773	.0006	
14,15-EET + 14,15-DHET	8.574	3.654	35.43	39.17	.0014	
5,6-EEQ + 5,6-DiHETE	8.119	5.428	28.67	32.50	.0344	
11,12-EEQ + 11,12-DiHETE	0.4307	0.2757	1.502	1.610	.0263	
14,15-EEQ + 14,15-DiHETE	0.3400	0.2008	1.260	1.377	.0170	
17,18-EEQ + 17,18-DiHETE	1.101	0.7089	4.671	4.833	.0042	
7,8-EDP + 7,8-DiHDPA	1.766	0.5502	3.930	2.449	.0045	
10,11-EDP + 10,11-DiHDPA	0.3813	0.1933	0.8080	0.5495	.0152	
16,17-EDP + 16,17-DiHDPA	1.425	0.4758	5.445	4.546	.0003	
19,20-EDP + 19,20-DiHDPA	2.126	0.6048	8.650	6.002	<.0001	
8,9-EEQ + 8,9-DiHETE	0.6840	0.4120	1.901	2.067	.1103	No effect or not significant
13,14-EDP + 13,14-DiHDPA	0.2453	0.1193	0.4880	0.4005	.1581	

(Continues)

Publication Ⅱ

TABLE 3 (Continued)

Epoxides or Diols (ng/mL)	Control (Mean	SD)	HD (Mean	SD)	p-value Mann-Whitney test	Data grouping effect
B: Ratios estimated using total concentrations of epoxides and diols in plasma.						
Ratio (9,10-DiHOME + 12,13-DiHOME) / (9,10-EpOME + 12,13-EpOME)	0.3009	0.1402	0.1559	0.3014	.0008	HD < Control
Ratio (5,6-DHET + 8,9-DHET + 11,12-DHET + 14,15-DHET) / (5,6-EET + 8,9-EET + 11,12 EET + 14,15-EET)	0.1406	0.07617	0.04724	0.04648	<.0001	
Ratio (5,6-DiHETE + 8,9-DiHETE + 11,12-DiHETE + 14,15-DiHETE + 17,18-DiHETE) / (5,6-EEQ + 8,9-EEQ + 11,12-EEQ + 14,15-EEQ + 17,18-EEQ)	0.04801	0.02220	0.02745	0.03105	.0028	

Publication Ⅱ

TABLE 3   (Continued)

Epoxides or Diols (ng/mL)	Control (Mean	SD)	HD (Mean	SD)	p-value Mann-Whitney test	Data grouping effect
Ratio (7,8-DiHDPA + 10,11-DiHDPA + 13,14-DiHDPA + 16,17-DiHDPA + 19,20-DiHDPA) / (7,8-EDP + 10,11-EDP + 13,14-EDP + 16,17-EDP + 19,20-EDP)	0.2242	0.1244	0.1145	0.1411	.0032	

Ratios	Control (Mean	SD)	HD (Mean	SD)	p-value Mann-Whitney test	Data grouping effect
C. Ratios estimated using individual total concentrations of epoxides and their diols in plasma.						
9,10-DiHOME / 9,10-EpOME	0.3487	0.1679	0.1792	0.3752	.0003	HD < Control
12,13-DiHOME / 12,13-EpOME	0.2567	0.1225	0.1320	0.2280	.0012	
5,6-DHET / 5,6-EET	0.1156	0.06784	0.03753	0.03869	.0002	
8,9-DHET / 8,9-EET	0.2790	0.1382	0.1206	0.1024	.0006	
11,12-DHET / 11,12-EET	0.2092	0.05280	0.07844	0.06571	.0002	
14,15-DHET / 14,15-EET	0.08377	0.05311	0.02045	0.02099	<.0001	
5,6-DiHETE / 5,6-EEQ	0.03749	0.01789	0.01923	0.02031	.0028	
8,9-DiHETE / 8,9-EEQ	0.04396	0.02798	0.02663	0.04312	.0021	
11,12-DiHETE / 11,12-EEQ	0.03184	0.01914	0.01553	0.02861	.0008	

(Continues)

Publication Ⅱ

TABLE 3 (Continued)

Ratios	Control (Mean SD)		HD (Mean SD)		p-value Mann-Whitney test	Data grouping effect
14,15-DiHETE / 14,15-EEQ	0.08126	0.04245	0.04268	0.05904	.0014	
17,18-DiHETE / 17,18-EEQ	0.1335	0.06799	0.07081	0.08064	.0070	
7,8-DiHDPA / 7,8-EDP	0.1699	0.1156	0.09037	0.09216	.0070	
10,11-DiHDPA / 10,11-EDP	0.2078	0.1351	0.08913	0.1152	.0008	
13,14-DiHDPA / 13,14-EDP	0.2631	0.1276	0.1662	0.1892	.0202	
16,17-DiHDPA / 16,17-EDP	0.08331	0.04474	0.03211	0.03420	.0004	
19,20-DiHDPA / 19,20-EDP	0.4071	0.2295	0.1934	0.2658	.0025	

increased several LOX/CYP ω/(ω-1)-hydroxylase metabolites, such as 13-HODE, 20-HETE, 5-HEPE, 15-HEPE, 18-HEPE, 19-HEPE, 7-HDHA, and 11-HDHA. No changes occurred in the levels of other CYP and LOX/CYP ω/(ω-1)-hydroxylase metabolites (Table 4A). No level variations of free oxylipins were found in response to hemodialysis, with the exception of 9,10-DiHOME, 11,12-EET, 19,20-DiHDPA, and 12-HpETE (Table 4B). While TXB2, PGE2, and PGD2 levels did not change by hemodialysis, this treatment did not cause accumulation of detectable levels of 11-dehydro TXB2, 15-keto-PGE2, 13,14-dihydro-15-keto-PGE2, 13,14-dihydro-15-keto-PGD2, PGJ2, 15-deoxy-delta 12,14-PGJ2, PGF2a, 8-iso-PGF2a, TXB3, 11-dehydro TXB3, PGE3, 6(S)-LXA4, LXA4, 15(R)-LXA4, LXB4, LXA5, MAR 1, 7-epi-MAR1, RvD1, 17(R)-RvD1, RvD2, RvD3, RvD5, and RvE1 in plasma (Table 4B) at a detection level of 0.05 ng/g, each.

3.5 | Diol/epoxide ratios

Our analysis of sums of the individual CYP epoxy metabolites and their diols (Table 5A) demonstrated increased accumulation of (9,10-EpOME + 9,10-DiHOME), (12,13-EpOME + 12,13-DiHOME), (5,6-EET + 5,6-DHET) (5,6-EEQ + 5,6-DiHETE), (8,9-EEQ + 8,9-DiHETE), (11,12-EEQ + 11,12-DiHETE), (14,15-EEQ + 14,15-DiHETE), (17,18-EEQ + 17,18-DiHETE), (7,8-EDP + 7,8-DiHDPA), (19,20-EDP + 19,20-DiHDPA), (8,9-EET + 8,9-DHET), (14,15-EET + 14,15-DHET), (10,11-EDP + 10,11-DiHDPA), (13,14-EDP + 13,14-DiHDPA) and (16,17-EDP + 16,17-DiHDPA). To provide insights into possible mechanisms, we calculated ratios of diols/epoxides. We found that the ratios were not influenced by hemodialysis (Table 5B and C). Together, the results indicate that the CYP epoxy metabolites are rather released and accumulated in the circulation during hemodialysis treatment than resulting from altered sEH activity in vivo. Furthermore, hemodialysis treatment is insufficient to change the majority of LOX/CYP ω/(ω-1)-hydroxylase metabolites in ESRD patients.

4 | DISCUSSION

Our data demonstrate that all four subclasses of CYP epoxy metabolites and several LOX/CYP ω/(ω-1)-hydroxylase metabolites are increased by the hemodialysis treatment. We found that these changes are unlikely related to altered sEH activity. The data are also not related to alterations of plasma or red blood cell (RBC) fatty acid levels, in particular RBC n-3 fatty acid status, which we demonstrated in our previous study (Gollasch, 2020). Despite significant changes in fatty acids signatures between healthy persons and CKD patients, we observed that hemodialysis does not alter plasma or RBC fatty acid levels to potentially explain the observed changes of oxylipins in the present study (Gollasch, 2020). Our data support the idea that 9,10-EpOME, 12,13-EpOME, 5,6-DHET,

TABLE 4 Effects of hemodialysis on oxylipins in the CKD patients before (pre-HD) and at cessation (post-HD) of hemodialysis ($n = 15$ each)

Amount ng/ml	Pre-HD (Mean SD)		Post-HD (mean SD)		p-value Paired t-Test ([#]paired Wilcoxon Test)	Data grouping effect
A. Total oxylipins in plasma.						
13-HODE	30.44	14.64	42.19	23.88	.016[#]	Post-HD
9,10-EpOME	57.77	53.82	145.71	161.87	.041[#]	>
12,13-EpOME	57.80	58.55	140.29	145.06	.041[#]	Pre-HD
9,10-DiHOME	4.07	4.37	6.35	4.81	.019[#]	
12,13-DiHOME	3.18	2.56	5.81	3.71	.004[#]	
5,6-EET	47.09	53.73	127.44	131.75	.035[#]	
14,15-EET	35.11	39.14	103.89	115.46	.048[#]	
8,9-DHET	1.10	1.25	1.29	1.49	.011[#]	
11,12-DHET	0.31	0.16	0.38	0.19	.022[#]	
8,9-EEQ	1.85	2.03	5.27	6.00	.019[#]	
11,12-EEQ	1.48	1.60	4.43	5.59	.035[#]	
14,15-EEQ	1.22	1.37	3.56	4.52	.030[#]	
17,18-EEQ	4.45	4.74	13.85	18.04	.048[#]	
14,15-DiHET	0.04	0.09	0.05	0.10	.019[#]	
17,18-DiHETE	0.22	0.48	0.25	0.49	.006[#]	
7,8-EDP	3.65	2.36	9.67	8.71	.041[#]	
10,11-EDP	0.75	0.54	1.98	2.23	.041[#]	
13,14-EDP	0.45	0.40	1.33	1.64	.048[#]	
16,17-EDP	5.34	4.55	17.46	18.62	.041[#]	
19,20-EDP	7.75	5.99	26.39	27.84	.035[#]	
7,8-DiHDPA	0.28	0.37	0.31	0.40	.016[#]	
10,11-DiHDPA	0.05	0.09	0.06	0.10	.011[#]	
13,14-DiHDPA	0.04	0.05	0.05	0.05	.022[#]	
16,17-DiHDPA	0.11	0.11	0.13	0.11	.002[#]	
19,20-DiHDPA	0.90	0.23	1.06	1.17	.016[#]	
20-HETE	0.72	0.26	0.86	0.26	.032	
5-HEPE	1.12	2.19	1.33	2.63	.022[#]	
15-HEPE	0.66	1.40	0.78	1.51	.013[#]	
18-HEPE	1.78	3.7	2.25	4.58	.041[#]	
7-HDHA	0.79	0.88	0.91	0.93	.048[#]	
11-HDHA	0.97	1.14	1.18	1.27	.041[#]	
19-HEPE	1.80	5.06	1.62	3.78	.041[#]	Pre-HD > Post-HD
8,9-EET	13.12	13.52	29.53	27.79	.056[#]	No effect or not significant
11,12-EET	7.29	8.74	12.97	11.42	.124[#]	
5,6-DHET	0.85	0.45	0.87	0.40	.826[#]	
14,15-DHET	0.32	0.10	0.36	0.10	.300	
5,6-EEQ	28.3 + 32.4		87.0 + 114.0		.132	
5,6-DiHETE	0.38	0.69	0.42	0.78	.272[#]	

(Continues)

Publication Ⅱ

TABLE 4 (Continued)

Amount ng/ml	Pre-HD (Mean SD)		Post-HD (mean SD)		p-value Paired t-Test ([#]paired Wilcoxon Test)	Data grouping effect
8,9-DiHETE	0.05	0.1	0.06	0.17	.221[#]	
11,12-DiHETE	0.02	0.07	0.03	0.08	.109[#]	
5-HETE	4.25	1.40	4.84	2.12	.213	
8-HETE	3.16	4.49	3.70	1.75	.108	
9-HETE	3.78	1.38	4.83	2.51	.083	
11-HETE	5.05	1.53	6.39	3.21	.116	
12-HETE	6.52	3.42	7.11	3.14	.158[#]	
15-HETE	8.82	3.30	10.82	6.77	.109[#]	
16-HETE	0.75	0.25	0.92	0.66	.221[#]	
17-HETE	0.30	0.23	0.33	0.31	.363[#]	
18-HETE	0.56	0.24	0.56	0.28	.638[#]	
19-HETE	0.58	0.2	0.58	0.27	.925[#]	
12-HpETE	12.32	10.44	15.78	19.17	.972[#]	
8-HEPE	0.46	1.04	0.54	1.17	.096[#]	
9-HEPE	0.48	1.05	0.53	1.08	.064[#]	
12-HEPE	1.33	3.32	1.52	3.64	.064[#]	
20-HEPE	0.35	0.81	0.29	0.49	.064[#]	
4-HDHA	1.61	1.32	1.94	1.70	.084[#]	
8-HDHA	1.02	1.29	1.11	1.32	.221[#]	
10-HDHA	1.00	1.00	1.16	1.08	.056[#]	
13-HDHA	0.90	0.80	1.10	0.93	.074[#]	
14-HDHA	1.18	1.33	1.42	1.58	.064[#]	
16-HDHA	0.76	0.84	0.91	0.92	.084[#]	
17-HDHA	1.85	1.83	2.26	2.02	.084[#]	
20-HDHA	2.90	2.48	3.35	3.00	.158[#]	
21-HDHA	1.53	3.35	1.29	2.14	.925[#]	
22-HDHA	0.63	1.55	0.51	0.81	.096[#]	
B. Free oxylipins in plasma.						
9,10-DiHOME	0.44	0.41	1.07	1.12	.034[#]	Post-HD
11,12-EET	0.03	0.02	0.04	0.02	.015[#]	>
19,20-DiHDPA	0.64	0.81	0.69	0.74	.019[#]	Pre-HD
12-HpETE	0.05	0.04	0.39	0.36	.027	
13-HODE	5.05	5.27	9.23	7.89		No effect or not significant
9,10-EpOME	1.73	2.01	3.55	2.62	.308[#]	
12,13-EpOME	1.59	1.89	4.28	4.22	.272[#]	
12,13-DiHOM	2.93	2.75	6.10	8.36	.099[#]	
5,6-EET	0.23	0.10	0.40	0.32	.071[#]	
8,9-EET	0.03	0.03	0.02	0.02	.347[#]	
14,15-EET	0.39	0.28	0.63	0.66	.433[#]	
5,6-DHET	0.01	0.01	0.01	0.01	.329	
8,9-DHET	0.09	0.05	0.10	0.05	.131[#]	
11,12-DHET	0.08	0.04	0.09	0.04	.306	

(Continues)

Publication Ⅱ

TABLE 4 (Continued)

Amount ng/ml	Pre-HD (Mean	SD)	Post-HD (mean	SD)	p-value Paired t-Test (#paired Wilcoxon Test)	Data grouping effect
14,15-DHET	0.04	0.01			0.05 0.02	
5,6-EEQ	0.32	0.19	0.29	0.34	.785	
8,9-EEQ	0.35	0.73	0.22	0.26	.753#	
11,12-EEQ	0.05	0.12	0.02	0.03	.310#	
14,15-EEQ	0.22	0.59	0.16	0.28	.674#	
17,18-EEQ	0.75	2.15	0.50	0.69	.071#	
5,6-DiHETE	0.01	0.02	0.01	0.01	1.000#	
8,9-DiHETE	0.01	0.03	0.01	0.02	.484#	
11,12-DiHETE	0.01	0.01	0.01	0.01	.169#	
14,15-DiHETE	0.02	0.05	0.03	0.04	.099#	
17,18-DiHETE	0.12	0.20	0.14	0.19	.084#	
7,8-EDP	0.15	0.21	0.18	0.17	.530#	
10,11-EDP	0.03	0.05	0.02	0.02	.594#	
13,14-EDP	0.02	0.02	0.02	0.01	.878#	
16,17-EDP−233	0.02	0.02	0.02	0.02	.010#	
19,20-EDP	0.49	1.43	0.26	0.46	.433#	
7,8-DiHDPA	0.01	0.01	0.01	0.02	.272#	
10,11-DiHDPA	0.01	0.01	0.01	0.01	.477#	
13,14-DiHDPA	0.01	0.01	0.01	0.01	.218	
16,17-DiHDPA	0.09	0.07	0.10	0.52	.136#	
5-HETE	0.09	0.11	0.08	0.07	.530#	
8-HETE	0.14	0.09	0.14	0.06	.695#	
9-HETE	0.09	0.12	0.09	0.07	.388#	
11-HETE	0.24	0.12	0.25	0.11	.893	
12-HETE	4.44	5.60	4.34	3.23	.875#	
15-HETE	0.41	0.22	0.54	0.29	.236	
16-HETE	0.25	0.10	0.30	0.14	.209#	
17-HETE	0.11	0.19	0.11	0.15	.530#	
18-HETE	0.03	0.05	0.03	0.03	.875#	
19-HETE	0.04	0.02	0.04	0.03	.068#	
20-HETE	0.35	0.19	0.39	0.18	.695#	
5-HEPE	0.15	0.42	0.09	0.12	.433#	
8-HEPE	0.08	0.23	0.07	0.22	1.000#	
9-HEPE	0.08	0.25	0.05	0.16	.754#	
12-HEPE	3.26	9.64	2.42	7.17	1.000#	
15-HEPE	0.13	0.35	0.12	0.28	.433#	
18-HEPE	0.58	1.67	0.44	1.18	.814#	
19-HEPE	1.45	4.24	0.78	1.35	.136#	
20-HEPE	0.24	0.50	0.09	0.20	.893#	
4-HDHA	0.23	0.73	0.14	0.40	.695#	
-HDHA	0.05	0.14	0.02	0.05	.209#	
8-HDHA	0.07	0.19	0.04	0.09	.272#	

(Continues)

Publication Ⅱ

TABLE 4 (Continued)

Amount ng/ml	Pre-HD (Mean	SD)	Post-HD (mean	SD)	p-value Paired t-Test ([#]paired Wilcoxon Test)	Data grouping effect
10-HDHA	0.23	0.50	0.18	0.33	.583[#]	
11-HDHA	0.28	0.74	0.18	0.34	.638[#]	
13-HDHA	0.10	0.20	0.08	0.12	.814[#]	
14-HDHA	1.30	2.23	1.17	1.61	.638[#]	
16-HDHA	0.12	0.37	0.09	0.23	.182[#]	
17-HDHA	0.85	2.33	0.63	1.24	.308[#]	
20-HDHA	0.16	0.37	0.12	0.16	.136[#]	
21-HDHA	2.02	5.94	1.06	2.35	.754[#]	
22-HDHA	1.10	3.00	0.61	1.20	.638[#]	
TXB2	0.14	0.16	0.10	0.08	.678[#]	
11-dehydro TXB2	n.d.		n.d.			
PGE2	0.04	0.03	0.03	0.03	.540	
15-keto-PGE2	n.d.		n.d.			
13,14-dihydro−15-keto-PGE2	n.d.		n.d.			
PGD2	0.03	0.02	0.02	0.01	.674[#]	
13,14-dihydro−15-keto-PGD2	n.d.		n.d.			
PGJ2	n.d.		n.d.			
15-deoxy-delta 12,14-PGJ2	n.d.		n.d.			
PGF2a8-iso-PGF2a	n.d.		n.d.			
TXB3	n.d.		n.d.			
11-dehydro TXB3	n.d.		n.d.			
PGE3	n.d.		n.d.			
6(S)-LXA4	n.d.		n.d.			
LXA4	n.d.		n.d.			
15(R)-LXA4	n.d.		n.d.			
LXB4	n.d.		n.d.			
LXA5	n.d.		n.d.			
MAR 1	n.d.		n.d.			
7-epi-MAR1	n.d.		n.d.			
RvD1	n.d.				n.d.	
17(R)-RvD1	n.d.		n.d.			
RvD2	n.d.		n.d.			
RvD3	n.d.		n.d.			
RvD5	n.d.		n.d.			
RvE1	n.d.		n.d.			

and 5-HETE are key markers to discriminate ESRD patients from healthy controls (Hu, 2018). It is unlikely that these changes occurred in response to chronic dialysis treatment since altered levels in 9,10-EpOME, 12,13-EpOME, 5,6-DHET, and 5-HETE levels were observed in patients with CKD before starting renal replacement therapy (Hu, 2018). While the ESRD patients in (Hu, 2018) were uremic Asians (eGFR 5–6 ml/min/1.73 m^2) and recruited before beginning renal replacement therapy for fistula construction surgery, our patients were Caucasian ESRD patients undergoing regular, thrice weekly dialysis. Nonetheless, we observed similar changes in 9,10-EpOME, 12,13-EpOME, 5,6-DHET, and 5-HETE levels. However, our study revealed also other oxylipins that is, specific signature, which are up- or down-regulated in plasma of the ESRD patients. The extent to which they exhibit beneficial or detrimental cardiovascular effects,

Publication Ⅱ

TABLE 5 Effects of hemodialysis on oxylipins and their ratios in the CKD patients before (pre-HD) and at cessation (post-HD) of hemodialysis ($n = 15$)

Epoxides or Diols (ng/mL)	Pre-HD (Mean	SD)	Post-HD (Mean	SD)	p-value Paired Wilcoxon test	Data grouping effect
A. Concentrations of individual total epoxides plus their respective diols in plasma.						
9,10-EpOME + 9,10-DiHOME	62.70	55.05	152.05	160.20	.035	Post HD > Pre-HD
12,13-EpOME + 12,13-DiHOME	62.12	60.44	146.11	144.84	.030	
5,6-EET + 5,6-DHET	49.70	55.40	128.30	131.89	.035	
5,6-EEQ + 5,6-DiHETE	29.28	33.64	87.44	113.99	.025	
8,9-EEQ + 8,9-DiHETE	1.89	2.14	5.33	6.90	.017	
11,12-EEQ + 11,12-DiHETE	1.52	1.67	4.46	5.58	.035	
14,15-EEQ + 14,15-DiHETE	1.27	1.43	3.60	4.50	.030	
17,18-EEQ + 17,18-DiHETE	4.70	5.01	14.10	18.00	.049	
7,8-EDP + 7,8-DiHDPA	4.03	2.51	9.97	8.70	.035	
19,20-EDP + 19,20-DiHDPA	8.82	6.19	27.45	27.56	.035	
8,9-EET + 8,9-DHET	14.65	14.23	30.82	28.47	.042	
14,15-EET + 14,15-DHET	35.52	40.42	104.25	115.45	.049	
10,11-EDP + 10,11-DiHDPA	0.81	0.57	2.05	2.22	.042	
13,14-EDP + 13,14-DiHDPA	0.49	0.41	1.37	1.63	.042	
16,17-EDP + 16,17-DiHDPA	5.53	4.70	17.58	18.59	.042	
11,12-EET + 11,12-DHET	8.01	8.96	13.36	11.42	.119	No effect or not significant

(Continues)

Publication Ⅱ

TABLE 5 (Continued)

Epoxides or Diols (ng/mL)	Pre-HD (Mean	SD)	Post-HD (Mean	SD)	*p*-value Paired Wilcoxon test	Data grouping effect
B. Ratios estimated using total concentrations of epoxides and diols in plasma.						
Ratio (9,10-DiHOME + 12,13-DiHOME) / (9,10-EpOME + 12,13-EpOME)	0.1624	0.3117	0.2179	0.4314	.670	No effect or not significant
Ratio (5,6-DHET + 8,9-DHET + 11,12-DHET + 14,15-DHET) / (5,6-EET + 8,9-EET + 11,12 EET + 14,15-EET)	0.0475	0.0482	0.0460	0.0634	.391	
Ratio (5,6-DiHETE + 8,9-DiHETE + 11,12-DiHETE + 14,15-DiHETE + 17,18-DiHETE) / (5,6-EEQ + 8,9-EEQ + 11,12-EEQ + 14,15-EEQ + 17,18-EEQ)	0.0279	0.0322	0.0353	0.0557	.626	

(Continues)

Publication Ⅱ

TABLE 5 (Continued)

Epoxides or Diols (ng/mL)	Pre-HD (Mean	SD)	Post-HD (Mean	SD)	*p*-value Paired Wilcoxon test	Data grouping effect
Ratio (7,8-DiHDPA + 10,11-DiHDPA + 13,14-DiHDPA + 16,17-DiHDPA + 19,20-DiHDPA) / (7,8-EDP + 10,11-EDP + 13,14-EDP + 16,17-EDP + 19,20-EDP)	0.1160	0.1462	0.1369	0.2039	0.502	

Ratios	Pre-HD (Mean	SD)	Post-HD (Mean	SD)	*p*-value Paired Wilcoxon test	Data grouping effect
C. Ratios estimated using individual total concentrations of epoxides and their diols in plasma.					
9,10-DiHOME / 9,10-EpOME	0.1881	0.3877	0.2402	0.4617	.903	No effect or not significant
12,13-DiHOME / 12,13-EpOME	0.1361	0.2361	0.1966	0.4089	.583	
5,6-DHET / 5,6-EET	0.0379	0.0401	0.0368	0.0537	.296	
8,9-DHET / 8,9-EET	0.1207	0.1062	0.1042	0.1197	.268	
11,12-DHET / 11,12-EET	0.0712	0.0616	0.0674	0.0650	.670	
14,15-DHET / 14,15-EET	0.0206	0.0218	0.0229	0.0313	.463	
5,6-DiHETE / 5,6-EEQ	0.0196	0.0210	0.0204	0.0313	.426	
8,9-DiHETE / 8,9-EEQ	0.0272	0.0447	0.0298	0.0494	.670	
11,12-DiHETE / 11,12-EEQ	0.0157	0.0297	0.0213	0.0460	.761	

(Continues)

Publication Ⅱ

T A B L E 5   (Continued)

Ratios	Pre-HD (Mean	SD)	Post-HD (Mean	SD)	*p*-value Paired Wilcoxon test	Data grouping effect
14,15-DiHETE / 14,15-EEQ	0.0438	0.0611	0.0768	0.1360	.761	
17,18-DiHETE / 17,18-EEQ	0.07161	0.0836	0.1085	0.1720	.855	
7,8-DiHDPA / 7,8-EDP	0.0912	0.0956	0.0820	0.1138	.391	
10,11-DiHDPA / 10,11-EDP	0.0924	0.1188	0.0928	0.1449	.903	
13,14-DiHDPA / 13,14-EDP	0.1745	0.1935	0.1417	0.1715	.502	
16,17-DiHDPA / 16,17-EDP	0.0329	0.0354	0.0415	0.0595	.583	
19,20-DiHDPA / 19,20-EDP	0.1952	0.2757	0.2417	0.3745	.542	

possibly in metabolite-interacting networks, remains to be explored. Furthermore, future studies can clarify whether specific underlying renal diseases may have specific oxylipin profiles to discriminate between ESRD patients.

4.1 | CYP epoxy metabolites

Hemodialysis increased all four subclasses of CYP epoxy metabolites (9,10-EpOME, 12,13-EpOME, 9,10-DiHOME, 12,13-DiHOME, 5,6-EET, 14,15-EET, 8,9-DHET, 11,12-DHET, 8,9-EEQ, 11,12-EEQ, 14,15-EEQ, 17,18-EEQ, 14,15-DiHETE, 17,18-DiHETE, 7,8-EDP, 10,11-EDP, 13,14-EDP, 16,17-EDP, 19,20-EDP, 7,8-DiHDPA, 10,11-DiHDPA, 13,14-DiHDPA, 16,17-DiHDPA, and 19,20-DiHDPA). Although these changes are unlikely related to altered sEH activity, but rather to the dialysis treatment itself, reduced in vivo sEH activity in CKD/ESRD (Zhang, 2015) may have contributed to the increased accumulation of all four epoxy metabolite classes in our CKD patients, compared to the healthy control subjects.

4.2 | EETs/DHETs

We demonstrated that hemodialysis increased EETs/DHETs levels, as detected for 5,6-EET, 14,15-EET, 8,9-DHET, and 11,12-DHET. Endothelial cells are reservoirs of EETs and the primary source of plasma EETs (Jiang, Anderson,

& McGiff, 2010, 2012; Jiang, 2011; Schunck, 2017), which produce profibrinolysis and reduce inflammation, vascular tone, and blood pressure (Jiang, Anderson, & McGiff, 2010, 2012; Jiang, 2011). 5,6-DHET as like 5,6-EET can produce vasodilation (Hercule, 2009; Lu, 2001), which could contribute to the cardiovascular response during maximal exercise (Gollasch, 2019a). The mechanisms of how epoxides and diols are released from the tissues and eventually become constituents of circulating lipoproteins are largely unknown, making it difficult to explain our findings. Cells preferentially release DHETs while storing the EETs (Roman, 2002), suggesting that certain diols might be overrepresented in the circulating blood compared with the respective diol/epoxide ratios (Fischer, 2014). Our data support the idea that DHETs/EETs are attractive signaling molecules for cardiovascular effects in ESRD because they are potent vasodilators (Campbell & Fleming, 2010), which could counteract circulating vasoconstrictor substances during dialysis. Therapeutic sEH inhibition is considered a novel approach for enhancing the beneficial biological activity of EETs (Spector & Kim, 2015). However, presumably higher levels of EETs in blood and tissue in vivo may have also detrimental cardiovascular side effects (Gschwendtner, 2008; Hutchens, 2008; Wutzler, 2013). Of note, levels of all four EETs (5,6-EET, 8,9-EET, 11,12-EET, and 14,15-EET) were high in the ESRD patients compared to the control. The extent to which this increase has beneficial or detrimental cardiovascular effects remains to be explored.

Publication Ⅱ

4.3 | EpOMEs/DiHOMEs

We observed increases in 9,10-EpOME, 12,13-EpOME, 9,10-DiHOME, and 12,13-DiHOME during dialysis. 9,10-EpOME (leukotoxins A) and 12,13-EpOME (leukotoxin B) were initially found to be generated by neutrophils during the oxidative burst to combat bacterial infection (Thompson & Hammock, 2007). Recent findings suggest that EpOMEs exhibit cardiodepressant (Fukushima, 1988; Siegfried, 1990; Sugiyama, 1987) and vasoactive properties, the latter by endothelial NO and O(2)(*-) production (Okamura, 2002). Moreover, 9,10-EpOME and 12,13-EpOME can exhibit vasoconstrictor responses in severe cardiac ischemia (Dudda, Spiteller, & Kobelt, 1996; Siegfried, 1990) and could contribute to the cardiovascular response during maximal exercise (Gollasch, 2019a). New data suggest that DiHOMEs cause detrimental effects on postischemic cardiac function (Bannehr, 2019b; Chaudhary, 2013). Our data support the notion that increases in EpOMEs/DiHOMEs could affect cardiac ischemia and hemodynamics in dialysis patients.

4.4 | EEQs/DiHETEs

We observed increases in 8,9-EEQ, 11,12-EEQ, 14,15-EEQ, 17,18-EEQ, 14,15-DiHETE, and 17,18-DiHETE during dialysis. While the putative biological functions of EEQs/DiHETEs have not received much attention, 17,18-EEQ has been identified as a potent vasodilator, which seems to be even more potent than EETs (Hercule, 2007; Lauterbach, 2002). Their diols could contribute to the cardiovascular response during maximal exercise (Gollasch, 2019a). The mechanisms of how EEQs/DiHETEs are released from the tissues are largely unknown, making it difficult to explain our findings. Based on our calculations of diol/epoxide ratios, we have no evidence that the higher levels of 14,15-DiHETE, 17,18-DiHETE result from in vivo sEH enzyme activation. Nevertheless, the role of circulating EEQs/DiHETEs has yet to be integrated into a physiological and pathophysiological context. This is particularly important since drugs that mimic 17,18-EEQ are viewed as novel promising drug candidates to overcome limitations of dietary EPA/DHA (C20:5 n–3/22:6 n–3) supplementation for cardiovascular health benefits (Schunck, 2017).

4.5 | EDPs/DiHDPAs

We observed increases in 7,8-EDP, 10,11-EDP, 13,14-EDP, 16,17-EDP, 19,20-EDP, 7,8-DiHDPA, 10,11-DiHDPA, 13,14-DiHDPA, 16,17-DiHDPA, and 19,20-DiHDPA during dialysis. Little is known about the biological functions of EDPs/DiHDPAs. 16,17-EDP and 19,20-EDP are potent vasodilators in coronary, pulmonary, and mesenteric

arteries. They lower blood pressure and exhibit cardioprotection by preservation of mitochondrial function (Morin, Fortin, & Rousseau, 2011; Schunck, 2017). Based on our calculations of diol/epoxide ratios, we have no evidence that the higher levels of DiHPAs metabolites observed in our study result from in vivo sEH enzyme activation. Our data indicate that both EDPs and DiHPAs metabolites are novel candidates for vasoactive substances potentially released by dialysis to affect hemodynamics in these conditions.

4.6 | LOX/CYP ω/(ω-1)-hydroxylase metabolites

We found that hemodialysis increased several LOX/CYP ω/(ω-1)-hydroxylase metabolites (13-HODE, 20-HETE, 5-HEPE, 15-HEPE, 18-HEPE, 19-HEPE, 7-HDHA, and 11-HDHA). Little is known about the biological functions of those metabolites. 13-HODE inhibits platelets (Buchanan, 1985) and could represent an important player in redox and immune homeostasis (Pecorelli, 2019; Vangaveti, 2018). 20-HETE is a potent vasoconstrictor, which modulates intracellular signal transduction pathways in neovascularization (Chen, 2019) and in renal and cardiac ischemia-reperfusion injury (Han, 2013; Hoff, 2011). Upregulation of 20-HETE contributes to inflammation, oxidative stress, endothelial dysfunction, and increased peripheral vascular resistance (Waldman, 2016). 5-HEPE promotes bovine neutrophil chemotaxis in vitro, but less potently than 5-HETE (Heidel, 1989). 18-HEPE is released by macrophages to inhibit cardiac fibrosis and inflammation in mice (Endo, 2014). Of note, 18-HEPE appears to downregulate proinflammatory and pro-proliferative factors, possibly via conversion to E-series resolvins (Sapieha, 2011). These resolvins have effects similar to the D-series resolvins, markedly reducing neutrophile infiltration, decreasing proinflammatory cytokines, and enhancing the resolution of inflammation (Sapieha, 2011). We have no evidence that hemodialysis affected resolvins, prostaglandins, thromboxanes, or other LOX/CYP ω/(ω-1)-hydroxylase metabolites in our patients (Shelmadine, 2017). Only few studies detected small changes in PGE2 or PGF2a (Losonczy, 1990; Schultze, 1984) and 5/12-HETE levels (Dolegowska, 2012) 4-HDHA is a mediator of antiangiogenic effects of n-3 PUFAs (Sapieha, 2011). Since we found that the majority of LOX metabolites measured were not affected by dialysis, we suggest that these metabolites are unlikely to play important roles in this scenario.

5 | CONCLUSIONS

To our knowledge, this is the first study to assess the impact of single hemodialysis treatment oxylipins in plasma using

Publication II

large-scale lipidomics. We confirmed our hypothesis that the oxylipins status is influenced by hemodialysis treatment. Our data demonstrate that all four subclasses of CYP epoxy metabolites and a number of LOX/CYP ω/(ω-1)-hydroxylase metabolites are increased by the treatment. Moreover, ESRD patients undergoing regular dialysis show marked differences in plasma oxylipin profiles, that is, specific signatures, compared to control subjects. Future research is required to determine the contribution of the identified oxylipins in reducing the risk from CVD in patients with kidney disease.

ACKNOWLEDGMENTS

CONFLICT OF INTEREST
None.

AUTHOR CONTRIBUTIONS
BG, MG, and FCL planned and designed the experimental studies. ID and MR performed the HPLC–MS spectrometry experiments. All authors contributed to the implementation and analyses of the experiments. BG drafted the article, and all authors, contributed to its completion.

ORCID
Benjamin Gollasch https://orcid.org/0000-0001-5267-518X

REFERENCES
Afshinnia, F., Zeng, L. Byun, J., Wernisch, S., Deo, R., Chen, J., … Townsend, R. R.. (2018). Elevated lipoxygenase and cytochrome P450 products predict progression of chronic kidney disease. *Nephrology, Dialysis, Transplantation*. https://doi.org/10.1093/ndt/gfy232

Bannehr, M., Löhr, L., Gelep, J., Haverkamp, W., Schunck, W. H., Gollasch, M., & Wutzler, A. (2019). Linoleic acid metabolite DiHOME decreases post-ischemic cardiac recovery in murine hearts. *Cardiovascular Toxicology*, *19*(4), 365–371.

Buchanan, M. R., Haas, T. A., Lagarde, M., & Guichardant, M. (1985). 13-Hydroxyoctadecadienoic acid is the vessel wall chemorepellant factor, LOX. *Journal of Biological Chemistry*, *260*(30), 16056–16059.

Campbell, W. B., & Fleming, I. (2010). Epoxyeicosatrienoic acids and endothelium-dependent responses. *Pflugers Archiv. European Journal of Physiology*, *459*(6), 881–895.

Campbell, W. B., Gebremedhin, D., Pratt, P. F., & Harder, D. R. (1996). Identification of epoxyeicosatrienoic acids as endothelium-derived hyperpolarizing factors. *Circulation Research*, *78*(3), 415–423.

Chaudhary, K. R., Zordoky, B. N., Edin, M. L., Alsaleh, N., El-Kadi, A. O., Zeldin, D. C., & Seubert, J. M. (2013). Differential effects of soluble epoxide hydrolase inhibition and CYP2J2 overexpression on postischemic cardiac function in aged mice. *Prostaglandins & Other Lipid Mediators*, *104–105*, 8–17.

Chen, L., Tang, S., Zhang, F. F., Garcia, V., Falck, J. R., Schwartzman, M. L., … Guo, A. M. (2019). CYP4A/20-HETE regulates

ischemia-induced neovascularization via its actions on endothelial progenitor and preexisting endothelial cells. *American Journal of Physiology. Heart and Circulatory Physiology*, *316*(6), H1468–H1479. https://doi.org/10.1152/ajpheart.00690.2018

Dolegowska, B., Błogowski, W., Stępniewska, J., Safranow, K., Jakubowska, K., & Olszewska, M. (2012). Presence of glucose in dialyzing fluid and synthesis of selected lipoxygenase-derived eicosanoids during hemodialysis. *International Urology and Nephrology*, *44*(6), 1799–1804. https://doi.org/10.1007/s11255-011-0089-5

Dudda, A., Spiteller, G., & Kobelt, F. (1996). Lipid oxidation products in ischemic porcine heart tissue. *Chemistry and Physics of Lipids*, *82*(1), 39–51.

Endo, J., Sano, M., Isobe, Y., Fukuda, K., Kang, J. X., Arai, H., & Arita, M. (2014). 18-HEPE, an n-3 fatty acid metabolite released by macrophages, prevents pressure overload-induced maladaptive cardiac remodeling. *Journal of Experimental Medicine*, *211*(8), 1673–1687. https://doi.org/10.1084/jem.20132011

Fan, F., & Roman, R. J. (2017). Effect of Cytochrome P450 metabolites of arachidonic acid in nephrology. *Journal of the American Society of Nephrology*, *28*(10), 2845–2855. https://doi.org/10.1681/ASN.2017030252

Fischer, R., Konkel, A., Mehling, H., Blossey, K., Gapelyuk, A., Wessel, N., … Schunck, W. (2014). Dietary omega-3 fatty acids modulate the eicosanoid profile in man primarily via the CYP-epoxygenase pathway. *Journal of Lipid Research*, *55*(6), 1150–1164. https://doi.org/10.1194/jlr.M047357

Fukushima, A., Hayakawa, M., SUGIYAMA, S., Ajioka, M., Ito, T., Satake, T., & Ozawa, T. (1988). Cardiovascular effects of leukotoxin (9, 10-epoxy-12-octadecenoate) and free fatty acids in dogs. *Cardiovascular Research*, *22*(3), 213–218. https://doi.org/10.1093/cvr/22.3.213

Gabbs, M., Leng, S., Devassy, J. G., Monirujjaman, M., & Aukema, H. M. (2015). Advances in our understanding of oxylipins derived from dietary PUFAs. *Advances in Nutrition*, *6*(5), 513–540. https://doi.org/10.3945/an.114.007732

Goetzl, E. J. (1980). A role for endogenous mono-hydroxy-eicosatetraenoic acids (HETEs) in the regulation of human neutrophil migration. *Immunology*, *40*(4), 709–719.

Gollasch, B., Dogan, I., Rothe, M., Gollasch, M., & Luft, F. C. (2019). Maximal exercise and plasma cytochrome P450 and lipoxygenase mediators: A lipidomics study. *Physiological Reports*, *7*(13), e14165. https://doi.org/10.14814/phy2.14165

Gollasch, B., Dogan, I., Rothe, M., Gollasch, M., & Luft, F. C. (2019). Maximal exercise and erythrocyte fatty-acid status: A lipidomics study. *Physiological Reports*, *7*(8), e14040.

Gollasch, B., Dogan, I., Rothe, M., Gollasch, M., & Luft, F. C. (2020). Effects of hemodialysis on blood fatty acids. *Physiol Rep*, *8*(2), e14332. https://doi.org/10.14814/phy2.14332

Gordon, E. E., Gordon, J. A., & Spector, A. A. (1991). HETEs and coronary artery endothelial cells: Metabolic and functional interactions. *American Journal of Physiology*, *261*(4 Pt 1), C623–C633.

Graber, M. N., Alfonso, A., & Gill, D. L. (1997). Recovery of Ca2+ pools and growth in Ca2+ pool-depleted cells is mediated by specific epoxyeicosatrienoic acids derived from arachidonic acid. *Journal of Biological Chemistry*, *272*(47), 29546–29553.

Gschwendtner, A., Ripke, S., Freilinger, T., Lichtner, P., Müller-Myhsok, B., Wichmann, H. E., … Dichgans, M. (2008). Genetic variation in soluble epoxide hydrolase (EPHX2) is associated with an increased risk of ischemic stroke in white Europeans. *Stroke*, *39*(5), 1593–1596.

Publication Ⅱ

Guidelines - Recommendations - Felasa | Federation for Laboratory Animal Science Associations. [Internet]; Available from: http://www.felasa.eu/recommendations/guidelines/

Han, Y., Zhao, H., Tang, H., Li, X., Tan, J., Zeng, Q., & Sun, C. (2013). 20-Hydroxyeicosatetraenoic acid mediates isolated heart ischemia/reperfusion injury by increasing NADPH oxidase-derived reactive oxygen species production. *Circulation Journal*, *77*(7), 1807–1816. https://doi.org/10.1253/circj.CJ-12-1211

Heidel, J. R., Taylor, S. M., Laegreid, W. W., Silflow, R. M., Liggitt, H. D., & Leid, R. W. (1989). In vivo chemotaxis of bovine neutrophils induced by 5-lipoxygenase metabolites of arachidonic and eicosapentaenoic acid. *American Journal of Pathology*, *134*(3), 671–676.

Hercule, H. C., Salanova, B., Essin, K., Honeck, H., Falck, J. R., Sausbier, M., … Gollasch, M. (2007). The vasodilator 17,18-epoxyeicosatetraenoic acid targets the pore-forming BK alpha channel subunit in rodents. *Experimental Physiology*, *92*(6), 1067–1076.

Hercule, H. C., Schunck, W. H., Gross, V., Seringer, J., Leung, F. P., Weldon, S. M., …Gollasch, M. (2009). Interaction between P450 eicosanoids and nitric oxide in the control of arterial tone in mice. *Arteriosclerosis, Thrombosis, and Vascular Biology*, *29*(1), 54–60. https://doi.org/10.1161/ATVBAHA.108.171298

Hoff, U., Lukitsch, I., Chaykovska, L., Ladwig, M., Arnold, C., Manthati, V. L., … Schunck, W.-H. (2011). Inhibition of 20-HETE synthesis and action protects the kidney from ischemia/reperfusion injury. *Kidney International*, *79*(1), 57–65. https://doi.org/10.1038/ki.2010.377

Hu, D. Y., Luo, Y., Li, C. B., Zhou, C. Y., Li, X. H., Peng, A., & Liu, J. Y. (2018). Oxylipin profiling of human plasma reflects the renal dysfunction in uremic patients. *Metabolomics*, *14*(8), 104.

Hutchens, M. P., Nakano, T., Dunlap, J., Traystman, R. J., Hurn, P. D., & Alkayed, N. J. (2008). Soluble epoxide hydrolase gene deletion reduces survival after cardiac arrest and cardiopulmonary resuscitation. *Resuscitation*, *76*(1), 89–94. https://doi.org/10.1016/j.resuscitation.2007.06.031

Jiang, H., Anderson, G. D., & McGiff, J. C. (2010). Red blood cells (RBCs), epoxyeicosatrienoic acids (EETs) and adenosine triphosphate (ATP). *Pharmacological Reports*, *62*(3), 468–474. https://doi.org/10.1016/S1734-1140(10)70302-9

Jiang, H., Anderson, G. D., & McGiff, J. C. (2012). The red blood cell participates in regulation of the circulation by producing and releasing epoxyeicosatrienoic acids. *Prostaglandins & Other Lipid Mediators*, *98*(3–4), 91–93. https://doi.org/10.1016/j.prostaglandins.2011.11.008

Jiang, H., Quilley, J., Doumad, A. B., Zhu, A. G., Falck, J. R., Hammock, B. D., …Carroll, M. A. (2011). Increases in plasma trans-EETs and blood pressure reduction in spontaneously hypertensive rats. *American Journal of Physiology. Heart and Circulatory Physiology*, *300*(6), H1990–H1996.

Kim, K. M., Jung, B. H., Paeng, K. J., Kim, S. W., & Chung, B. C. (2004). Alteration of plasma total F2-isoprostanes before and after hemodialysis in end-stage renal disease patients. *Prostaglandins Leukotrienes and Essential Fatty Acids*, *70*(5), 475–478.

Kovac, A., Boldizsar, J., Földes, O., & Pavlovic, M. (1992). Prostaglandins during haemodialysis treatment. *Materia Medica Polona*, *24*(4), 241–242.

Lauterbach, B., Barbosa-Sicard, E., Wang, M. H., Honeck, H., Kärgel, E., Theuer, J., … Schunck, W. H. (2002). Cytochrome P450-dependent eicosapentaenoic acid metabolites are novel BK channel activators. *Hypertension*, *39*(2 Pt 2), 609–613.

Losonczy, G., Walter, J., Mucha, I., & Taraba, I. (1990). Changes of arterial prostaglandin E2 during haemodialysis. *Nephrology, Dialysis, Transplantation*, *5*(11), 937–941. https://doi.org/10.1093/ndt/5.11.937

Lu, T., Katakam, P. V., VanRollins, M., Weintraub, N. L., Spector, A. A., & Lee, H. C. (2001). Dihydroxyeicosatrienoic acids are potent activators of Ca(2+)-activated K(+) channels in isolated rat coronary arterial myocytes. *Journal of Physiology*, *534*(Pt 3), 651–667.

Luft, F. C. (2000). Renal disease as a risk factor for cardiovascular disease. *Basic Research in Cardiology*, *95*(Suppl 1), I72–I76. https://doi.org/10.1007/s003950070013

McGill, R. L., Bragg-Gresham, J. L., He, K., Lacson, E. K. Jr, Miskulin, D. C., & Saran, R. (2019). Chronic disease burdens of incident U.S. dialysis patients, 1996–2015. *Clinical Nephrology*.

Morin, C., Fortin, S., & Rousseau, E. (2011). 19,20-EpDPE, a bioactive CYP450 metabolite of DHA monoacyglyceride, decreases Ca(2)(+) sensitivity in human pulmonary arteries. *American Journal of Physiology. Heart and Circulatory Physiology*, *301*(4), H1311–H1318.

Nayeem, M. A. (2018). Role of oxylipins in cardiovascular diseases. *Acta Pharmacologica Sinica*, *39*(7), 1142–1154. https://doi.org/10.1038/aps.2018.24

Okamura, S., Ameshima, S., Demura, Y., Ishizaki, T., Matsukawa, S., & Miyamori, I. (2002). Leukotoxin-activated human pulmonary artery endothelial cell produces nitric oxide and superoxide anion. *Pulmonary Pharmacology & Therapeutics*, *15*(1), 25–33.

Pecorelli, A., Cervellati, C., Cordone, V., Amicarelli, F., Hayek, J., & Valacchi, G. (2019). 13-HODE, 9-HODE and ALOX15 as potential players in Rett syndrome oxinflammation. *Free Radical Biology and Medicine*, *134*, 598–603.

Roman, R. J. (2002). P-450 metabolites of arachidonic acid in the control of cardiovascular function. *Physiological Reviews*, *82*(1), 131–185.

Sapieha, P., Sapieha, P., Stahl, A., Chen, J., Seaward, M. R., Willett, K. L., … Carughi, A. (2011). 5-Lipoxygenase metabolite 4-HDHA is a mediator of the antiangiogenic effect of omega-3 polyunsaturated fatty acids. *Science Translational Medicine*, *3*(69), p. 69ra12.

Schultze, G., Maiga, M., Neumayer, H. H., Wagner, K., Keller, F., Molzahn, M., & Nigam, S. (1984). Prostaglandin E2 promotes hypotension on low-sodium hemodialysis. *Nephron*, *37*(4), 250–256.

Schunck, W. H., Konkel, A., Fischer, R., & Weylandt, K. H. (2017). Therapeutic potential of omega-3 fatty acid-derived epoxyeicosanoids in cardiovascular and inflammatory diseases. *Pharmacology & Therapeutics*. https://doi.org/10.1016/j.pharmthera.2017.10.016

Shelmadine, B. D., Bowden, R. G., Moreillon, J. J., Cooke, M. B., Yang, P., Deike, E., … Wilson, R. L. (2017). A Pilot Study to Examine the Effects of an Anti-inflammatory Supplement on Eicosanoid Derivatives in Patients with Chronic Kidney Disease. *Journal of Alternative and Complementary Medicine*, *23*(8), 632–638. https://doi.org/10.1089/acm.2016.0007

Siegfried, M. R., Aoki, N., Lefer, A. M., Elisseou, E. M., & Zipkin, R. E. (1990). Direct cardiovascular actions of two metabolites of linoleic acid. *Life Sciences*, *46*(6), 427–433. https://doi.org/10.1016/0024-3205(90)90086-7

Spector, A. A., Fang, X., Snyder, G. D., & Weintraub, N. L. (2004). Epoxyeicosatrienoic acids (EETs): Metabolism and biochemical function. *Progress in Lipid Research*, *43*(1), 55–90. https://doi.org/10.1016/S0163-7827(03)00049-3

Spector, A. A., & Kim, H. Y. (2015). Cytochrome P450 epoxygenase pathway of polyunsaturated fatty acid metabolism. *Biochimica*

Publication Ⅱ

Et Biophysica Acta, *1851*(4), 356–365. https://doi.org/10.1016/j.bbalip.2014.07.020

Stenson, W. F., & Parker, C. W. (1980). Monohydroxyeicosatetraenoic acids (HETEs) induce degranulation of human neutrophils. *The Journal of Immunology*, *124*(5), 2100–2104.

Sugiyama, S., Hayakawa, M., Nagai, S., Ajioka, M., & Ozawa, T. (1987). Leukotoxin, 9, 10-epoxy-12-octadecenoate, causes cardiac failure in dogs. *Life Sciences*, *40*(3), 225–231.

Thompson, D. A., & Hammock, B. D. (2007). Dihydroxyoctadecamonoenoate esters inhibit the neutrophil respiratory burst. *Journal of Biosciences*, *32*(2), 279–291. https://doi.org/10.1007/s12038-007-0028-x

Tourdot, B. E., Ahmed, I., & Holinstat, M. (2014). The emerging role of oxylipins in thrombosis and diabetes. *Front Pharmacol*, *4*, 176.

Valone, F. H., Franklin, M., Sun, F. F., & Goetzl, E. J. (1980). Alveolar macrophage lipoxygenase products of arachidonic acid: Isolation and recognition as the predominant constituents of the neutrophil chemotactic activity elaborated by alveolar macrophages. *Cellular Immunology*, *54*(2), 390–401.

Vangaveti, V., Shashidhar, V., Collier, F., Hodge, J., Rush, C., Malabu, U. … Kennedy, R. L. (2018). 9- and 13-HODE regulate fatty acid binding protein-4 in human macrophages, but does not involve HODE/GPR132 axis in PPAR-gamma regulation of FABP4. *Therapeuti Advances in Endocrinology and Metabolism*, *9*(5), 137–150.

Waldman, M., Peterson, S. J., Arad, M., & Hochhauser, E. (2016). The role of 20-HETE in cardiovascular diseases and its risk factors. *Prostaglandins & Other Lipid Mediators*, *125*, 108–117. https://doi.org/10.1016/j.prostaglandins.2016.05.007

Wutzler, A., Kestler, C., Perrot, A., Loehr, L., Huemer, M., Parwani, A. S. … Haverkamp, W. (2013). Variations in the human soluble epoxide hydrolase gene and recurrence of atrial fibrillation after catheter ablation. *International Journal of Cardiology*, *168*(4), 3647–3651. https://doi.org/10.1016/j.ijcard.2013.05.010

Zhang, K., Liu, Y., Liu, X., Chen, J., Cai, Q., Wang, J., & Huang, H. (2015). Apocynin improving cardiac remodeling in chronic renal failure disease is associated with up-regulation of epoxyeicosatrienoic acids. *Oncotarget*, *6*(28), 24699–24708. https://doi.org/10.18632/oncotarget.5084

Publication Ⅱ

9.3 Publication #3

Hemodialysis and erythrocyte epoxy fatty acids.

Not included in SCIE and SSCI.

Physiological Reports is a peer-reviewed open access online only scientific journal covering original research in all areas of physiology. It is published by Wiley-Blackwell on behalf of The Physiological Society and the American Physiological Society.

ORIGINAL RESEARCH

The Physiological Society · american physiological society · **Physiological** Reports

Hemodialysis and erythrocyte epoxy fatty acids

Benjamin Gollasch[1,2] (ID) | **Guanlin Wu**[1,3] | **Tong Liu**[1] | **Inci Dogan**[4] | **Michael Rothe**[4] | **Maik Gollasch**[1,5,6] | **Friedrich C. Luft**[5]

[1]Experimental and Clinical Research Center (ECRC), A Joint Institution Between the Charité University Medicine and Max Delbrück Center (MDC) for Molecular Medicine, Berlin-Buch, Germany

[2]HELIOS Klinikum Berlin-Buch, Berlin, Germany

[3]Max Delbrück Center for Molecular Medicine (MDC) in the Helmholtz Association, Berlin, Germany

[4]LIPIDOMIX GmbH, Berlin, Germany

[5]Nephrology/Intensive Care Section, Charité Campus Virchow, Berlin, Germany

[6]Department of Internal and Geriatric Medicine, University Medicine Greifswald, Greifswald, Germany

Correspondence
Benjamin Gollasch, Experimental and Clinical Research Center (ECRC), Lindenberger Weg 80, 13125 Berlin, Germany.
Email: benjamin.gollasch@charite.de

Abstract

Fatty acid products derived from cytochromes P450 (CYP) monooxygenase and lipoxygenase (LOX)/CYP ω/(ω-1)-hydroxylase pathways are a superclass of lipid mediators with potent bioactivities. Whether or not the chronic kidney disease (CKD) and hemodialysis treatments performed on end-stage renal disease (ESRD) patients affect RBC epoxy fatty acids profiles remains unknown. Measuring the products solely in plasma is suboptimal. Since such determinations invariably ignore red blood cells (RBCs) that make up 3 kg of the circulating blood. RBCs are potential reservoirs for epoxy fatty acids that regulate cardiovascular function. We studied 15 healthy persons and 15 ESRD patients undergoing regular hemodialysis treatments. We measured epoxides derived from CYP monooxygenase and metabolites derived from LOX/CYP ω/(ω-1)-hydroxylase pathways in RBCs by LC–MS/MS tandem mass spectrometry. Our data demonstrate that various CYP epoxides and LOX/CYP ω/(ω-1)-hydroxylase products are increased in RBCs of ESRD patients, compared to control subjects, including dihydroxyeicosatrienoic acids (DHETs), epoxyeicosatetraenoic acids (EEQs), dihydroxydocosapentaenoic acids (DiHDPAs), and hydroxyeicosatetraenoic acids (HETEs). Hemodialysis treatment did not affect the majority of those metabolites. Nevertheless, we detected more pronounced changes in free metabolite levels in RBCs after dialysis, as compared with the total RBC compartment. These findings indicate that free RBC eicosanoids should be considered more dynamic or vulnerable in CKD.

KEYWORDS
chronic kidney disease (CKD), dialysis, erythrocytes, fatty acids, lipidomics

Publication III

1 | INTRODUCTION

Chronic kidney disease (CKD) is a risk factor for the composite outcome of all-cause mortality and cardiovascular disease (Weiner et al., 2004). Although mortality and cardiovascular disease burden have decreased for end-stage renal disease (ESRD) hemodialysis patients in the United States, the 5-year mortality is still ~50% (McGill et al., 2019), Most of these deaths are related to cardiovascular disease (CVD) (Felasa | Federation for Laboratory Animal Science Associations, 2012; Luft, 2000). Dietary omega-3 (n-3) fatty acid intake is associated with a reduced CVD risk (Harris et al., 2008; Huang et al., 2011; InterAct Consortium et al., 2011). Erythrocyte red-blood-cell (RBC) n-3 fatty-acid status is inversely related to cardiovascular events, such as cardiac arrhythmias, myocardial infarction, and sudden cardiac death (Bucher et al., 2002).

Epoxides and hydro(pero)xy fatty acids (or oxylipins) are lipid peroxidation products of polyunsaturated fatty acids (PUFA), including C18:2 linoleic (LA), C20:0 arachidonic (AA), C20:5 n-3 eicosapentaenoic (EPA), and C22:5 n-3 docosahexaenoic acids (DHA). These products are derived from CYP monooxygenase, cyclooxygenase (COX), and LOX/CYP ω/(ω-1)-hydroxylase pathways, which catalyze the production in a highly tissue-dependent and regioisomer-specific manner (Figure 1). The resulting products are epoxyoctadecenoic acids (EpOMEs), epoxyeicosatrienoic acid (EETs), epoxyeicosatetraenoic acids (EEQs), epoxydocosapentaenoic acids (EDPs), hydroperoxylinoleic acids (HpODEs), hydroxyoctadecadienoic acids (HODEs), hydroxydocosahexaenoic acids (HDHAs), hydroperoxyeicosatetraenoic acids (HPETEs), and hydroxyeicosatetraenoic acids (HETEs) (Figure 1). EpOMEs, EETs, EEQs, and EDPs are converted depending on cell type, into secondary eicosanoids and their metabolites. The major metabolic route of CYP epoxides is incorporation into phospholipids and hydrolysis to corresponding diols by the enzyme soluble epoxide hydrolase (sEH) (Spector & Kim, 2015). CYP-derived EETs and other epoxides, such as 17,18-EEQ, serve as endothelium-derived hyperpolarizing factors (EDHFs) to cause vasodilation (Campbell et al., 1996; Hercule et al., 2007; Hu & Kim, 1993). Recently, RBCs (~3 kg in human body) have been identified as a reservoir for CYP epoxides, in particular EETs, which on release may act in a vasoregulatory capacity (Jiang et al., 2010, 2011). Maximal exercise has been found to increase such erythro-epoxides in RBCs, including 9,10-EpOME, 12,13-EpOME, 5,6-EET, 11,12-EET, 14,15-EET, 16,17-EDP, and 19,20-EDP (Gollasch et al., 2019). Furthermore, sEH in the RBC and the resulting increase in EETs presumably contribute to a greater degree on regional blood flow than sEH inhibition localized in the arterial wall (Jiang et al., 2011; Yu et al., 2004). Nonetheless, the impact of epoxy and hydroxy fatty acids measurements in the RBCs for the prediction of CVD and mortality have not been previously elucidated. Whether or not CKD or hemodialysis treatment itself affect RBC-epoxids and hydroxy metabolites remains unknown. We tested the hypotheses that CKD and hemodialysis treatments performed on end-stage renal disease (ESRD) patients affect RBC epoxy fatty acids profiles.

2 | METHODS

The Charité University Medicine Institutional Review Board approved this duly registered study (ClinicalTrials.gov, Identifier: NCT03857984). Recruitment was primarily *via* person-to-person interview. Prior to participation in the study, 15 healthy volunteers (6 male and 9 female) and 15 CKD patients (7 male and 8 female) undergoing regular hemodialysis treatment signed informed consent forms which outlined the treatments to be taken and the possible risks involved. All healthy control subjects were not taking medications. Venous blood was collected in each healthy subject by subcutaneous arm vein puncture in the sitting position. In the group of dialyzed patients (CKD group), all the blood samples were collected on the fistula arm right before beginning of the dialysis (starting of the HD, pre-HD) and at the end of the dialysis (5–15 min before termination, post-HD). Patients underwent thrice-weekly dialysis, which lasted from 3 hr 45 min to 5 hr, based on high flux AK 200 dialyzers (Gambro GmbH, Hechingen, Germany). All samples were analyzed for RBC lipids. All blood samples were obtained by 4°C precooled EDTA vacuum extraction tube systems. Cells were separated from plasma by centrifugation for 10 min at 1,000–2,000 g using a refrigerated centrifuge RBCs were separated from EDTA blood by centrifugation as previously described (Gollasch, et al., 2020). RBC lipidomics was performed using LC–MS/MS tandem mass spectrometry as described in (Fischer et al., 2014; Gollasch et al., 2019; Gollasch et al., 2019). Concentrations are given in nanogram/g.

Descriptive statistics were calculated and variables were examined for meeting assumptions of normal distribution without skewness and kurtosis. In order to determine statistical significance, t test or Mann–Whitney test was used to compare the values of CKD versus control groups. Paired t-test or paired Wilcoxon test were used to compare pre-HD versus post-HD values. In order to determine statistical significance between the four classes of epoxy-metabolites hydrolyzed to appear in the circulation, Friedman's test followed by applying Dunn's multiple comparison test was used. In order to determine statistical significance between the four classes of epoxy-metabolites hydrolyzed to appear in the circulation, Friedman's test followed by applying Dunn's multiple comparison test was used. The analysis included Mauchly's test of sphericity followed by applying the test of within-subjects effects with Greenhouse–Geisser correction to ensure sphericity assumption (Gollasch et al., 2019; Gollasch et al., 2019). The .05 level of significance (p) was chosen. All data are

Publication Ⅲ
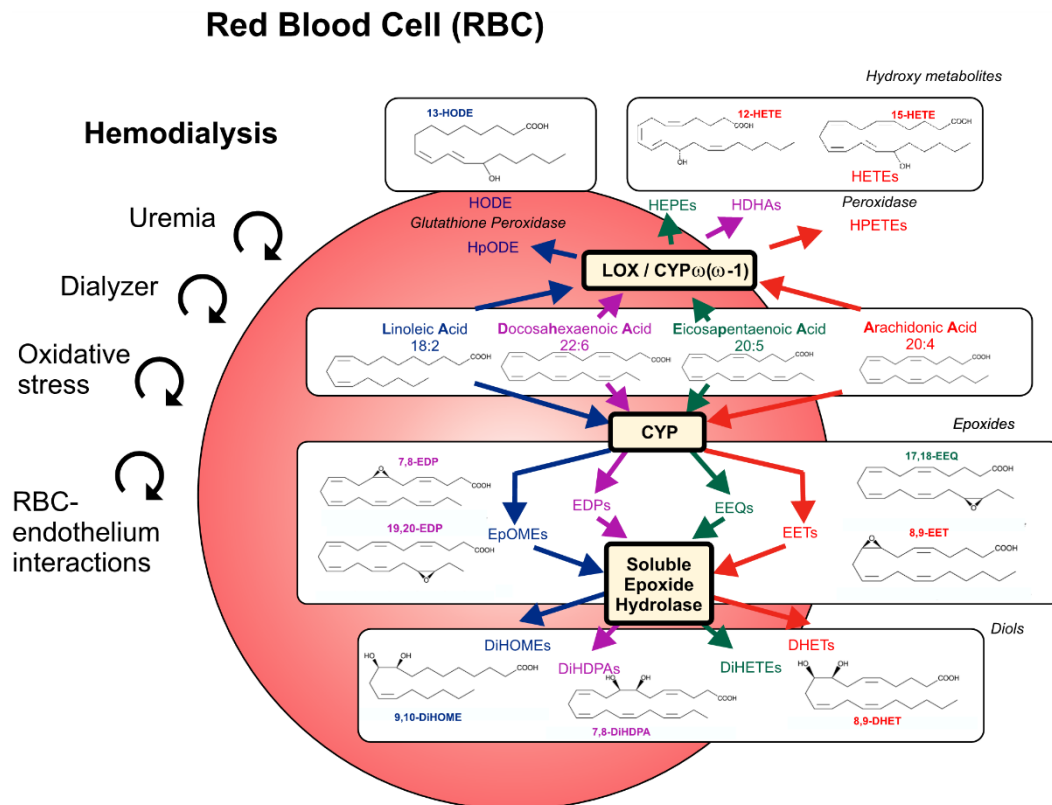
Red Blood Cell (RBC)

FIGURE 1 Hypothetic influence of CKD and hemodialysis associated with shear stress, red blood cell (RBC)-dialyzer interactions, red blood cell (RBC)-endothelial interactions, and oxidative stress affecting the content of cytochrome P450 epoxygenase (CYP) and 12- and 15-lipoxygenase (LOX)/CYP omega-hydroxylase metabolites in RBCs. The scheme illustrates the epoxide and hydroxy metabolites pathways studied. Linoleic (LA), arachidonic (AA), eicosapentaenoic (EPA), and docosahexaenoic acids (DHA) are converted to epoxyoctadecenoic acids (EpOMEs, e.g., 9,10-EpOME), epoxyeicosatrienoic acid (EETs, e.g., 8,9-EET), epoxyeicosatetraenoic acids (EEQs, e.g., 17,18-EEQ), and epoxydocosapentaenoic acids (EDPs, e.g., 17,18-EDP and 19,20-EDP) by CYP, respectively. EpOMEs, EETs, EEQs, and EDPs are converted to dihydroxyctadecenoic acids (DiHOMEs, e.g., 9,10-DiHOME), dihydroxyeicosatrienoic acids (DHETs, e.g., 8,9-DHET), dihydroxyeicosatetraenoic acids (DiHETEs), and dihydroxydocosapentaenoic acids (DiHDPAs, e.g., 7,8-DiHDPA), respectively, by the soluble epoxide hydrolase (sEH) enzyme. LA, AA, EPA, and DHA are converted to hydroperoxylinoleic acids (HpODEs), hydroxyoctadecadienoic acids (HODEs, e.g., 13-HODE), hydroxydocosahexaenoic acids (HDHAs), hydroperoxyeicosatetraenoic acids (HPETEs), and hydroxyeicosatetraenoic acids (HETEs, e.g., 12-HETE and 15-HETE) by LOX, CYP omega/(omega-1)-hydroxylase and peroxidase pathways. The metabolites measured within these pathways track the changes observed. Arrows demarcate metabolic pathways evaluated

presented as mean $\pm$ SD. All statistical analyses were performed using SPSS Statistics software (IBM Corporation) or All-Therapy statistics beta (AICBT Ltd).

3 | RESULTS

3.1 | Clinical characteristics

The age between ESRD patients and the healthy subjects was not different (50 ± 18 years vs. 47 ± 12 years, respectively, $p > .05$, $n = 15$ each). The body mass indices between the two groups were also not different (24.8 ± 3.4 kg/m^2 and 24.7 ± 4.6 kg/m^2, respectively, $p > .05$, $n = 15$ each). The patients in the group CKD were diagnosed for the following conditions: diabetes mellitus ($n = 4$ patients), hypertension ($n = 3$), membranous glomerulonephritis ($n = 2$), autosomal dominant polycystic kidney disease ($n = 1$), other or unknown ($n = 5$). Major cardiovascular complications in the CKD group included peripheral artery disease ($n = 3$), cardiovascular ($n = 2$) and cerebrovascular ($n = 1$) events. Subjects were Caucasians, with the exception of one Black

Publication III

patient in the CKD group and one Asian subject in the control group.

3.2 | RBC epoxy and hydroxy metabolites in CKD

We first determined the total levels of various CYP epoxides and LOX/CYP ω/(ω-1)-hydroxylase products in RBCs of the HD patients (Table 1) and compared the results with the healthy control subjects. Total CYP epoxides were analyzed for each member (Table 1A) and together within the four subclasses (Table 2A). RBCs of hemodialysis patients showed increased total levels of various individual CYP epoxides, namely 8,9-DHET, 14,15-DHET, 5,6-EEQ, 11,12-EEQ, 14,15-EEQ, 17,18-EEQ, 7,8-DiHDPA, 10,11-DiHDPA, 13,14-DiHDPA, and 16,17-DiHDPA in the RBCs (Table 1A). EpOMEs, DiHOMEs, EETs, EDPs (with exception of 19,20-EDP), and DiHETEs were not different between both groups (Table 1A). Free CYP epoxides in the RBCs were also not different or only slightly decreased (8,9-EET, 14,15-EET, and 5,6-EEQ) in RBCs of hemodialysis patients. Nonetheless, our analysis of the four CYP epoxide classes demonstrates that ESRD patients can be discriminated from controls by characteristic increases in three epoxide classes, that is, signatures, namely increased levels of total DHETs, EEQs, and DiHDPAs in the RBCs, that is, 5,6-DHET+8,9-DHET+11,12-DHET+14,15-DHET, 5,6-EEQ+8,9-EEQ+11,12-EEQ+14,15-EEQ+17,18-EEQ, and 7,8-DiHDPA+10,11-DiHDPA+13,14-DiHDPA+16,17-DiHDPA+19,20-DiHDPA (Table 2A). We next inspected the total levels of various LOX/CYP ω/(ω-1)-hydroxylase products in RBCs of the HD patients (Table 1A). We found that 5-HETE, 8-HETE, 9-HETE, 11-HETE, 12-HETE, 15-HETE, and 19-HETE levels were increased in the hemodialysis patients, whereas 13-HODE, 16-HETE, 17-HETE, 18-HETE, 20-HETE, 12 -HpETE, 5-HEPE, 8-HEPE, 9-HEPE, 12-HEPE, 15-HEPE, 18-HEPE, 19-HEPE, 20-HEPE, 4-HDHA, 7-HDHA, 8-HDHA, 10-HDHA, 11-HDHA, 13-HDHA, 14-HDHA, 16-HDHA, 17-HDHA, 20-HDHA, 21-HDHA, and 22-HDHA levels, were normal or nondetectable (Table 1A). Of note, free LOX/CYP ω/(ω-1)-hydroxylase products were generally increased in RBCs of hemodialysis patients, with exception of 17-HETE, 18-HETE, 19-HETE, 20-HETE, 12-HpETE, 19-HEPE, 20-HEPE, and 20-HDHA which were normal or non-detectable (Table 1B). Together, the findings indicate that ESRD patients show an altered RBC fatty acid metabolite status, that is, individual signature, which shows the accumulation of three CYP epoxide classes (DHETs,

EEQs, and DiHDPAs) and various HETEs and other LOX/CYP ω/(ω-1) metabolites in RBCs, the latter mostly accumulated in free state.

3.3 | Ratios

The main route of EpOMEs, EETs, EEQs, and EDPs metabolism in many cells is conversion into DiHOMEs, DHETs, dihydroxyeicosatetraenoic acids (DiHETEs), and dihydroxydocosapentaenoic acids (DiHDPAs) by the sEH, respectively (Figure 1). To provide possible insights into the nature of the observed accumulation of DHETs, EEQs, and DiHDPAs in RBCs of ESRD patients, we calculated diol/epoxide ratios in RBCs and compared the results with the control subjects (Table 2B). We found that the four classes of epoxy-metabolites are unequally hydrolyzed and appear in the RBCs (Table 2B for controls). Compared to EETs and EEQs (ratios diols/epoxy-metabolites, 0.0096 ± 0.0017 vs. 0.0042 ± 0.00012, Dunn's multiple comparison test, $p > .05$), EpOMEs and EDPs (ratios diols/epoxy-metabolites, 0.1628 ± 0.0658 vs. 0.0244 ± 0.0053, Dunn's multiple comparison test, $p > .05$) are preferentially metabolized into their diols. In fact, the following order of ratios was identified: DiHOMEs/EpOMEs=DiHDPA/EDPs>DHETs/EETs=DiHETEs/EEQs (Dunn's multiple comparison test, $p < .05$). ESRD patients showed increased ratios for DHET/EET and DiHDPA/EDP, which indicates that increased sEH activity preferred for EET and EDP substrate classes in vivo may have caused the observed accumulation of 8,9-DHET, 14,15-DHET, 7,8-DiHDPA, 10,11-DiHDPA, 13,14-DiHDPA, and 16,17-DiHDPA in the RBCs in ESRD. The observed accumulation of EEQs is unlikely to result from changes in sEH activity (Table 2B) or accumulation of eicosapentaenoic acid (EPA) as EPA levels are not increased in RBCs of our patients (Gollasch et al., 2020) (Figure 1).

3.4 | Effects of hemodialysis

With the exception of 7,8-DiHDPA, the data (Table 3) demonstrate no change of total CYP epoxides and LOX/CYP ω/(ω-1)-hydroxylase metabolites in response to a single dialysis (Table 3A). Accordingly, the diol/epoxide ratios were not altered (Table 4). However, hemodialysis treatment increased several CYP epoxides and LOX/CYP ω/(ω-1)-hydroxylase metabolites in free state, such as 11,12-DHET, 13-HODE, 5-HETE, 8-HETE, 9-HETE, 11-HETE, 15-HETE, 5-HEPE, 8-HDHA, 10-HDHA, 13-HDHA, 16-HDHA, and 17-HDHA (Table 3B).

Publication III

TABLE 1 Comparison of epoxy- and hydroxy-metabolites between control subjects versus CKD patients before hemodialysis (HD) ($n = 15$ each)

Amount (ng/g)	Control (Mean SD)		HD (mean SD)		p value, t test (#Mann-Whitney test)
(A) Total metabolites in RBCs					
CYP epoxy-metabolites					
(a) EpOMEs/DiHOMES					
9,10-EpOME	29.36	12.01	25.48	6.59	.267#
12,13-EpOME	13.67	9.22	10.62	6.16	.305#
9,10-DiHOME	4.12	1.30	5.13	1.92	.081#
12,13-DiHOME	2.26	0.90	2.92	1.45	.161#
(b) EETs/DiHOMEs					
5,6-EET	170.67	29.90	148.54	44.94	.124
8,9-EET	39.03	6.25	39.90	9.00	.761
11,12-EET	39.46	5.51	37.86	11.98	.644
14,15-EET	66.17	11.64	59.58	22.69	.328
5,6-DHET	0.89	0.17	0.98	0.43	.457
8,9-DHET	**1.07**	**0.23**	**2.03**	**1.81**	**.001#**
11,12-DHET	0.62	0.14	0.96	0.61	.081#
14,15-DHET	**0.40**	**0.05**	**0.51**	**0.16**	**.030**
(c) EEQs/DiHETEs					
5,6-EEQ	**41.54**	**13.39**	**51.78**	**98.53**	**.019#**
8,9-EEQ	2.48	0.89	3.51	6.41	.126#
11,12-EEQ	**2.09**	**0.68**	**2.56**	**4.74**	**.016#**
14,15-EEQ	**1.44**	**0.48**	**1.91**	**3.57**	**.041#**
17,18-EEQ	**3.25**	**1.03**	**3.90**	**7.31**	**.021#**
5,6-DiHETE	0.21	0.10	0.28	0.49	.202#
8,9-DiHETE	0.01	0.01	0.01	0.01	.776#
11,12-DiHETE	0.01	0.01	0.01	0.01	.677#
14,15-DiHETE	0.01	0.01	0.01	0.01	.697#
17,18-DiHETE	0.01	0.01	0.01	0.01	.787#
(d) EDPs/DiHDPAs					
7,8-EDP	15.58	4.55	18.16	12.19	.838#
10,11-EDP	1.22	0.43	1.35	0.47	.463
13,14-EDP	0.39	0.25	0.44	0.15	.158#
16,17-EDP	4.49	1.34	4.72	1.78	.967#
19,20-EDP	**6.72**	**4.26**	**4.22**	**1.52**	**.026#**
7,8-DiHDPA	**0.21**	**0.10**	**0.40**	**0.30**	**.041#**
10,11-DiHDPA	**0.50**	**0.20**	**0.09**	**0.05**	**.007**
13,14-DiHDPA	**0.08**	**0.02**	**0.11**	**0.04**	**.037#**
16,17-DiHDPA	**0.14**	**0.03**	**0.19**	**0.06**	**.022**
19,20-DiHDPA	0.20	0.07	0.26	0.16	.187#
LOX/CYP ω/(ω−1) metabolites					
13-HODE	69.46	19.97	77.47	18,89	.098#
5-HETE	**38.43**	**7.90**	**53.45**	**14.83**	**.002**
8-HETE	**27.30**	**5.72**	**35.11**	**10.20**	**.015**
9-HETE	**27.49**	**4.72**	**37.84**	**9.77**	**.001**
11-HETE	**41.90**	**7.00**	**54.16**	**14.84**	**.009**
12-HETE	**32.71**	**5.66**	**43.47**	**12.68**	**.007**

(Continues)

Publication Ⅲ

TABLE 1 (Continued)

Amount (ng/g)	Control (Mean SD)		HD (mean SD)		p value, t test (#Mann-Whitney test)
15-HETE	**74.29**	**14.38**	**93.95**	**24.59**	**.012**
16-HETE	4.60	0.82	4.91	1.43	.461
17-HETE	0.18	0.03	0.22	0.10	.512#
18-HETE	0.24	0.05	0.32	0.21	.461#
19-HETE	**0.26**	**0.11**	**0.42**	**0.11**	**.001#**
20-HETE	0.59	0.09	0.62	0.08	.371
12-HpETE	n.d.		n.d.		n/a
5-HEPE	1.47	0.51	2.05	2.64	.838#
8-HEPE	0.75	0.31	1.15	1.55	.744#
9-HEPE	0.93	0.37	1.35	1.64	.744#
12-HEPE	1.38	0.52	2.15	3.12	.935#
15-HEPE	1.18	0.41	2.06	2.74	.345#
18-HEPE	3.19	1.30	5.28	7.10	.567#
19-HEPE	1.32	0.50	1.89	2.80	.902#
20-HEPE	n.d.		n.d.		n/a
4-HDHA	9.11	2.99	11.20	4.61	.267#
7-HDHA	4.56	1.36	5.90	2.69	.137#
8-HDHA	5.27	1.77	7.16	3.11	.061#
10-HDHA	6.39	1.99	8.05	3.79	.148
11-HDHA	7.38	2.41	9.43	4.47	.217#
13-HDHA	9.35	2.80	10.43	4.20	.414
14-HDHA	5.41	1.75	6.82	3.38	.345#
16-HDHA	8.79	2.69	9.80	3.88	.486#
17-HDHA	12.98	3.97	15.55	6.92	.227
20-HDHA	19.16	5.89	22.57	9.88	.261
21-HDHA	3.04	1.18	3.76	1.70	.184
22-HDHA	n.d.		n.d.		n/a
(B) Free metabolites in RBCs					
CYP epoxy-metabolites					
(a) EpOMEs/DiHOMES					
9,10-EpOME	1.42	0.59	1.79	1.00	.367#
12,13-EpOME	1.22	0.63	1.25	0.91	.624#
9,10-DiHOME	0.43	0.29	0.52	0.34	.595#
12,13-DiHOME	1.70	0.96	2.20	1.52	.412#
(b) EETs/DiHOMEs					
5,6-EET	0.55	0.21	0.45	0.19	.170
8,9-EET	**0.12**	**0.06**	**0.06**	**0.04**	**.013#**
11,12-EET	0.24	0.07	0.20	0.08	.100
14,15-EET	**1.08**	**0.40**	**0.74**	**0.36**	**.015#**
5,6-DHET	n.d.		n.d.		n/a
8,9-DHET	n.d.		n.d.		n/a
11,12-DHET	0.01	0.01	0.01	0.01	.467
14,15-DHET	**0.01**	**0.01**	**0.01**	**0.01**	**.074#**
(c) EEQs/DiHETEs					
5,6-EEQ	**1.29**	**1.14**	**0.90**	**3.39**	**.010#**
8,9-EEQ	0.22	0.12	0.31	0.50	.351#

Publication III

TABLE 1 (Continued)

Amount (ng/g)	Control (Mean	SD)	HD (mean	SD)	p value, t test (#Mann-Whitney test)
11,12-EEQ	0.06	0.04	0.07	0.14	.116#
14,15-EEQ	0.14	0.10	0.20	0.23	.851#
17,18-EEQ	0.39	0.19	0.53	1.02	.217#
5,6-DiHETE	n.d.		n.d.		n/a
8,9-DiHETE	n.d.		n.d.		n/a
11,12-DiHETE	n.d.		n.d.		n/a
14,15-DiHETE	0.01	0.01	0.01	0.04	.285#
17,18-DiHETE	0.04	0.02	0.11	0.23	.902#
(d) EDPs/DiHDPAs					
7,8-EDP	0.12	0.05	0.17	0.17	.539#
10,11-EDP	0.01	0.01	0.01	0.01	.222#
13,14-EDP	n.d.		n.d.		n/a
16,17-EDP	n.d.		n.d.		n/a
19,20-EDP	0.06	0.05	0.11	0.22	.505#
7,8-DiHDPA	n.d.		n.d.		n/a
10,11-DiHDPA	n.d.		n.d.		n/a
13,14-DiHDPA	n.d.		n.d.		n/a
16,17-DiHDPA	0.01	0.01	0.02	0.01	.461#
19,20-DiHDPA	0.12	0.06	0.15	0.14	.744#
LOX/CYP ω/(ω−1) metabolites					
13-HODE	**8.96**	**4.64**	**36.76**	**31.23**	**<.001#**
5-HETE	**0.21**	**0.07**	**0.60**	**0.37**	**<.001#**
8-HETE	**0.28**	**0.14**	**0.90**	**0.59**	**<.001#**
9-HETE	**0.55**	**0.32**	**1.85**	**1.46**	**<.001#**
11-HETE	**0.84**	**0.32**	**2.66**	**1.64**	**<.001#**
12-HETE	**4.23**	**2.53**	**28.11**	**33.78**	**<.001#**
15-HETE	**0.65**	**0.25**	**2.15**	**1.05**	**<.001**
16-HETE	**0.10**	**0.03**	**0.15**	**0.06**	**.003**
17-HETE	n.d.		n.d.		n/a
18-HETE	n.d.		n.d.		n/a
19-HETE	n.d.		n.d.		n/a
20-HETE	0.10	0.05	0.10	0.04	.877
12-HpETE	n.d.		n.d.		n/a
5-HEPE	**0.03**	**0.02**	**0.14**	**0.34**	**.021#**
8-HEPE	**0.04**	**0.03**	**0.32**	**0.87**	**<.001#**
9-HEPE	**0.05**	**0.04**	**0.35**	**0.96**	**.003#**
12-HEPE	**0.97**	**0.52**	**8.06**	**14.72**	**.006#**
15-HEPE	**0.06**	**0.04**	**0.70**	**1.82**	**<.001#**
18-HEPE	**0.12**	**0.06**	**1.52**	**3.96**	**<.001#**
19-HEPE	0.03	0.02	0.22	0.69	.367#
20-HEPE	n.d.		n.d.		n/a
4-HDHA	**0.03**	**0.02**	**0.18**	**0.32**	**.001#**
7-HDHA	**0.02**	**0.01**	**0.11**	**0.05**	**.001#**
8-HDHA	**0.04**	**0.02**	**0.22**	**0.35**	**<.001#**
10-HDHA	**0.06**	**0.03**	**0.63**	**1.07**	**<.001#**
11-HDHA	**0.19**	**0.08**	**0.87**	**1.32**	**<.001#**

(Continues)

Publication III

T A B L E 1 (Continued)

Amount (ng/g)	Control (Mean SD)		HD (mean SD)		p value, t test (#Mann-Whitney test)
13-HDHA	**0.08**	**0.04**	**0.44**	**0.61**	**<.001#**
14-HDHA	**0.35**	**0.17**	**2.81**	**3.60**	**<.001#**
16-HDHA	**0.07**	**0.03**	**0.37**	**0.63**	**<.001#**
17-HDHA	**0.42**	**0.15**	**2.59**	**4.22**	**<.001#**
20-HDHA	0.27	0.09	0.67	1.00	.050#
21-HDHA	**0.11**	**0.05**	**0.42**	**0.59**	**.002#**
22-HDHA	**0.72**	**0.29**	**1.27**	**0.71**	**.013**

Note: Bold font indicates statistical significance.

Abbreviations: n.d., not detected; n/a, not applicable.

T A B L E 2 Comparison of epoxy-metabolites and their ratios between control subjects versus CKD patients before hemodialysis (HD) ($n = 15$ each)

(A) Concentrations of individual total epoxides together or their respective diols in RBCs

Epoxides or Diols (ng/g)	Control (Mean SD)		HD (Mean SD)		p-value, Mann-Whitney test
9,10-EpOME+12,13-EpOME	43.03	21.07	36.10	10.60	.3195
9,10-DiHOME+12,13-DiHOME	6.377	2.104	8.049	3.178	.0971
5,6-EET+8,9-EET+11,12 EET+14,15-EET	315.3	51.27	285.9	86.25	.2998
5,6-DHET+8,9-DHET+11,12-DHET+14,15-DHET	**2.986**	**0.5208**	**4.477**	**2.789**	**.0421**
5,6-EEQ+8,9-EEQ+11,12-EEQ+14,15-EEQ+17,18-EEQ	**50.81**	**16.35**	**63.65**	**120.5**	**.0225**
5,6-DiHETE+8,9-DiHETE+11,12-DiHETE+14,15-DiHETE+17,18-DiHETE	0.2153	0.1021	0.3420	0.7263	.1835
7,8-EDP+10,11-EDP+13,14-EDP+16,17-EDP+19,20-EDP	28.40	9.805	28.86	14.26	.6187
7,8-DiHDPA+10,11-DiHDPA+13,14-DiHDPA+16,17-DiHDPA+19,20-DiHDPA	**0.6813**	**0.2123**	**1.039**	**0.5678**	**.0464**

(B) Ratios estimated using total concentrations of epoxides and diols in RBCs

Ratios	Control (Mean SD)		HD (Mean SD)		p-value, Mann-Whitney test
Ratio (9,10-DiHOME+12,13-DiHOME)/(9,10-EpOME+12,13-EpOME)	0.1628	0.06583	0.2425	0.1255	.0564
Ratio (5,6-DHET+8,9-DHET+11,12-DHET+14,15-DHET)/(5,6-EET+8,9-EET+11,12 EET+14,15-EET)	**0.0096**	**0.001705**	**0.01652**	**0.009067**	**.0279**
Ratio (5,6-DiHETE+8,9-DiHETE+11,12-DiHETE+14,15-DiHETE+17,18-DiHETE)/(5,6-EEQ+8,9-EEQ+11,12-EEQ+14,15-EEQ+17,18-EEQ)	0.00416	0.001188	0.005927	0.004070	.2627
Ratio (7,8-DiHDPA+10,11-DiHDPA+13,14-DiHDPA+16,17-DiHDPA+19,20-DiHDPA)/(7,8-EDP+10,11-EDP+13,14-EDP+16,17-EDP+19,20-EDP)	**0.02445**	**0.005347**	**0.03765**	**0.01382**	**.0025**

Note: Bold font indicates statistical significance.

Publication III

TABLE 3 Effects of hemodialysis on epoxy- and hydroxy-metabolites in the CKD patients before (pre-HD) and at cessation (post-HD) of hemodialysis ($n = 15$ each)

Amount, (ng/g)	Pre-HD (Mean	SD)	Post-HD (mean	SD)	p value, paired t test ([#]paired Wilcoxon test)
(A) Total metabolites in RBCs					
CYP epoxy-metabolites					
(a) EpOMEs/DiHOMES					
9,10-EpOME	25.48	6.59	25.91	5.94	.802
12,13-EpOME	10.62	6.16	11.52	7.93	.307[#]
9,10-DiHOME	5.13	1.92	5.27	1.42	.623
12,13-DiHOME	2.92	1.45	3.00	0.90	.914
(b) EETs/DiHOMEs					
5,6-EET	148.54	44.94	162.71	46.95	.198
8,9-EET	39.90	9.00	43.76	8.50	.134
11,12-EET	37.86	11.98	41.54	11.54	.112
14,15-EET	59.58	22.69	63.97	21.75	.162
5,6-DHET	0.98	0.43	1.06	0.43	.117
8,9-DHET	2.03	1.81	2.13	1.67	.112[#]
11,12-DHET	0.96	0.61	0.99	0.50	.334[#]
14,15-DHET	0.51	0.16	0.53	0.12	.148
(c) EEQs/DiHETEs					
8,9-EEQ	3.51	6.41	3.39	5.75	1.000[#]
5,6-EEQ	51.78	98.53	45.89	69.79	.650[#]
11,12-EEQ	2.56	4.74	2.40	3.49	.125[#]
14,15-EEQ	1.91	3.5	1.66	2.55	.910[#]
17,18-EEQ	3.90	7.31	3.66	5.81	.460[#]
5,6-DiHETE	0.28	0.49	0.24	0.32	.733[#]
8,9-DiHETE	n.d.		n.d.		n/a
11,12-DiHETE	n.d.		n.d.		n/a
14,15-DiHETE	n.d.		n.d.		n/a
17,18-DiHETE	n.d.		n.d.		n/a
(d) EDPs/DiHDPAs					
7,8-EDP	18.16	12.19	19.48	12.59	.307[#]
10,11-EDP	1.35	0.47	1.50	0.73	.427[#]
13,14-EDP	0.44	0.15	0.52	0.31	.551[#]
16,17-EDP	4.72	1.78	5.46	2.50	.078[#]
19,20-EDP	4.22	1.52	5.14	2.84	.109
7,8-DiHDPA	**0.40**	**0.30**	**0.48**	**0.42**	**.036[#]**
10,11-DiHDPA	0.09	0.05	0.10	0.07	.256[#]
13,14-DiHDPA	0.11	0.04	0.12	0.04	.363[#]
16,17-DiHDPA	0.19	0.06	0.20	0.07	.124
19,20-DiHDPA	0.26	0.16	0.27	0.14	.173[#]
LOX/CYP ω/(ω−1) metabolites					
13-HODE	77.47	18,89	82.00	18.35	.391
5-HETE	53.45	14.83	56.62	10.08	.295
8-HETE	35.11	10.20	36.63	7.23	.379

Publication Ⅲ

T A B L E 3   (Continued)

Amount, (ng/g)	Pre-HD (Mean	SD)	Post-HD (mean	SD)	p value, paired t test (#paired Wilcoxon test)
9-HETE	37.84	9.77	39.89	7.07	.268
11-HETE	54.16	14.84	56.92	10.96	.323
12-HETE	43.47	12.68	45.33	8.36	.466
15-HETE	93.95	24.59	99.31	18.34	.281
16-HETE	4.91	1.43	5.14	1.08	.412
17-HETE	0.22	0.10	0.22	0.08	.363#
18-HETE	0.32	0.21	0.34	0.23	.112#
19-HETE	0.42	0.11	0.49	0.17	.085
20-HETE	0.62	0.08	0.65	0.23	.602
12-HpETE	n.d.		n.d.		
5-HEPE	2.05	2.64	2.30	3.25	.281#
8-HEPE	1.15	1.55	1.26	1.88	.363#
9-HEPE	1.35	1.64	1.51	2.11	.281#
12-HEPE	2.15	3.12	2.29	3.38	.307#
15-HEPE	2.06	2.74	2.23	2.95	.053#
18-HEPE	5.28	7.10	5.63	7.64	.140#
19-HEPE	1.89	2.80	1.80	2.32	.910#
20-HEPE	n.d.		n.d.		
4-HDHA	11.20	4.61	12.71	5.81	.140#
7-HDHA	5.90	2.69	6.33	2.85	.233#
8-HDHA	7.16	3.11	7.74	3.35	.112#
10-HDHA	8.05	3.79	8.57	3.93	.334#
11-HDHA	9.43	4.47	10.03	4.90	.140#
13-HDHA	10.43	4.20	11.22	4.95	.173#
14-HDHA	6.82	3.38	7.41	3.41	.156#
16-HDHA	9.80	3.88	10.55	4.14	.112#
17-HDHA	15.55	6.92	16.83	7.47	.078#
20-HDHA	22.57	9.88	24.53	10.60	.112#
21-HDHA	3.76	1.70	3.71	1.32	.790
22-HDHA	n.d.		n.d.		n/a
(B) Free metabolites in RBCs					
CYP epoxy-metabolites					
(a) EpOMEs/DiHOMES					
9,10-EpOME	1.79	1.00	2.08	0.48	.156#
12,13-EpOME	1.25	0.91	1.89	0.88	.053#
9,10-DiHOME	0.52	0.34	0.65	0.29	.147
12,13-DiHOME	2.20	1.52	2.91	1.87	.256#
(b) EETs/DiHOMEs					
5,6-EET	0.45	0.19	0.54	0.21	.114
8,9-EET	0.06	0.04	0.07	0.10	.480#
11,12-EET	0.20	0.08	0.21	0.06	.654
14,15-EET	0.74	0.36	0.93	0.35	.100#
5,6-DHET	<0.01	0.01	<0.01	0.01	n/a

(Continues)

Publication III

TABLE 3 (Continued)

Amount, (ng/g)	Pre-HD (Mean	SD)	Post-HD (mean	SD)	p value, paired t test (#paired Wilcoxon test)
8,9-DHET	0.02	0.01	0.03	0.03	.131#
11,12-DHET	**<0.02**	**0.01**	**0.02**	**0.01**	**.005**
14,15-DHET	0.01	0.01	0.02	0.01	.427#
(c) EEQs/DiHETEs					
5,6-EEQ	0.90	3.39	1.08	3.52	.068#
8,9-EEQ	0.31	0.50	0.20	0.55	.128#
11,12-EEQ	0.07	0.14	0.07	0.09	.424#
14,15-EEQ	0.20	0.23	0.17	0.24	.477#
17,18-EEQ	0.53	1.02	0.49	0.80	.955#
5,6-DiHETE	<0.01	0.01	<0.01	0.01	.477
8,9-DiHETE	<0.01		<0.01		n/a
11,12-DiHETE	<0.01		<0.01		n/a
14,15-DiHETE	0.01	0.04	0.02	0.04	.394#
17,18-DiHETE	0.11	0.23	0.16	0.38	.394#
(d) EDPs/DiHDPAs					
7,8-EDP	0.17	0.17	0.22	0.18	.112#
10,11-EDP	0.01	0.01	0.01	0.01	.463#
13,14-EDP	n.d.		n.d.		n/a
16,17-EDP	n.d.		n.d.		n/a
19,20-EDP	0.11	0.22	0.09 + 0.09		.507#
7,8-DiHDPA	n.d.		n.d.		n/a
10,11-DiHDPA	<0.01	0.01	<0.01	0.01	n/a
13,14-DiHDPA	<0.01	0.01	0.01	0.01	.465#
16,17-DiHDPA	0.02	0.01	0.03	0.02	.140#
19,20-DiHDPA	0.15	0.14	0.18	0.18	.334#
LOX/CYP ω/(ω−1) metabolites					
13-HODE	**36.76**	**31.23**	**45.70**	**31.56**	**.031#**
5-HETE	**0.60**	**0.37**	**0.85**	**0.53**	**.023#**
8-HETE	**0.90**	**0.59**	**1.24**	**0.83**	**.008#**
9-HETE	**1.85**	**1.46**	**2.51**	**1.84**	**.031#**
11-HETE	**2.66**	**1.64**	**3.37**	**2.16**	**.017#**
12-HETE	28.11	33.78	34.20	33.78	.334#
15-HETE	**2.15**	**1.05**	**2.78**	**1.54**	**.008#**
16-HETE	0.15	0.06	0.15	0.04	.999
17-HETE	n.d.		n.d.		n/a
18-HETE	n.d.		n.d.		n/a
19-HETE	n.d.		n.d.		n/a
20-HETE	0.10 + 0.04		0.12	0.06	.155
12-HpETE	n.d.		n.d.		n/a
5-HEPE	**0.14**	**0.34**	**0.18**	**0.45**	**.031#**
8-HEPE	0.32	0.87	0.35	0.98	.394#
9-HEPE	0.35	0.96	0.42	1.14	.112#
12-HEPE	8.06	14.72	10.61	21.49	.191#
15-HEPE	0.70	1.82	0.75	1.96	.307#

(Continues)

Publication Ⅲ

TABLE 3   (Continued)

Amount, (ng/g)	Pre-HD (Mean	SD)	Post-HD (mean	SD)	p value, paired t test (#paired Wilcoxon test)
18-HEPE	1.52	3.96	1.53	3.96	.776#
19-HEPE	0.22	0.69	0.21	0.64	.955#
20-HEPE	n.d.		n.d.		n/a
4-HDHA	0.18	0.32	0.25	0.45	.061#
7-HDHA	0.11	0.05	0.15	0.28	.112#
8-HDHA	**0.22**	**0.35**	**0.31**	**0.49**	**.031#**
10-HDHA	**0.63**	**1.07**	**0.79**	**1.39**	**.023#**
11-HDHA	0.87	1.32	1.07	1.60	.100#
13-HDHA	**0.44**	**0.61**	**0.55**	**0.74**	**.036#**
14-HDHA	2.81	3.60	3.40	4.40	.078#
16-HDHA	**0.37**	**0.63**	**0.50**	**0.93**	**.012#**
17-HDHA	**2.59**	**4.22**	**3.35**	**5.24**	**.031#**
20-HDHA	0.67	1.00	0.83	1.37	.112#
21-HDHA	0.42	0.59	0.48	0.68	.256#
22-HDHA	1.27	0.71	1.30	0.78	.837

Note: Bold font indicates statistical significance.

TABLE 4   Effects of hemodialysis on epoxide and their respective diol ratios in the CKD patients before (pre-HD) and at cessation (post-HD) of hemodialysis ($n = 15$ each). Ratios were estimated using total concentrations of epoxides and diols in RBCs

Ratios	Pre-HD (Mean	SD)	Post-HD (Mean	SD)	p-value, Paired Wilcoxon test
Ratio (9,10-DiHOME+12,13-DiHOME)/ (9,10-EpOME+12,13-EpOME)	0.2425	0.1255	0.2435	0.1043	.8904
Ratio (5,6-DHET+8,9-DHET+11,12-DHET+14,15-DHET)/(5,6-EET+8,9-EET+11,12 EET+14,15-EET)	0.01652	0.009067	0.01623	0.008816	.8647
Ratio (5,6-DiHETE+8,9-DiHETE+14,15-DiHETE+17,18-DiHETE)/(5,6-EEQ+8,9-EEQ+11,12-EEQ+14,15-EEQ+17,18-EEQ)	0.005927	0.004070	0.005647	0.003565	.4896
Ratio (7,8-DiHDPA+10,11-DiHDPA+13,14-DiHDPA+16,17-DiHDPA+19,20-DiHDPA)/ (7,8-EDP+10,11-EDP+13,14-EDP+16,17-EDP+19,20-EDP)	0.03765	0.01382	0.03873	0.01658	.4887

4 | DISCUSSION

Our data demonstrate that RBCs of ESRD patients accumulated three CYP epoxide classes (DHETs, EEQs, and DiHDPAs) and various HETEs, including 5-HETE, 8-HETE, 9-HETE, 11-HETE, 12-HETE, 15-HETE, and 19-HETE, compared to control subjects. Furthermore, hemodialysis treatment is insufficient to change the total concentrations of these and other LOX/CYP metabolites in RBCs of ESRD patients. Since the four subclasses of CYP epoxy metabolites increase in plasma after the dialysis treatment (Gollasch et al., 2020), we suggest that total CYP metabolites in RBCs are relatively invulnerable in CKD and hemodialysis

(possibly due to slow exchange). Of note, ESRD is associated with increased levels of several free CYP epoxides and LOX/CYP ω/(ω-1)-hydroxylase metabolites in RBCs. Since several of those mediators are also increased by hemodialysis treatment itself, we suggest that free RBC eicosanoids constitute a fraction of lipid mediators, which are particularly vulnerable in CKD and hemodialysis. The extent to which the RBC eicosanoids exhibit beneficial or detrimental cardiovascular effects in CKD, possibly in comprehensive lipidomic (patho)physiological networks, remains to be explored. Nonetheless, our results indicate that RBCs could represent a reservoir for PUFA CYP epoxy-metabolites and LOX/CYP hydroxy metabolites, which on release may act in a

Publication III

vasoregulatory capacity to affect cardiovascular responses in hemodialysis patients.

4.1 | EETs

RBCs are reservoir of EETs which on release may act in a vasoregulatory capacity (Jiang et al., 2010, 2011). In addition to serving as carriers of O_2, RBCs are known to regulate the microvascular perfusion by liberating adenosine triphosphate (ATP) and EETs upon exposure to a low O_2 environment (Jiang et al., 2010; Sprague et al., 2010). The release of EETs is activated by $P2X_7$ receptor stimulation *via* ATP to cause the circulatory response (Jiang et al., 2007). RBCs are believed to serve as a source of plasma EETs, which are esterified to the phospholipids of lipoproteins. Therefore, levels of free EETs in plasma are found to be low (~3% of circulating EETs) (Jiang et al., 2010, 2011). Erythro-EETs are produced by direct oxidation of AA and the monooxygenase-like activity of hemoglobin (Jiang et al., 2010, 2011, 2012). On release, EETs and their diols (DHETs) produce vasodilation (Hercule et al., 2009; Lu et al., 2001), are profibrinolytic and reduce inflammation (Jiang et al., 2010, 2011, 2012). Exhaustive exercise increases the circulating levels of 5,6-DHET (Gollasch et al., 2019). In this study, we were able to demonstrate that RBCs of ESRD patients show increased accumulation of total DHETs. In particular, we observed increases in total concentrations of 8,9-DHET and 14,15-DHET in the RBCs. Hemodialysis did not affect this accumulation. It remains unknown whether RBCs are capable of liberating erythro-DHETs into the blood and/or tissues in kidney patients. Our results indicate that CKD affects the RBC reservoir for DHETs, but not EETs, which on release may affect the cardiovascular response.

4.2 | Other PUFA metabolites

We observed increases in total concentrations of EEQs (5,6-EEQ, 11,12-EEQ, 14,15-EEQ, 17,18-EEQ) and EDP/DiHDPAs (19,20-EDP, 7,8-DiHDPA, 10,11- DiHDPA, 13,14-DiHDPA, 16,17-DiHDPA) and HETEs (5-HETE, 8-HETE, 9-HETE, 11-HETE, 12-HETE, 15-HETE, 19-HETE) in RBCs of our ESRD patients. Little is known about the functions of EEQs and EDPs. Both EEQs and EDPs are potent vasodilators (Hercule et al., 2007; Lauterbach et al., 2002; Morin et al., 2011; Ulu et al., 2014). EDPs have antiangiogenic (McDougle et al., 2017), anti-fibrotic (Sharma et al., 2016) and protective effects in post-ischemic functional recovery, at least in particular by maintaining mitochondrial function and reducing inflammatory responses (Arnold et al., 2010; Darwesh et al., 2019). It is possible that their diols (DiHDPAs) are also biologically active and may exert beneficial effects in cardiac

arrhythmias (Zhang et al., 2016). DiHDPAs dilate coronary microvessels with similar potency to EEQ isomers in canine and porcine models (Zhang et al., 2001) and inhibit human platelet aggregation with moderately lower potency to EDPs and EEQs (VanRollins, 1995). Specific 17,18-EEQ analogs are in development to serve as novel antiarrhythmic agents (Adebesin et al., 2019). HETEs are involved in many chronic diseases such as inflammation, obesity, cardiovascular disease, kidney disease, and cancer, for review see (Gabbs et al., 2015). Nonetheless, it remains unknown whether RBCs are capable of liberating EEQs, DiHDPAs, or HETEs into blood or tissues. Our data indicate that both metabolite classes are novel candidates potentially released by RBCs to exhibit cardiovascular effects in health and CKD.

Surprisingly, we did detect increases in various free CYP epoxides and LOX/CYP $\omega/(\omega\text{-}1)$-hydroxylase metabolites in RBCs in ESRD, which were augmented by hemodialysis. The mechanism by which CKD and hemodialysis raises the levels of those erythro-metabolites is not known. Since those metabolites cannot be synthesized endogenously in appreciable amounts, accelerated release into and uptake from plasma could be a possible explanation. The more pronounced changes observed in free metabolite levels within the RBCs, as compared with the total RBC compartment, indicate that free erythro-eicosanoids should be considered more dynamic or vulnerable with respect to metabolite flux. The design of our study does not differentiate between patient groups undergoing long-term dialysis therapy with regard to the specific underlying renal disease. Nevertheless, the impact of those epoxides and hydroxy metabolites has yet to be integrated into a (patho)physiological context.

5 | CONCLUSIONS

Our results show that CKD affects the levels of numerous CYP epoxides and hydroxy metabolites (DHETs, EEQs, DiHDPAs, and HETEs) in circulating RBCs compared to control subjects, which on release may act in a vasoregulatory capacity. Although hemodialysis treatment was insufficient to change the majority of those total metabolites, we detected pronounced changes in free metabolite levels within the ESRD RBCs and in response to hemodialysis, indicating that free erythro-epoxides could also contribute to the cardiovascular risk, for example, in diabetes or hypertension. More research is needed to determine the contribution of RBC epoxy- and hydroxy-metabolites to cardiac performance and blood pressure regulation in health, cardiovascular, and specific kidney diseases.

Publication III

CONFLICT OF INTEREST
None.

AUTHOR CONTRIBUTIONS
BG, MG, and FCL planned and designed the experimental studies. MR and ID performed the LC–MS/MS spectrometry experiments. All authors contributed to the implementation and analyses of the experiments. BG drafted the article, and all authors, contributed to its completion.

ORCID

Benjamin Gollasch https://orcid.org/0000-0001-5267-518X

REFERENCES

Adebesin, A. M., Wesser, T., Vijaykumar, J., Konkel, A., Paudyal, M., Lossie, J., Zhu, C., Westphal, C., Puli, N., Fischer, R., Schunck, W.-H., & Falck, J. R. (2019). Development of robust 17(R),18(S)-epoxyeicosatetraenoic acid (17,18-EEQ) analogs as potential clinical antiarrhythmic agents. *Journal of Medicinal Chemistry*, *62*(22), 10124–10143. https://doi.org/10.1021/acs.jmedchem.9b00952

Arnold, C., Markovic, M., Blossey, K., Wallukat, G., Fischer, R., Dechend, R., Konkel, A., von Schacky, C., Luft, F. C., Muller, D. N., Rothe, M., & Schunck, W.-H. (2010). Arachidonic acid-metabolizing cytochrome P450 enzymes are targets of {omega}-3 fatty acids. *The Journal of Biological Chemistry*, *285*(43), 32720–32733.

Bucher, H. C., Hengstler, P., Schindler, C., & Meier, G. (2002). N-3 polyunsaturated fatty acids in coronary heart disease: A meta-analysis of randomized controlled trials. *American Journal of Medicine*, *112*(4), 298–304. https://doi.org/10.1016/S0002-9343(01)01114-7

Campbell, W. B., Gebremedhin, D., Pratt, P. F., & Harder, D. R. (1996). Identification of epoxyeicosatrienoic acids as endothelium-derived hyperpolarizing factors. *Circulation Research*, *78*(3), 415–423. https://doi.org/10.1161/01.RES.78.3.415

Darwesh, A. M., Jamieson, K. L., Wang, C., Samokhvalov, V., & Seubert, J. M. (2019). Cardioprotective effects of CYP-derived epoxy metabolites of docosahexaenoic acid involve limiting NLRP3 inflammasome activation (1). *Canadian Journal of Physiology and Pharmacology*, *97*(6), 544–556. https://doi.org/10.1139/cjpp-2018-0480

Felasa | Federation for Laboratory Animal Science Associations. (2012). Guidelines - Recommendations. [Internet]. http://www.felasa.eu/recommendations/guidelines/.

Fischer, R., Konkel, A., Mehling, H., Blossey, K., Gapelyuk, A., Wessel, N., von Schacky, C., Dechend, R., Muller, D. N., Rothe, M., Luft, F. C., Weylandt, K., & Schunck, W.-H. (2014). Dietary omega-3 fatty acids modulate the eicosanoid profile in man primarily via the CYP-epoxygenase pathway. *Journal of Lipid Research*, *55*(6), 1150–1164. https://doi.org/10.1194/jlr.M047357

Gabbs, M., Leng, S., Devassy, J. G., Monirujjaman, M., & Aukema, H. M. (2015). Advances in our understanding of oxylipins derived from dietary PUFAs. *Advances in Nutrition*, *6*(5), 513–540. https://doi.org/10.3945/an.114.007732

Gollasch, B., Dogan, I., Rothe, M., Gollasch, M., & Luft, F. C. (2019). Maximal exercise and erythrocyte fatty-acid status: A lipidomics study. *Physiological Reports*, *7*(8), e14040.

Gollasch, B., Dogan, I., Rothe, M., Gollasch, M., & Luft, F. C. (2019). Maximal exercise and plasma cytochrome P450 and lipoxygenase

mediators: A lipidomics study. *Physiological Reports*, *7*(13), e14165. https://doi.org/10.14814/phy2.14165

Gollasch, B., Dogan, I., Rothe, M., Gollasch, M., & Luft, F. C. (2020). Effects of hemodialysis on blood fatty acids. *Physiological Reports*, *8*(2), e14332. https://doi.org/10.14814/phy2.14332

Gollasch, B., Wu, G., Dogan, I., Rothe, M., Gollasch, M., & Luft, F. C. (2020). Effects of hemodialysis on plasma oxylipins. *Physiological Reports*, *8*(12), e14447. https://doi.org/10.14814/phy2.14447

Harris, W. S., Kris-Etherton, P. M., & Harris, K. A. (2008). Intakes of long-chain omega-3 fatty acid associated with reduced risk for death from coronary heart disease in healthy adults. *Current Atherosclerosis Reports*, *10*(6), 503–509. https://doi.org/10.1007/s11883-008-0078-z

Hercule, H. C., Salanova, B., Essin, K., Honeck, H., Falck, J. R., Sausbier, M., Ruth, P., Schunck, W.-H., Luft, F. C., & Gollasch, M. (2007). The vasodilator 17,18-epoxyeicosatetraenoic acid targets the pore-forming BK alpha channel subunit in rodents. *Experimental Physiology*, *92*(6), 1067–1076.

Hercule, H. C., Schunck, W.-H., Gross, V., Seringer, J., Leung, F. P., Weldon, S. M., da Costa Goncalves, A. C., Huang, Y., Luft, F. C., & Gollasch, M. (2009). Interaction between P450 eicosanoids and nitric oxide in the control of arterial tone in mice. *Arteriosclerosis, Thrombosis, and Vascular Biology*, *29*(1), 54–60. https://doi.org/10.1161/ATVBAHA.108.171298

Hu, S., & Kim, H. S. (1993). Activation of K+ channel in vascular smooth muscles by cytochrome P450 metabolites of arachidonic acid. *European Journal of Pharmacology*, *230*(2), 215–221. https://doi.org/10.1016/0014-2999(93)90805-R

Huang, J., Frohlich, J., & Ignaszewski, A. P. (2011). The impact of dietary changes and dietary supplements on lipid profile. *Canadian Journal of Cardiology*, *27*(4), 488–505. https://doi.org/10.1016/j.cjca.2010.12.077

InterAct Consortium, Romaguera, D., Guevara, M., Norat, T., Langenberg, C., Forouhi, N. G., Sharp, S., Slimani, N., Schulze, M. B., Buijsse, B., Buckland, G., Molina-Montes, E., Sánchez, M. J., Moreno-Iribas, M. C., Bendinelli, B., Grioni, S., van der Schouw, Y. T., Arriola, L., Beulens, J. W., … Wareham, N. J. (2011). Mediterranean diet and type 2 diabetes risk in the European Prospective Investigation into Cancer and Nutrition (EPIC) study: The InterAct project. *Diabetes Care*, *34*(9), 1913–1918.

Jiang, H., Anderson, G. D., & McGiff, J. C. (2010). Red blood cells (RBCs), epoxyeicosatrienoic acids (EETs) and adenosine triphosphate (ATP). *Pharmacological Reports*, *62*(3), 468–474. https://doi.org/10.1016/S1734-1140(10)70302-9

Jiang, H., Anderson, G. D., & McGiff, J. C. (2012). The red blood cell participates in regulation of the circulation by producing and releasing epoxyeicosatrienoic acids. *Prostaglandins & Other Lipid Mediators*, *98*(3–4), 91–93. https://doi.org/10.1016/j.prostaglandins.2011.11.008

Jiang, H., Quilley, J., Doumad, A. B., Zhu, A. G., Falck, J. R., Hammock, B. D., Stier, C. T. Jr, & Carroll, M. A. (2011). Increases in plasma trans-EETs and blood pressure reduction in spontaneously hypertensive rats. *American Journal of Physiology. Heart and Circulatory Physiology*, *300*(6), H1990–H1996.

Jiang, H., Zhu, A. G., Mamczur, M., Falck, J. R., Lerea, K. M., & McGiff, J. C. (2007). Stimulation of rat erythrocyte P2X7 receptor induces the release of epoxyeicosatrienoic acids. *British Journal of Pharmacology*, *151*(7), 1033–1040.

Lauterbach, B., Barbosa-Sicard, E., Wang, M.-H., Honeck, H., Kärgel, E., Theuer, J., Schwartzman, M. L., Haller, H., Luft, F. C., Gollasch,

Publication Ⅲ

M., & Schunck, W.-H. (2002). Cytochrome P450-dependent eicosapentaenoic acid metabolites are novel BK channel activators. *Hypertension*, *39*(2 Pt 2), 609–613. https://doi.org/10.1161/hy0202.103293

Lu, T., Katakam, P. V. G., VanRollins, M., Weintraub, N. L., Spector, A. A., & Lee, H.-C. (2001). Dihydroxyeicosatrienoic acids are potent activators of Ca(2+)-activated K(+) channels in isolated rat coronary arterial myocytes. *Journal of Physiology*, *534*(Pt 3), 651–667.

Luft, F. C. (2000). Renal disease as a risk factor for cardiovascular disease. *Basic Research in Cardiology*, *95*(Suppl 1), I72–I76. https://doi.org/10.1007/s003950070013

McDougle, D. R., Watson, J. E., Abdeen, A. A., Adili, R., Caputo, M. P., Krapf, J. E., Johnson, R. W., Kilian, K. A., Holinstat, M., & Das, A. (2017). Anti-inflammatory omega-3 endocannabinoid epoxides. *Proceedings of the National Academy of Sciences of the United States of America*, *114*(30), E6034–E6043.

McGill, R. L., Bragg-Gresham, J. L., He, K., Lacson, E. K. Jr, Miskulin, D. C., & Saran, R. (2019). Chronic disease burdens of incident U.S. dialysis patients, 1996–2015. *Clinical Nephrology*, *93*(1), 1–8.

Morin, C., Fortin, S., & Rousseau, E. (2011). 19,20-EpDPE, a bioactive CYP450 metabolite of DHA monoacyglyceride, decreases Ca(2)(+) sensitivity in human pulmonary arteries. *American Journal of Physiology. Heart and Circulatory Physiology*, *301*(4), H1311–H1318.

Sharma, A., Khan, M., Levick, S., Lee, K., Hammock, B., & Imig, J. (2016). Novel omega-3 fatty acid epoxygenase metabolite reduces kidney fibrosis. *International Journal of Molecular Sciences*, *17*(5), 751. https://doi.org/10.3390/ijms17050751

Spector, A. A., & Kim, H. Y. (2015). Cytochrome P450 epoxygenase pathway of polyunsaturated fatty acid metabolism. *Biochimica Et Biophysica Acta*, *1851*(4), 356–365. https://doi.org/10.1016/j.bbalip.2014.07.020

Sprague, R. S., Goldman, D., Bowles, E. A., Achilleus, D., Stephenson, A. H., Ellis, C. G., & Ellsworth, M. L. (2010). Divergent effects of low-O(2) tension and iloprost on ATP release from erythrocytes of humans with type 2 diabetes: Implications for O(2) supply to skeletal muscle. *American Journal of Physiology. Heart and Circulatory Physiology*, *299*(2), H566–H573.

Ulu, A., Stephen Lee, K. S., Miyabe, C., Yang, J., Hammock, B. G., Dong, H., & Hammock, B. D. (2014). An omega-3 epoxide of docosahexaenoic acid lowers blood pressure in angiotensin-II-dependent hypertension. *Journal of Cardiovascular Pharmacology*, *64*(1), 87–99. https://doi.org/10.1097/FJC.0000000000000094

VanRollins, M. (1995). Epoxygenase metabolites of docosahexaenoic and eicosapentaenoic acids inhibit platelet aggregation at concentrations below those affecting thromboxane synthesis. *Journal of Pharmacology and Experimental Therapeutics*, *274*(2), 798–804.

Weiner, D. E., Tighiouart, H., Amin, M. G., Stark, P. C., MacLeod, B., Griffith, J. L., Salem, D. N., Levey, A. S., & Sarnak, M. J. (2004). Chronic kidney disease as a risk factor for cardiovascular disease and all-cause mortality: A pooled analysis of community-based studies. *Journal of the American Society of Nephrology*, *15*(5), 1307–1315. https://doi.org/10.1097/01.ASN.0000123691.46138.E2

Yu, Z., Davis, B. B., Morisseau, C., Hammock, B. D., Olson, J. L., Kroetz, D. L., & Weiss, R. H. (2004). Vascular localization of soluble epoxide hydrolase in the human kidney. *American Journal of Physiology. Renal Physiology*, *286*(4), F720–F726. https://doi.org/10.1152/ajprenal.00165.2003

Zhang, Y., Guallar, E., Blasco-Colmenares, E., Harms, A. C., Vreeken, R. J., Hankemeier, T., Tomaselli, G. F., & Cheng, A. (2016). Serum-based oxylipins are associated with outcomes in primary prevention implantable cardioverter defibrillator patients. *PLoS One*, *11*(6), e0157035. https://doi.org/10.1371/journal.pone.0157035

Zhang, Y., Oltman, C. L., Lu, T., Lee, H. C., Dellsperger, K. C., & VanRollins, M. (2001). EET homologs potently dilate coronary microvessels and activate BK(Ca) channels. *American Journal of Physiology. Heart and Circulatory Physiology*, *280*(6), H2430–H2440.

Publication III

10. Curriculum Vitae

My curriculum vitae does not appear in the electronic version of my paper for reasons of data protection.

11. Complete list of publications

Original Publishing

1. **G. Wu**, M. Gotthardt, and M. Gollasch, Assessment of nanoindentation in stiffness measurement of soft biomaterials: kidney, liver, spleen and uterus. Sci Rep, 2020. 10(1): p. 18784. **Impact Factor (2019): 3.998**

2. B. Gollasch, **G. Wu**, I. Dogan, M. Rothe, M. Gollasch, and F. C. Luft, Maximal exercise and erythrocyte epoxy fatty acids: a lipidomics study. Physiol Rep, 2019. 7(22): p. e14275.

3. B. Gollasch, **G. Wu**, I. Dogan, M. Rothe, M. Gollasch, and F. C. Luft, Effects of hemodialysis on plasma oxylipins. Physiol Rep, 2020. 8(12): p. e14447.

4. B. Gollasch, **G. Wu**, T. Liu, I. Dogan, M. Rothe, M. Gollasch, and F. C. Luft, Hemodialysis and erythrocyte epoxy fatty acids. Physiol Rep, 2020. 8(20): p. e14601.

12. Acknowledgements